Fakultät Wissenschaftszentrum Weihenstephan für Ernährung,
Landnutzung und Umwelt

Professur für Ökoklimatologie

Remote sensing of vegetation phenology by MODIS - challenges in data processing and validation by multispecies ground observation and LiDAR.

Gourav Misra

Vollständiger Abdruck der von der Fakultät Wissenschaftszentrum Weihenstephan für Ernährung, Landnutzung und Umwelt der Technischen Universität München zur Erlangung des akademischen Grades eines

Doktors der Naturwissenschaften (Dr. rer. nat.)

genehmigten Dissertation.

Vorsitzende: Prof. Dr. Anja Rammig

Prüfer der Dissertation: 1. Prof. Dr. Annette Menzel
2. Prof. Dr. Christopher Conrad

Die Dissertation wurde am 06.02.2019 bei der Technischen Universität München eingereicht und durch die Fakultät Wissenschaftszentrum Weihenstephan für Ernährung, Landnutzung und Umwelt am 07.10.2019 angenommen.

Abstract

Phenology, cyclic events in living organisms, is among others triggered by climatic conditions and hence affected by climate change. The timing of such events are important factors influencing species interactions and ecosystem functioning. Thus, phenology is an indicator of any changes in climate and the well-being of an ecosystem. Traditionally, phenology has been observed through surveying of species locally and sporadically in time. In contrast, remote sensing based estimations of phenology provide avenues for repetitive and cost-effective solutions for monitoring plant development at both local and global scales. The central idea of this thesis revolves around remote sensing based estimation of key phenophases of plants (Land Surface Phenology or LSP), their drivers, and their validation with observed ground phenology (GP). Several phenological metrics such as Start of Season (SOS), End of Season (EOS), Length of Season (LOS), maximum NDVI value (NDVImax), NDVI integrated over the growing season (NDVIsum) and day of maximum NDVI (maxDOY) were estimated from remote sensing based time series of MODIS NDVI data.

This thesis consists of three case studies carried out in Germany with sites near Stuttgart (southwestern Germany), in the Bavarian Forest National Park, and in the Bavarian Alps that posed different challenges in terms of land cover, climate, and topography. Different methods for smoothing and extraction of phenological metrics were also discussed in this thesis. The phenological metrics derived from remote sensing data were validated with ground phenological records and LiDAR observations. It was found that the earliest phenological phases such as bud burst or the first leaf are difficult to detect from satellite data. The 50% amplitude method of estimating LSP-SOS provided superior results in detecting leaf unfolding as compared to other available techniques. A further analysis revealed other controls on phenology apart from climatic drivers. Homogeneity of land cover or the mixing of broad leaves and conifers in a pixel also significantly affected the estimated LSP. The final case study in the Bavarian Alps provided clues regarding the changing nature of elevational rates of LSP in the Alpine and pre-Alpine regions which are primarily driven by variations in spring and winter temperatures.

Zusammenfassung

Phänologie, zyklische Ereignisse in lebenden Organismen, wird unter anderem durch klimatische Bedingungen gesteurt und ist folglich auch vom Klimawandel betroffen. Die Eintrittstermine dieser Ereignisse sind wichtige Faktoren, die Arteninteraktionen und Ökosystemfunktionen beeinflussen. Die Phänologie kann als Indikator über Veränderungen des Klimas und den Zustand des Ökosystems Auskunft geben. Phänologie wurde herkömmlicherweise über lokale und sporadische Beobachtungen von Arten durchgeführt. Im Gegensatz dazu bieten fernerkundliche Abschätzungen der Phänologie neue Wege für repetitive und kostengünstige Lösungen, um die Pflanzenentwicklung sowohl lokal als auch global zu überwachen. Der Grundgedanke dieser Arbeit dreht sich um die fernerkundlich basierte Abschätzung von Schlüsselphasen der Pflanzenphänologie (Phänologie der Landschaftsoberfläche oder LSP), ihre Antriebe und ihre Validierung mittels phänologischer Bodenbeobachtungen (ground phenology, GP). Verschiedene phänologische Kennzahlen wie Beginn der Saison (Start of Season, SOS), Ende der Saison (End of Season EOS), Länge der Saison (Length of Season LOS), Wert des maximalen NDVI (NDVImax), über die Wachstumsperiode integrierter NDVI (NDVIsum) und Tag des maximalen NDVI (maxDOY) wurden über Satellitenbasierten Zeitreihen von MODIS NDVI-Daten abgeschätzt.

Diese Arbeit besteht aus drei Fallstudien in Deutschland, die unterschiedliche Herausforderungen aufgrund der Landbedeckung, des Klimas und der Topographie stellten. Diese Studien wurden durchgeführt mit Flächen nahe Stuttgart (Südwestdeutschland), im Nationalpark Bayerischer Wald und in den bayerischen Alpen. Zusätzlich wurden verschiedene Methoden zur Glättung und Gewinnung von phänologischen Kennzahlen diskutiert. Die aus phänologischen fernerkundlichen Daten abgeleiteten Kennzahlen wurden mit phänologischen Bodenbeobachtungen und LiDAR-Beobachtungen validiert. Es zeigte sich, dass die frühesten phänologischen Phasen, wie erste Blätter und Laubaustrieb, sich nur schwer über Satellitendaten erkennen lassen. Im Vergleich mit anderen verfügbaren Techniken lieferte die Kennzahl der 50%-Amplitude zur Abschätzung von LSP-SOS die besten Ergebnisse, um den Laubaustrieb zu erkennen. Eine weitere Analyse ergab, dass die Phänologie neben den klimatischen Antriebsfaktoren von weiteren Einflüssen kontrolliert wird. Es zeigte sich, dass die Homogenität der Landbedeckung oder die Mischung von Laub- und Nadelbäumen innerhalb eines Pixels signifikant die abgeschätzte LSP beeinflusste. Die letzte Fallstudie in den bayerischen Alpen lieferte Hinweise, dass Veränderungen der Höhenabhängigkeit von LSP im alpinen und voralpinen Bereich hauptsächlich durch Winter- und Frühjahrestemperaturen ausgelöst werden.

1 Table of Contents

1. Introduction

Phenology, the study of annual recurring events in the life cycle of living organisms has been well documented (Schwartz, 2003; Zhang et al., 2012). The cyclic events of leaf unfolding, flowering, fruiting and leaf-fall, etc. of plants (i.e. the primary producers) influence ecosystem productivity, succession and migration of species (Pettorelli et al., 2017). These events are primarily driven by temperature and other meteorological parameters and hence are also affected by climate change (Menzel and Fabian, 1999; Parmesan and Yohe, 2003). Diez et al. (2012) showed the varied responses to climate change across different spatial scales and levels of organisation (Figure 1). In the context of the already established climate driven phenology of organisms and the implications of future climate change on the timing of key phases, very little justification is needed for more intensive efforts in studying of phenology for understanding its changing patterns and drivers (Chang et al., 2017; Cleland et al., 2007; Garonna et al., 2018; Ovaskainen et al., 2013). Monitoring of phenology is also important due to the species specific responses to similar climatic drivers (Basler and Körner, 2014), which may lead to desynchronisation of interaction among species and consequent loss of biodiversity (Burgess et al., 2018; Visser et al., 1998). For e.g. across the trophic levels, shifts in plant phenology could lead to mismatches in food availability and peak species abundance leading to decoupling of the food web phenology. Therefore, a comprehensive understanding of the spatial and temporal variability of phenology is essential to develop strategies for adaptation to and mitigation of risks of climate change (Doi et al., 2008; Thackeray et al., 2016).

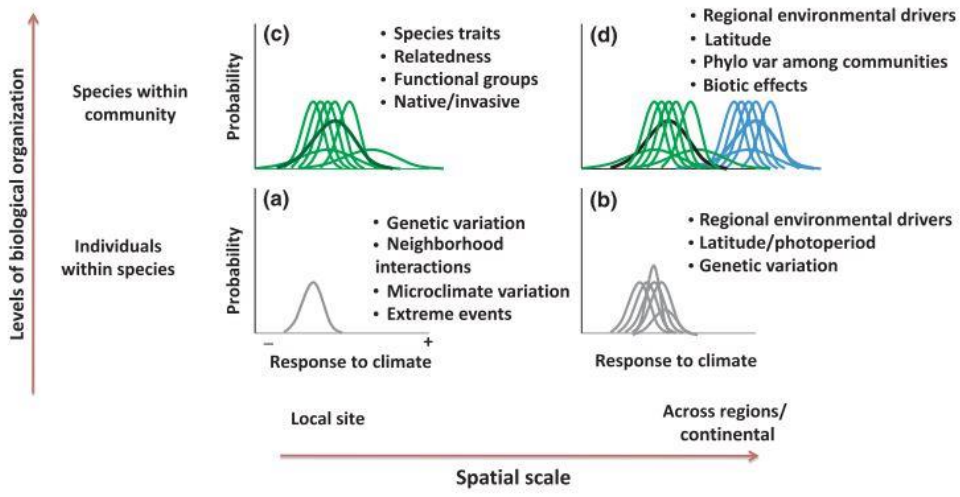

Figure 1. A conceptual diagram of species' responses to climate change at various levels of organisation and scales (source: Diez et al., 2012).

1.1 History of phenology

Traditionally phenology has been observed by volunteers who traverse a fixed path periodically and record key phases in the life cycle of both plants and animals. The oldest evidences of phenological records have been found in the early civilisations of Egypt, Mesopotamia and China (Schwartz, 2003). It was probably after Carl Linnaeus in the end of eighteenth century that phenology was studied systematically as a science and the first survey networks of phenology were established around the globe (Giovanna, 2007). An example of an early phenological record by Carl Linnaeus is shown in Figure 2. Some of the best known phenological records are hundreds of years old i.e. the Japanese cherry blossoms of the 9th century, the grape harvest dates of central Europe from the 1300s and the 200 year old Marsham phenological records from the UK (Chuine et al., 2004; Nagai et al., 2016; Sparks and Carey, 1995). Such long term records of phenology are important works of history documenting distribution and the life cycles of plants, animals and agricultural systems, and also provide critical clues to the climate of the past (Chuine et al., 2004; Sparks and Carey, 1995).

Many global and regional phenological networks such as the National Phenological Network in the USA (USA-NPN), International Phenological Gardens (IPG) in Europe and the camera based Japanese Phenological Eyes Network (PEN) among several others are operating currently and continue to provide information on phenology of plants (Zhang et al., 2012). A comprehensive list of phenological networks is available at the website of Potsdam Institute for Climate Research (http://www.pik-potsdam.de/~rachimow/epn/html/frameok.html). The earliness in the timing of spring events in Europe and North America (Diez et al., 2012; Walther et al., 2002), the extension of growing season in Europe (Menzel and Fabian, 1999), decrease in elevational rates of phenology in central Europe (Vandvik et al., 2018; Vitasse et al., 2017), increased biodiversity and shifting treelines in the higher latitudes (Kullman, 2010; Leonelli et al., 2011) and asynchrony in community level phenology (Ovaskainen et al., 2013; Visser et al., 1998) are few of the climate change induced anomalies observed in ground phenology records and confirmed by satellite remote sensing. In view of the climate induced changes in phenology and also the feedbacks of phenology on climate, observing phenological phases that started as a pastime for naturalists has now therefore become a critical yardstick for studying the global climate change process (Menzel, 2002; Peñuelas, 2009; Richardson et al., 2013).

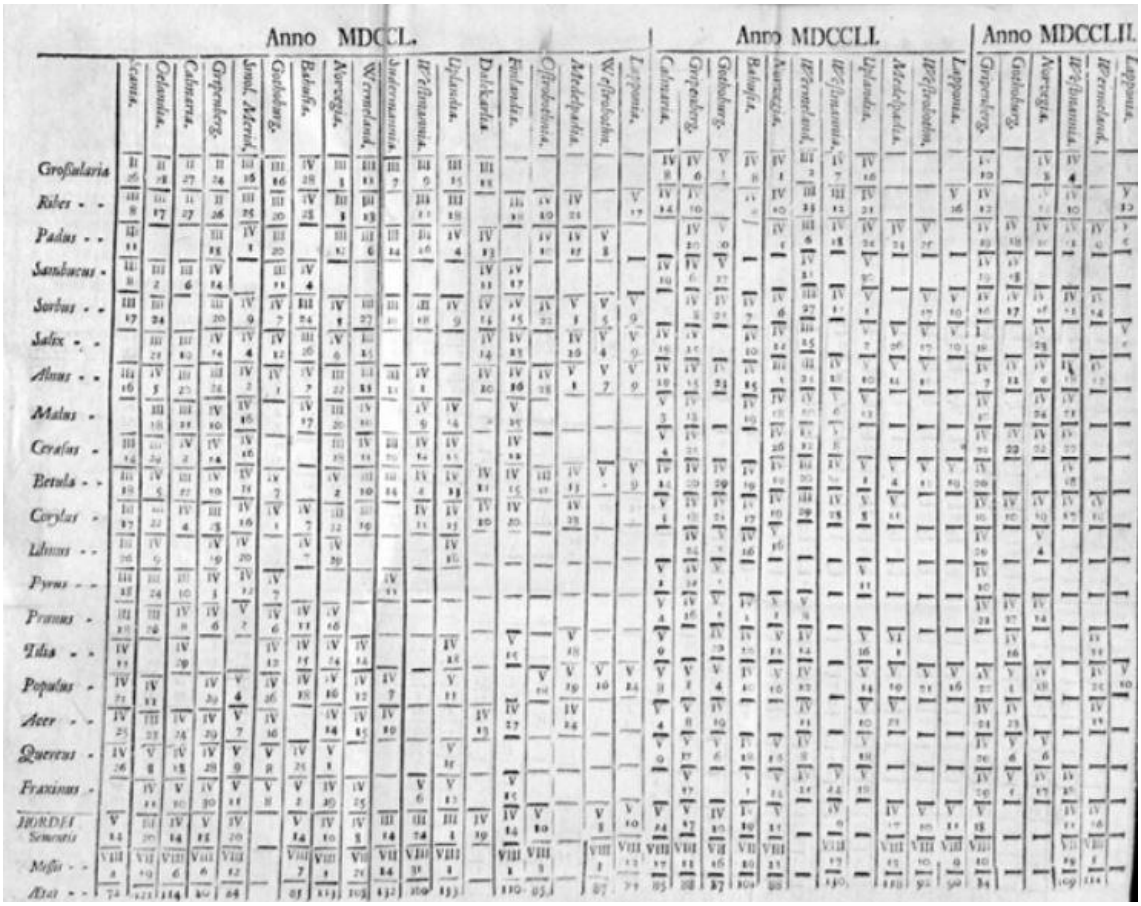

Figure 2. Carl Linnaeus' record of phenological timings of few common trees and shrubs in Northern Europe during 1750-1752 (source: Giovanna, 2007).

1.2 Remote sensing of phenology

Remotely sensed data from space-borne satellite platforms provide periodic information on the earth's surface and its atmosphere. The revolution in earth observation satellites for imaging of the earth's surface and its natural resources started in 1972 with the launch of the Landsat Mission under the "Project Eros" by the United States of America (Wulder et al., 2019). Subsequently, other satellites such as the SPOT, NOAA-AVHRR, Resoucesat, MODIS and Sentinel among several others were launched that provide a myriad of information about the earth's surface and not limited to mapping of vegetation status, moisture stress, atmospheric components (clouds, aerosols and precipitation), ocean properties, surface temperature, etc. The advent of remote sensing technology provided easy access to high resolution information both in time and space, and are cost-effective in comparison to land based survey methods. The promise of monitoring of vegetation through remote sensing was first recognised in the early 1970s when vegetation indices were found to

be well correlated with biomass (Rouse et al., 1974). Later, with the improvement in sensing technologies, several other properties of vegetation such as fractional cover, leaf area index, plant pigments (chlorophyll and carotenoids), etc. could be determined with great precision from satellite sensors (Frampton et al., 2013; Glenn et al., 2008; Verger et al., 2016).

The Normalised Difference Vegetation Index (NDVI) is the preferred and most commonly used measure among several vegetation indices that were developed over time (Helman, 2018). It is the ratio of the difference and the sum of the reflectance of an object in the near infra-red and red region of the spectrum. Its values ranges from -1 and +1, and helps exploiting the fact that green vegetation reflects strongly in the near infra-red and absorbs in the red region (Glenn et al., 2008). The vegetation spectral response curve in shown in Figure 3. NDVI is easy to calculate and is directly correlated to properties such as carbon assimilation, photosynthetic activity and plant transpiration (Glenn et al., 2008). Temporal NDVI data is known to be sensitive to seasonal changes in vegetation and have also been used to study effects of extreme events and pest infestation, map species abundance (Berner et al., 2011; Pettorelli et al., 2005; Spruce et al., 2011), and identify species based on their unique phenology (Clerici et al., 2012; Massey et al., 2017).

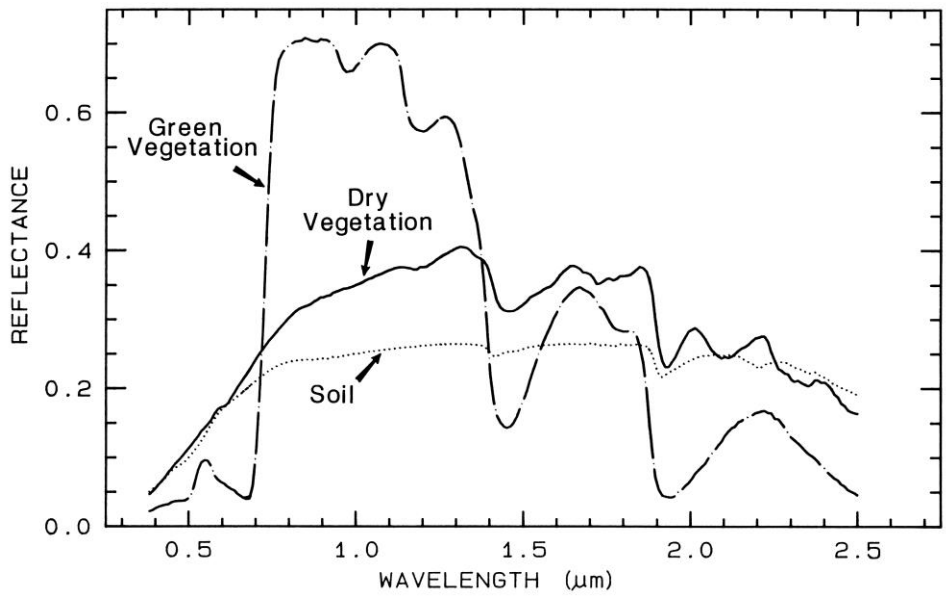

Figure 3. The spectral response curve of vegetation and soil (source: Clark, 1999). The contrasting near infra-red reflectance of the green and dry (stressed) vegetation is clear. The chlorophyll present in the green vegetation also leads to strong absorption in the visible range of the spectrum.

In addition to conventional space based platforms, several near surface measuring techniques such as fixed digital cameras or phenocams and drone mounted cameras have also emerged in the past decade that work with the same principle of repeated photography of land surface and help in monitoring of vegetation phenology at multiple scales (Browning et al., 2017; Klosterman and Richardson, 2017). Figure 4 is a vivid representation of capturing vegetation phenology through different remote sensing platforms (drones or UAV are not shown in the picture). Recently, Hufkens et al. (2019) demonstrated the suitability of inexpensive smartphones in close range monitoring of crop phenology in India. Data from remote sensing platforms have been able to provide critical insights into vegetation performance and ecosystem functioning in response to biotic and abiotic triggers that aid developing strategies for adaptation and policy measures (Foster et al., 2019; Heumann et al., 2007; Ma et al., 2015). Some studies demonstrating advancements in the science of remote sensing of vegetation phenology or land surface phenology (LSP) are listed in Table 1.

Figure 4. Remote sensing of vegetation phenology through various platforms. (Source: Bennet and Hope, 2018)

Table1. Few major developments in land surface phenology studies.

S/No.	Findings	Data	Time period	Author
1)	Measures of central tendency, variability of phenological measures (timing of key events) and the NDVI value at key phases estimated from time series NDVI data over coterminous USA corresponded well with the observed phenology of grasslands, deciduous and conifer forests, and spring wheat.	AVHRR (1 km and 14 day maximum value composite or MVC)	1989-1992	(Reed et al., 1994)
2)	Increased seasonal amplitude of NDVI and lengthening of the growing season in the northern hemisphere.	NOAA-GIMMS NDVI (8km and monthly averaged values)	1981-1991	(Myneni et al., 1997)
3)	Integrated seasonal NDVI (I-NDVI) provided a good estimate of biomass in the semi-arid and arid regions of Australia and correlated well with rainfall patterns.	AVHRR-GIMMS (14 day MVC)	1992-1999	(Holm et al., 2003)
4)	An advance in spring and delay in autumn timings globally. Phenological timings were highly correlated with climatic indices based on ocean currents and sea surface temperature.	AVHRR-GIMMS (8 km and 15 MVC)	1981-2003	(Julien and Sobrino, 2009)
5)	Apart from elevation, distance to urban land cover was found to strongly influence phenological timing of vegetation near Baltimore and Washington cities in the USA. Green down in summer was found to affect estimates of autumn onset in the study area.	Landsat TM and ETM+ data (16 day and 30m resolution) Phenocam data based greenness and redness (2004-2008; daily data)	1983-2008	(Elmore et al., 2012)
6)	Vegetation phenology in semi-arid regions in South-eastern Australia showed higher sensitivity to climate anomalies. Years with	MODIS EVI (16 days and 0.05 degree) and Standardized Precipitation	2000-2014	(Ma et al., 2015)

	extreme droughts revealed a complete loss of vegetation seasonality.	Evaporation Index or SPEI (3 month interval and 0.05 degree)		
7)	Phenocam based greenness was able detect the invasive mesquite shrub phenology better than satellite based NDVI which tracked the dominant native grassland species seasonality. This study validates the reliability of phenocams in bridging the gap in observations from field and space.	Digital camera (20m from horizontal and capturing images every 15 mins from 10:00 to 16:00 hrs) and MODIS NDVI (250m and 16 day interval)	2012-2016	(Browning et al., 2017)
8)	Drone based repeated imaging at mixed forest sites in Harvard forest, USA revealed species specific differences in phenology. Greenness and redness based indices from the drone mounted camera correlated strongly with field observations of start and end of season. Few Oak trees displayed redness at leaf out which had to be processed accordingly.	Drone mounted digital camera (16MP, flight frequency- 5days during leaf out and weekly during leaf colouring).	2015	(Klosterman and Richardson, 2017)
9)	SOS, peak and EOS obtained from high temporal and spatial resolution Sentinel 2 data were strongly linked to phenological metrics estimates from close range cameras in the Netherlands.	Green colour coordinate or GCC from Sentinel 2 data (10 m spatial and 5 day temporal resolution)	2016	(Vrieling et al., 2018)

Review of literature provide evidence of increased interest in plant phenology with almost a 10 times growth in peer-reviewed articles on the topic in the last 30 years (Tang et al., 2016). This renewed interest in plant phenology is mainly due to the debate around the global climate change, especially after the 1990s, and the ability of plant phenology to track such changes in climate (Richardson et al., 2013). This has led to enhanced curiosity in the performance of pioneer techniques such as remote sensing for improving monitoring of phenology at multiple temporal and spatial scales. Processing of remote sensing data however requires high expertise and skills in data and image processing, which could prove to be a

hindrance in the further advancement of this field. But confidence can be drawn from the fact that the scientific community in last decade has developed several open source software and packages that help now help in processing time series remote sensing data. TIMESAT (Jönsson and Eklundh, 2004), Phenopix (Filippa et al., 2016), green-brown (Forkel et al., 2013), Phenor (Hufkens et al., 2018) and nnphen (Estay and Chavez, 2018) are few such noteworthy packages and software. However, caution must be exercised while using these packages and their appropriateness and accuracy must be tested before being used for specific studies. The existence of several free to use remote sensing data (i.e. Landsat, AVHRR, MODIS, etc.) and open source software provides an incredible opportunity to critically study the various drivers of Land Surface Phenology (LSP) that were non-existent in the past.

Despite huge advancements in sensor technologies and data processing techniques, remote sensing of phenology has its own limitations. Several studies have discussed the limitations of remote sensing data and suggested solutions to overcome those. Most notably the processing of raw satellite data is crucial in time series analysis of LSP and so are the choice of methods adopted that are known to affect conclusions derived from studies (Jönsson and Eklundh, 2004). Since no single method can be claimed to address all the issues with data processing sufficiently and applied to all case studies equally, it is pertinent that such decisions are based on the characteristics of the data and area under study (Cai et al., 2017; Hufkens et al., 2019).

The versatility of LSP in revealing various aspects of ecosystem functioning and its performances is evident from the case studies carried out as part of this thesis and Table 1, however utmost care should be taken to ensure high quality of data used in such studies to generate high confidence in the results. For example, divergent effects of droughts on the Amazon forests were reported during the droughts of 2005 and 2010. The greening of the Amazon in 2005 as reported by Saleska et al., (2007) and the decreased greenness of forests in 2010 as concluded by Xu et al., (2011) cannot be attributed to droughts alone. Quality of data in form of gaps in the time series of vegetation indices and sensor degradation (Atkinson et al., 2011; Samanta et al., 2010), and other climatic factors such as clouds, aerosols and variability in the received solar radiation are also known to influence data and introduce errors (Saleska et al., 2007).

The inability of coarse resolution satellite data to discriminate among individual species is another major hindrance in fruitfully deriving conclusions from LSP based studies (Panchen

et al., 2015). Fu et al., (2014) reported a reversal of the advancing trends in spring phenology in Western Central Europe post year 2000. The delayed trends in LSP were probably driven by a combination of the inability of satellite data to discriminate between species and the delay in the SOS of earliest species that are affected by cooling in late winter. In contrast, the ground observed phenology revealed an advancing but weakened trend in the spring phases of species during the same period. Most importantly, issues concerned with matching LSP with ground phenology or GP arise due to the absence of attribution of a biological meaning to the various methods of estimating phenology from remote sensing data i.e. LSP (Eklundh and Jonsson, 2015). As stated earlier, an arbitrary selection from a myriad of methods available for estimating LSP can complicate matters when comparing LSP with GP observations. Therefore, it is essential to carefully chose pre-processing methods and the framework for analysing data to minimise errors and uncertainties in results.

2. Aims and outline of the thesis

This thesis aims to better understand the process of estimating phenology from remote sensing data. The basic premise of the studies carried out in this thesis revolves around a) challenges in pre-processing of data, b) matching pixel based LSP with point based GP observations, and c) interpreting LSP patterns in light of various drivers such as climate, topography and LiDAR based forest stand information.

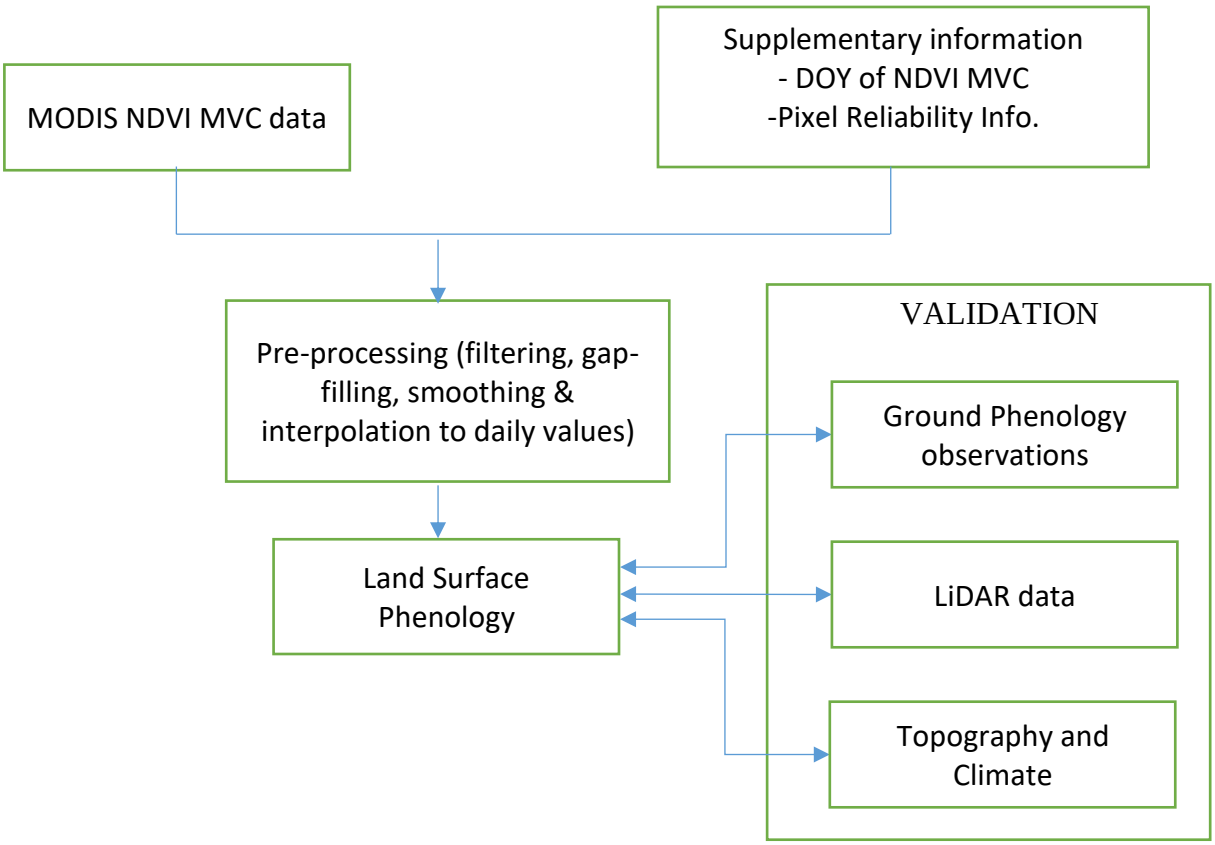

Figure 5. Flowchart depicting the various themes in the case studies undertaken as part of this thesis.

Remote sensing based estimation of phenology (Land Surface Phenology or LSP) provides promising alternatives to time consuming, labour intensive and localised ground based observations (Ground Phenology or GP) of phenological phases. Though various methods of extracting phenological information from time series of remote sensing data have been studied in detail (Beck et al., 2006; Forkel et al., 2015; Ivits et al., 2013; White et al., 2009), there still lack successful efforts in the temporal matching of LSP estimates with GP

observations. Chapter 4.1 of this thesis deals with extraction of various start of season (SOS) estimates of LSP and correlating it temporally with observed dates of GP-SOS of several understory, broadleaf and conifer species. Chapter 4.1 also discusses the challenges in the pre-processing of raw NDVI times series data and subsequently the problems faced in matching pixel based LSP estimates with species specific GP observations. The central aim of the study in this chapter was to test whether different LSP-SOS metrics correspond to specific GP-SOS observations, and if the GP-SOS observations match with the LSP-SOS in terms of their long term trends, mean values and interannual variability.

Apart from the influence of pre-processing of remotely sensed NDVI data, the LSP at the pixel level is also affected by several other drivers. The validation of pixel based LSP following segregation of pixels using popular land cover maps such as CORINE and GlobeCover, etc. and its matching with GP observations of dominant species on the ground is commonly advocated (Hamunyela et al., 2013; Rodriguez-Galiano et al., 2015). However, as completely homogenous pixels are rarely found in nature, it is important to consider the accuracy of such land cover maps and subpixel mixing of classes to correctly interpret the meaning of the LSP metrics estimated from a pixel. In absence of high resolution or sub-pixel information, it is difficult to ascribe the variability in the estimated LSP to climate alone. Therefore, the role of subpixel information on forest stands in driving the spatial variability in mean LSP metrics is discussed in chapter 4.2. The advantage of using LiDAR data to include subpixel information on forest stand with respect to percentages of broadleaf and conifer species, crown volume and Shannon's entropy helped in studying the variability observed in LSP metrics, which is not otherwise discernible through coarse resolution remote sensing data. The neglected end of season (EOS) metric along with several other phenological measures are also discussed in this chapter.

Climate change is known to have differential effects on the phenology of different plant species. Moreover, there are now evidences for the weakening of the widely accepted Hopkin's bioclimatic law dealing with the elevation linked lapse rates of leaf out in trees (Vitasse et al., 2017). In such a situation, not only long term climate change impacts but also the inter-annual or seasonal temperature patterns need to be investigated for their role in affecting vegetation phenology. Chapter 4.3 discusses the role of spring and winter temperatures in driving variability in elevation linked lapse rates of vegetation phenology in the pre-Alpine and Alpine regions of Bavaria. A synopsis of results from remote sensing and

ground observations-based phenology and their elevational lapse rates is also presented in the chapter.

The succeeding sections of this thesis contain description of the data and complete methodology followed for three studies (two individual accepted publications and one case study to be submitted). Also listed are the abstracts of the three studies in the subsections of chapter 4. A short description of the results of the and their implications are also presented in chapter 5. The reprints of the published articles and the case study (to be submitted) is attached at the end of this thesis.

3. Data and Methods

3.1 Data used

The data used in this thesis have been described in detailed in the two individual publications and one case study (to be submitted). However, a brief overview of the data and its sources are listed in this section as below.

3.1.1. Satellite remote sensing based NDVI data

The 16-day maximum value composite (MVC) Normalised Difference Vegetation Index (NDVI) data (MOD13Q1) and its corresponding pixel reliability information for the years 2001-2013 (used in chapter 4.1) was downloaded from the now retired MRTweb application (https://lpdaac.usgs.gov/tools/modis_reprojection_tool) of the United State Geological Survey (USGS) website. This data can now be downloaded from the AppEARS portal of USGS (https://lpdaacsvc.cr.usgs.gov/appeears/).

A 4-day MVC NDVI data along with its respective pixel quality and exact day of the year for the composites were accessed from EURAC, Bolzano (Asam et al., 2018) for use in chapter 4.2 and 4.3. This 4-day MVC product was derived from the daily MOD09GQ product collection 6 and use in conjunction with MOD09GA product for constraints on quality and viewing geometry of the pixels. The NDVI measure was calculated from the red and near infra-red bands of the of the satellite product. The details of this NDVI product are discussed in detail in Misra et al. (2018) and Asam et al. (2018).

3.1.2. LiDAR based forest stand data

A LiDAR based spatial points data frame was obtained from the Bavarian Forest National Park (BFNP) administration. The LiDAR data is based on an aerial survey carried out in June 2012 using a Riegl LMS-680i scanner under leaf-on conditions at a height of 650 m with a density of 30 points/m^2. The database contained structural information of individual trees (i.e. tree type, crown volume, height, species type (conifer or broadleaf), etc.) in the BFNP, which was later resampled and rasterized to 250 m grids for comparison with MODIS pixels. Several aggregated measures of forest stand characteristics were calculated (in chapter 4.2) such as average tree height, average crown volume, average crown area, broadleaf %, conifer

% and Shannon's entropy for comparison with MODIS based phenology. The LiDAR data used in chapter 4.2 is described in detail in Misra et al. (2018).

3.1.3. Topography data

The digital elevation model at a spatial resolution of 30 metres was downloaded from the Shuttle Radar Topography Mission (SRTM) data available through the earthexplorer portal of the United State Geological Survey website (USGS, 2018) for use in chapter 4.3. The digital terrain model (DTM) used in chapter 4.2 from the LiDAR survey of the Bavaria Forest National Park (BFNP) was obtained from the BFNP at 1-meter resolution and was resampled to 250 metres. The slope and aspect were calculated from the LiDAR- DTM using the terrain function available in raster package of R (Hijmans, 2016).

3.1.4. Land cover maps

The CORINE (COoRdination of INformation on the Environment) land cover maps used in for chapters 4.1, 4.2 and 4.3 were downloaded from the Copernicus Land Monitoring Service of the European Environment Agency (EEA, 2012). The land cover maps were downloaded in raster format at a spatial resolution of 250 meters for the year 2012, and consist of land cover classes such as broadleaf, conifer, mixed forests, pasture, urban areas, transitional woodlands, arable land and water bodies. The classes in the land cover map were used as such in chapter 4.2, and aggregated to forested (broadleaf, conifer and mixed forests) and non-forested areas in chapter 4.3 and masked for broadleaf forests in chapter 4.1.

A habitat map generated was also obtained from the BFNP administration. This land cover map used in chapter 4.2 was generated by visual interpretation of digital colour infra-red images from a DMC camera in the year 2012. The habitat map consists of various land cover classes such as urban areas, broadleaf, conifer and mixed forests, clear-cut areas, water, dead-wood lying and regenerating areas. Further details of the habitat map is available in Dupke et al., (2017).

3.1.5. Ground phenology data

The ground phenology data used in chapter 4.1 was obtained from a dedicated naturalist who previously worked at the German Meteorological Service (DWD) for decades. He provided

records of phenological phases of several broadleaf, conifer and understory species present around a single site near Stuttgart, Germany, covering a transect of 8-10 km in the surrounding woods and agricultural areas (48.73°N/9.26°E, 410 m a.s.l). The dates of leaf unfolding and leaf greening of several species for years 2001- 2013 were used in this study. Further details of species and their phenophases are provided in the supplementary information of Misra et al. (2016).

The International Phenological Gardens (IPG, n.d.) and the German Meteorological Service (DWD) monitor phenological phases of species through a network of stations in Germany. The ground phenological data for the BFNP used in chapter 4.2 was collected at IPG station Freyung Waldhaeuser (956 m a.sl.), and DWD stations Neureichenau (770m a.sl.), Schönbrunn (775m a.s.l.) and Großer Arber (1436 m a.s.l.). The dates of leaf unfolding and leaf fall of broadleaf species i.e. mountain ash (*Sorbus aucuparia* L.) and European beech (*Fagus sylvatica* L.), and the may shoot dates for conifer species i.e. Norway spruce (*Picea abies* L.) were collected for the years 2002-2015.

Gridded phenological information from DWD for the years 2001-2016 were used for validation of MODIS based phenological data in chapter 4.3. The grids for start of season (leaf unfolding) and end of season (i.e. leaf colouring and leaf fall) for European beech trees were downloaded from the Climate Date Center web portal of the German Meteorological Service (DWD, n.d.). These DWD annual gridded values at 1km x 1 km resolution are a result of spatial interpolation of species and site specific phenological phases reported by observers (as day of the year or DOY). The spatial interpolation of these values are based on latitude, longitude, height and weighted by distance to four nearest observations (DWD, n.d.).

3.2 Methods of processing and analysis of data

This section describes the methods used in pre-processing of remote sensing data and the various statistical methods used for modelling and validation with ground phenological observations.

3.2.1 Pre-processing of NDVI data

Remote sensing data in the form of Normalised Difference Vegetation Index (NDVI) was used for various case studies carried out in this thesis. The NDVI data available as maximum

value composites (MVC) were first stacked in chronological order. However, they could not be used in their available form and required special treatment before extraction of different phenological metrics. Satellite based remote sensing data are many times contaminated by atmospheric components such as clouds, rain, snow, aerosols, etc., and such errors or contamination in observations were identified and accounted for before any further analysis of time series of NDVI data. The complimentary pixel reliability information obtained along with the NDVI MVC data were used in this regard and pixels with only high confidence (pixels labelled as good or marginal) were retained.

The gaps introduced in the NDVI data due to removal of outliers were then filled in two steps: a) gaps occurring in the winter period (January and December) of the NDVI times series were filled with averages of available high confidence values from the same period in other years and b) linear interpolation of the remaining gaps (in non-winter period). Another round of outlier detection in the NDVI values was necessary after the removal of outliers and the subsequent filling of gaps. Such outliers were present as sudden spikes in time series of NDVI data (assuming NDVI profile of vegetation to follow a gradual rate of increase or decrease) and hence needed further attention. A Gaussian filter was applied twice to the NDVI time series: (1) in the first instance to detect high differences (values beyond two standard deviations) in NDVI values in comparison to its neighbouring values and such values were subsequently removed and replaced with the average of nearest available values, and (2) a second time to obtain a smooth NDVI times series that would represent the smooth and gradual transition of values over the growing season of vegetation. In chapter 4.1, the NDVI time series was alternatively fitted with a Double Logistic function after the initial Gaussian smoothing to compare the performance of two different smoothing approaches. The NDVI MVC data was then set to their day of year (from the ancillary information layer) and linearly interpolated to daily values.

The Gaussian function used in the case studies in this thesis was so designed that the weights (W_i) of the of each value within a window followed a Gaussian distribution (see equation 1). These fractional weights were distributed symmetrically around the central value.

$$W_i = \left({}^{1}\!/_{0.5 * k * \sqrt{\pi}}\right) * exp * \left({}^{w_i^2}\!/_{(0.5 * k)^2}\right) \ldots\ldots\ldots\ldots\ldots\ldots \text{(equation 1)}$$

where, k is the half window size of the filter and w_i is the i^{th} value in the local window of sequence –k to k. The weight W_i was normalised by its sum to add to 1. The pre-processing and smoothing of NDVI data are explained in detail in Misra et al. (2016).

Instead of using the readily available 16 day NDVI MVC (MOD13Q1) data, a 4 day NDVI MVC data was used in chapters 4.2 and 4.3 of this thesis. This 4 day NDVI time series data was generated from MOD09GA and MOD09GQ reflectance products of the MODIS sensor. The NDVI values were calculated from the red and near infra-red bands and were filtered according to geometry information (sun and senor zenith angles) and scene acquisition quality flags. This NDVI product was obtained from the Institute for Earth Observation, EURAC, Italy and the methods are explained in detail in Asam et al. (2018). A similar pre-processing algorithm as in chapter 4.1 for outlier detection, gap filling, smoothing and interpolation was applied to this 4-day NDVI MVC product.

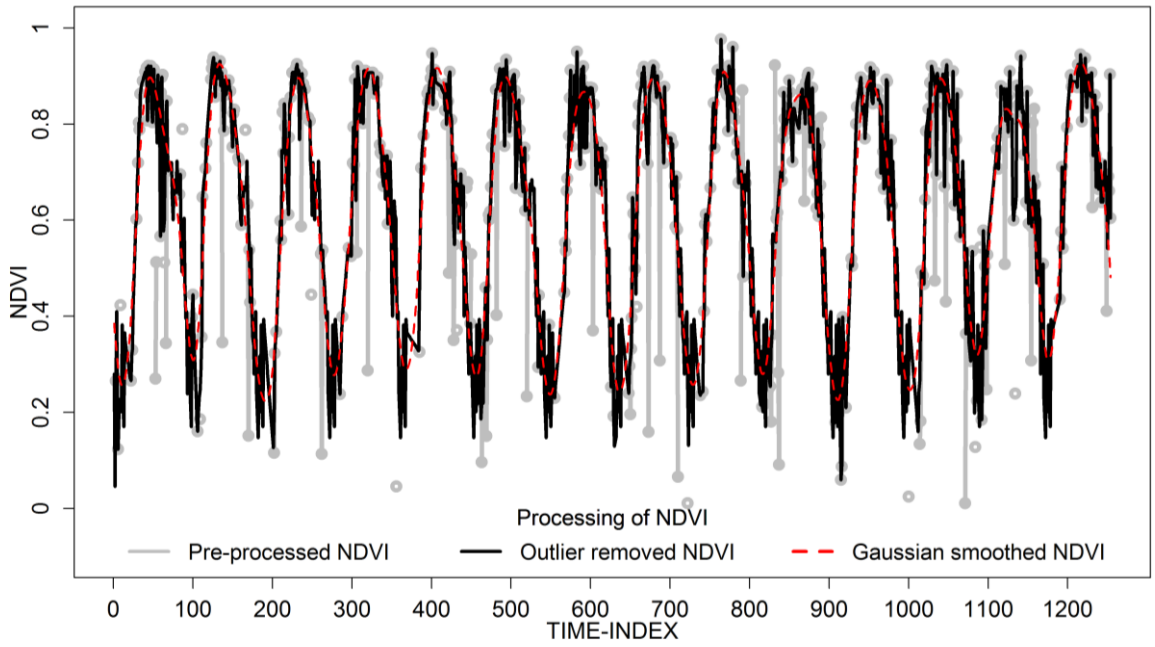

Figure 5. Example of pre-processing and smoothing of raw NDVI (time series) from a pixel. Note: The raw NDVI values are shown as circles, the good and marginal NDVI values (using the pixel reliability information) are shown as grey lines, the outlier removed and gap filled values are shown as black lines, and the Gaussian filtered NDVI time series is shown as a dashed red line.

3.2.2 Extraction of phenological information (Land Surface Phenology) from NDVI time series

The pre-processed daily NDVI time series data was used to extract several phenological metrics (land surface phenology or LSP). In chapter 4.1 various thresholds based start of season (SOS) were computed from the NDVI time series by determining the time period when the increasing curve of NDVI values reached the 20%, 50%, 60% and 75% of the seasonal amplitude. Similarly, a derivative (first, second and third derivatives) based SOS was also calculated for determining the time of greatest rate of change occurring in the growing or greening phase of the NDVI profile. Additionally, a delayed moving average (DMA) method of estimating phenology was also evaluated. Subsequently, in chapters 4.2 and 4.3, the SOS and EOS (by determining the time period when the receding curve of NDVI profile reached the 50% of the seasonal amplitude) were calculated using the 50% amplitude method for its robustness in terms of its application to a variety of ecosystems (Hamunyela et al., 2013; Wang et al., 2016; White et al., 2009, 1997). Apart from calculating the SOS and EOS, several other phenological metrics such as DOYmax (day of maximum NDVI value), NDVImax (the maximum NDVI value), NDVIsum (NDVI values integrated over the growing season) and length of season or LOS (difference between annual EOS and SOS) were calculated in chapter 4.2.

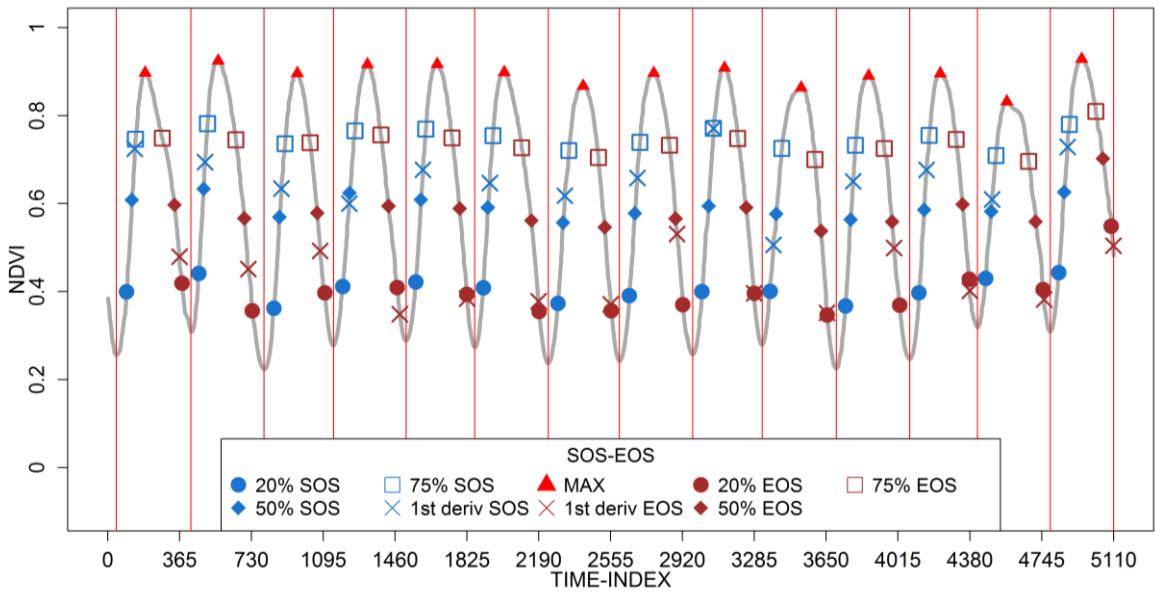

Figure 6. Estimation of different LSP metrics from the smoothed and daily interpolated times series of a pixel.

3.2.3 Validation of Land Surface Phenology

To begin with, in chapter 4.1, the validation of the different LSP metrics was carried out through a measure of Spearman's rank correlation strength with observer reported dates of different phenological phases (ground phenology or GP) to check for their match in inter-annual variations. For this purpose, annual LSP-SOS calculated from threshold and derivative based approaches were compared with the annual GP records of leaf unfolding of several common understory and conifer species, and leaf unfolding and greening of broadleaf species found at the study site. A comparison of means and trends of LSP and GP was undertaken to assess the match in seasonality and climate change impacts respectively.

In chapter 4.2, the match between annual phenology of LSP and GP were evaluated. The LSP were first segregated for broadleaf and conifers using the land cover map and their correlation strength with GP i.e. leaf unfolding and fall for broadleaf and conifer species was analysed. Additionally, the drivers of spatial variability of mean LSP metrics were evaluated with respect to LiDAR based topography (slope, aspect and elevation) and forest stand characteristics (broadleaf%, conifer%, average crown volume, average height, Shannon's entropy, etc.). First the predictors were subjected to a variance inflation factor (VIF) analysis and variables with VIF> 10 were removed from further analysis. Additionally, a non-parametric Kruskal-Wallis test followed by a posthoc Dunn's test was conducted to test whether different land cover types reveal significant differences in their LSP. The uncorrelated predictors were then applied to a stepwise multiple regression analysis to predict various LSP metrics. As an initial model, multiple regressions were run on mean LSP metrics as response and topography variables as predictors respectively. Subsequently, additional predictors in form of land cover information and LiDAR based forest stand information were included to evaluate improvements in the explained variance of models. A stepwise BIC function (stepAIC function from MASS package in R) (Venables et al., 2002) was applied to the different models in order to select the predictors resulting in minimum BIC. Subsequently, the relative importance of the predictors in the selected best models were also calculated (from calc.relimp function in relaimpo package in R) (Grömping, 2006). A bootstrapping analyses of all modelled parameters as described in Buras et al., (2017) was also carried out to evaluate stability of the models.

In chapter 4.3, the elevation linked lapse rates of MODIS based LSP-SOS and EOS were calculated using a bootstrapping analysis. The LSP-SOS and EOS dates of pre-Alpine and Alpine regions in Bavaria were sampled separately for each year from 2001-2016. The slope from a linear regression analysis of LSP with elevation was calculated over 1000 iterations. The different years from 2001-2016 were then analysed for their mean spring and winter temperatures and classified in to four groups of warmest and coldest seasons. These calculated slopes were then grouped into their location (Alpine and pre-Alpine) and the years grouped according to their spring-winter temperatures. A Kruskal-Wallis test followed by a posthoc Dunn's test was then conducted to test for differences in the groups for the elevational linked lapse rates of LSP. The ground phenology observations of leaf unfolding and leaf colouring/ fall obtained in the form of gridded datasets from the German Meteorological Sevice (DWD) were used to validate both the distribution of annual LSP-SOS and EOS values and their elevational rates.

3.2.4 Software and tools used

All data handling, pre-processing, analysis and plotting of figure in the above mentioned case studies were carried out in the R statistical programming environment (Core Team, 2014). The ArcGIS and ERDAS Imagine software were also used for preliminary exploration and visualisation of spatial data.

4. Abstracts of individual publications

4.1 Effects of different methods on the comparison between Land Surface and Ground Phenology - A methodological case study from South-Western Germany

Gourav Misra, Allan Buras & Annette Menzel. *Remote Sens. 8, 753* (2016). doi: 10.3390/rs8090753

Several methods exist for extracting plant phenological information from time series of satellite data. However, there have been only a few successful attempts to temporarily match satellite observations (Land Surface Phenology or LSP) with ground based phenological observations (Ground Phenology or GP). The classical pixel to point matching problem along with the temporal and spatial resolution of remote sensing data are some of the many issues encountered. In this study, MODIS-sensor's Normalised Difference Vegetation Index (NDVI) time series data were smoothed using two filtering techniques for comparison. Several start of season (SOS) methods established in the literature, namely thresholds of amplitude, derivatives and delayed moving average, were tested for determination of LSP-SOS for broadleaf forests at a site in southwestern Germany using 2001–2013 time series of NDVI data. The different LSP-SOS estimates when compared with species-rich GP dataset revealed that different LSP-SOS extraction methods agree better with specific phases of GP, and the choice of data processing or smoothing strongly affects the LSP-SOS extracted. LSP methods mirroring late SOS dates, i.e., 75% amplitude and 1st derivative, indicated a better match in means and trends, and high, significant correlations of up to 0.7 with leaf unfolding and greening of late understory and broadleaf tree species. GP-SOS of early understory leaf unfolding partly were significantly correlated with earlier detecting LSP-SOS, i.e., 20% amplitude and 3rd derivative. Early understory SOS were, however, more difficult to detect from NDVI due to the lack of a high resolution land cover information.

Contributions: The study was conceptualized and designed by me and Annette Menzel. I wrote the manuscript and carried out the data processing with support from Allan Buras. All authors contributed to the interpretation of results and editing of the manuscript. About 70% of the work was done by me.

4.2 LiDAR derived topography and forest stand characteristics largely explain the spatial variability observed in MODIS land surface phenology

Gourav Misra, Allan Buras, Marco Heurich, Sarah Asam & Annette Menzel. *Remote Sens. Environ. 218, 231–244* (2018). doi: 10.1016/j.rse.2018.09.027

In the past, studies have successfully identified climatic controls on the temporal variability of the land surface phenology (LSP). Yet we lack a deeper understanding of the spatial variability observed in LSP within a land cover type and the factors that control it. Here we make use of a high resolution LiDAR based dataset to study the effect of subpixel forest stand characteristics on the spatial variability of LSP metrics based on MODIS NDVI. Multiple linear regression techniques (MLR) were applied on forest stand information and topography derived from LiDAR as well as land cover information (i.e. CORINE and proprietary habitat maps for the year 2012) to predict average LSP metrics of the mountainous Bavarian Forest National Park, Germany. Six different LSP metrics, i.e. start of season (SOS), end of season (EOS), length of season (LOS), NDVI integrated over the growing season (NDVIsum), maximum NDVI value (NDVImax) and day of maximum NDVI (maxDOY) were modelled in this study. It was found that irrespective of the land cover, the mean SOS, LOS and NDVIsum were largely driven by elevation. However, inclusion of detailed forest stand information improved the models considerably. The EOS however was more complex to model, and the subpixel percentage of broadleaf forests and the slope of the terrain were found to be more strongly linked to EOS. The explained variance of the NDVImax improved from 0.45 to 0.71 when additionally considering land cover information, which further improved to 0.84 when including LiDAR based subpixel forest stand characteristics. Since completely homogenous pixels are rare in nature, our results suggest that incorporation of subpixel forest stand information along with land cover type leads to an improved performance of topography based LSP models. The novelty of this study lies in the use of topography, land cover and subpixel vegetation characteristics derived from LiDAR in a stepwise manner with increasing level of complexity, which demonstrates the importance of forest stand information on LSP at the pixel level.

Contributions: The study was conceptualized and designed by me and Annette Menzel. I wrote the manuscript and carried out the data processing and statistical analyses for this study. The raw LiDAR data and raw 4-day composite NDVI data were processed and provided by

Marco Heurich and Sarah Asam respectively. All authors contributed to the interpretation of results and editing of the manuscript. About 80% of the work was done by me.

4.3 Elevation linked phenological lapse rates show differences in the pre-alpine and alpine regions of Bavaria: Overview from ground and satellite observations

Gourav Misra, Sarah Asam & Annette Menzel. (to be submitted to Environmental Research Letters)

The role of temperature in driving phenology of vegetation is well established. However, with the changing climate leading to differences in temperature regimes during the year and especially also during winter chilling, a pronounced variability in the already established phenological rates is now being observed along the elevational gradient of mountains. In this study, we analysed the elevation linked lapse rates of phenological dates in the pre-alpine and alpine regions of the Bavarian Alps in Germany. The dates for the start of season (SOS) and the end of season (EOS) were extracted from a 4-day maximum value composite Moderate Resolution Imaging Spectrometer (MODIS) sensor's Normalised Difference Vegetation Index (NDVI) time series data for the years 2001-2016. Analyses of SOS data showed higher elevational lapse rates in the alpine areas than the pre-alpine areas, possibly due to longer duration of snow. Maximal differences in rates of SOS of alpine and pre-alpine areas were observed in years with preceding warm winters with lack of chilling. Minimum differences in the rates of SOS were found along the elevational gradient during cold spring and cold winter years. The MODIS based SOS showed the highest correspondence when validated against the gridded German Meteorological Service (DWD) leaf unfolding data. The EOS dates showed a comparatively lower correspondence to DWD data and their lapse rates in the pre-alpine and alpine regions were tricky to validate. Contrary to SOS, EOS dates revealed lower, but still positive lapse rate in the alpine areas than the pre-alpine areas.

Contributions: I and Annette Menzel led and conceptualised the design of the study. I wrote the manuscript and carried out the data processing and statistical analyses for this study. The raw 4-day composite NDVI data was processed and provided by Sarah Asam. All authors contributed to the interpretation of results and editing of the manuscript. About 70% of the work was done by me. Special thanks to Dr. Nicole Estrella and Dr. Stefan Haerer for their support in analysing the temperature and DWD data respectively.

5. Discussion

This thesis describes and tests different pre-processing methods for MODIS NDVI data, estimation of various LSP metrics and its interpretation, and its validation with various species-specific GP and LiDAR data. In this chapter a general discussion of the results from two publications and the paper to be submitted is presented.

5.1 Issues and considerations in pre-processing of NDVI data

Pre-processing of data is the first consideration in any study and was predictably crucial in the case studies (two published papers and one to be submitted) carried out as part of this thesis. The methods of pre-processing of data are known to affect LSP estimates (Clerici et al., 2012; White et al., 2009) and hence requires careful consideration of several issues for decision making. To begin with, the decision to use daily or a composited NDVI product is critical in LSP studies. Previous research suggests using satellite data with a temporal resolution not more than the phase of vegetation growth period or phenophase under study (Ahl et al., 2006; Kross et al., 2011; Zhang et al., 2009). In chapters 4.2 and 4.3 of this thesis, a 4 day NDVI MVC product as suggested by Asam et al. 2018 was used. In contrast to the 8 day, bi-weekly or monthly composites, the 4 day MVC aimed at capturing fast occurring changes in the phenology of vegetation and potentially increases the temporal sampling of valid observations that were discarded in the 8 day NDVI MVC. NDVI data with lower compositing periods i.e. less than 8 days and a high quality criteria for data inclusion, may lead to larger data gaps but did not impair subsequent fitting of phenological models and concurrently improved the accuracy of mean NDVI estimates (Asam et al., 2018). Moreover, the use of maximum value composites, especially for MODIS data, helped minimise error in data and also mitigate problems due to the variable daily footprint of MODIS sensor that may lead to inconsistency in spectral signatures (Jin and Sader, 2005; Tan et al., 2006; Xin et al., 2013).

Though the MVC NDVI data consisted of fewer outliers than the daily values and the pixel reliability layer provides indication of contaminated data, there still existed unexplained deviations or outliers in the temporal NDVI profile of the pixels. Existing methods of outlier detection such as from Hamunyela et al., (2013), evaluating the n+1 and n-1 values in time series of data for unusually high deviations or “spikes”, were found to be sub-optimal in our case. NDVI time series with longer durations of unexplained deviations from the normal course of NDVI development had to be removed by using a unique two-step function operating in a larger temporal window as described in Misra et al., (2016). Removal of

outliers in any time series data presents challenges in filling of gaps. The choice of gap filling technique can introduce errors in the time series data and hence must be decided according to the area and subject under study. For example, Beck et al. (2006) filled the winter gaps in high northern latitudes by assuming the NDVI values to be constant (i.e. complete cessation of vegetation activity) between the last and first snow free observation. However, in the case studies carried as part of this thesis, the filling of winter gaps with mean of available winter values from other years was found to provide satisfactory results as suggested by previous studies (Bradley et al., 2007; Clerici et al., 2012). The summer gaps however had to be filled using mean of available neighbouring values in the time series, as filling of gaps in the growing season from other years would have introduced artificial similarity in the annual growing season NDVI values and hence defeated the purpose of studying the impacts of drivers on vegetation phenology. Subsequently, a decision to choose from various existing smoothing functions also had to be made for the smoothing of NDVI data in order to mimic a gradually progressing phenological curve. In chapter, 4.1, a Gaussian function was found to be superior to a double logistic function in modelling both the winter and summer NDVI values. Cai et al., (2017) showed very similar results in their study, where they demonstrated the improved performance of local filtering methods over function fitting methods in smoothing of time series NDVI. The Gaussian algorithm was therefore the preferred choice for outlier detection and smoothing in all the case studies carried out as a part of this thesis.

Remote sensing data such as Landsat and MODIS have associated pixel quality information that helps identify and remove poor quality pixels from time series analyses of data. However, it has been observed that such information alone is not sufficient to completely remove outliers from a data. In such a situation, experiences from the case studies in chapter 4 of this thesis and previous studies (Asam et al., 2018; Tan et al., 2011) suggest use of ancillary information from other sensors or sources that can provide details on meteorological conditions such as snow depth, temperature and cloud cover, etc. and aid in explaining any aberrations in the NDVI time series. Apart from removal of outliers, attention should be given to the choice of gap filling and smoothing functions, ensuring that such choices do not introduce bias into the data.

5.2 Matching LSP with GP

Chapter 4 of this thesis consists of different sections that deal with the validation of LSP estimates with GP observations at various scales i.e. time, space and elevation. Chapter 4.1

examines the challenge in the temporal matching of several LSP-SOS estimates to GP observations. The pixel (LSP) to point (GP) matching of phenology was a major challenge and as suggested by previous studies (Hamunyela et al., 2013; Rodriguez-Galiano et al., 2015) had to be carried out by pairing LSP masked by land cover maps and GP observations of dominant species in the study area. In chapter 4.1, the strong similarities observed in the inter-annual behaviour of different species-specific GP observations indicates serious issues when correlating LSP estimates with GP observations in the absence of a very detailed land cover map. A species level map as generated by Brus et al., (2012) would be best way to validate LSP estimates, however, such maps require considerable efforts and statistical skills. A careful selection of LSP methods for studying and interpreting phenological behaviour is also of utmost importance. Equally high correlation strengths between LSP and GP might be observed at locations (pixels) where GP consist of several species having similar meteorological forcing (Rodriguez-Galiano et al., 2015), and in turn making it difficult to rationally match LSP with all or any of the different species that are reported from a study area. The correlation between inter-annual estimates of LSP and GP also showed different strengths with each different method. The phenology of late understory and broadleaf species revealed a strong match in their inter-annual behaviour. Results from chapter 4.1 suggest the use of 20% amplitude and 3rd derivative that best correspond with leaf unfolding of early understory species, and 75% amplitude and 1st derivative to detect broadleaf SOS (greening). In contrast to Nagai et al. (2010) analyses in chapter 4.1 demonstrate the limitation of an overall threshold (of an absolute NDVI value) in detecting species specific differences in phenology.

The results of from chapter 4.1 corroborates the findings of previous studies that suggest attributing specific LSP methods to specific GP (Eklundh and Jonsson, 2015; Schwartz et al., 2002). Analyses of phenological data in this cases study also reveal a higher inter-annual variability in the GP-SOS of early species that are generally limited by the frost period and have a higher sensitivity to temperature fluctuations (C Cornelius et al., 2013; Wang et al., 2015). In agreement with Helman (2018), we find that the absence of detailed land cover maps (including understory distribution) and mixing of signals from pre-existing understory and the growing overstory before reaching its full canopy maturity, makes the matching of early season LSP-SOS with a species specific GP a major challenge.

Another major source of variability in LSP and GP observations is the lack of a common definition for senescence across species (Gill et al., 2015; Panchen et al., 2015). Additionally, it is difficult to compare species specific observations of minute and detailed changes such as bud burst or fruiting in vegetation as reported by observers on the ground with remote sensing based estimates of phenology that are based on change in the average greenness of vegetation in a pixel (Badeck et al., 2004; White et al., 2014). Additionally, observation of GP dates are often affected by inconsistent collection of data that renders missing data in phenological records. This was evident in Chapter 4.2 where the broadleaf species (i.e. *Fagus sylvatica* and *Sorbus aucuparia*) had EOS as day of leaf fall reported but the conifer species i.e. *Picea abies* did not have an equivalent day of senescence in the records. Hence, the EOS extracted from the remote sensing data could not be compared to any equivalent GP-EOS. Analysis was also hampered in chapter 4.2 due to many years of missing entries for the GP dates at higher elevations (> 900 metres) of BFNP. The GP information used in chapter 4.3 was generated by interpolating observer reported dates of SOS and EOS, hence the method of interpolation and the changes in the observation network might be partly responsible for the inter-annual variability in GP values (DWD, n.d.), and hence further complicated validation of LSP.

In agreement with previous studies (Fisher and Mustard, 2007; Hamunyela et al., 2013) strong correlations in the inter-annual behaviour were detected in the 50% amplitude based LSP-SOS estimates and GP-SOS (leaf unfolding) observations in chapters 4.2 and 4.3. This was also shown in chapter 4.1 where 50% and 75% amplitude both revealed high correlations with leaf unfolding and greening. However, very weak linkages were found in the LSP-EOS estimates and GP observations of senescence i.e. leaf fall. In chapter 4.3, GP-EOS depicting the leaf fall rather than the leaf colouring was more closely linked to the LSP-EOS estimates. In contrast to the spring, the autumn or EOS has received very limited attention in previous studies. The difficulty in identifying EOS in the NDVI time series and its weak correlation with GP observations are evident in chapters 4.2 and 4.3 of this thesis. The limitations of LSP based estimates in detecting the senescence or EOS have been discussed in several studies. This is because EOS unlike SOS is very subjective and lasts a period of gradual change in leaf colouring to complete leaf fall, which makes senescence difficult to observe (Estrella and Menzel, 2006; Gallinat et al., 2015; Richardson and O'Keefe, 2009; Stöckli et al., 2008). The overreliance on greenness based measures such as NDVI for tracking the entire phenology might be one of the limiting factors of existing studies. Inclusion of redness based indices and pigment ratios such as the chlorophyll to carotenoid index (CCI) might help in better

detection of colouring of leaves and photosynthetic activity of plants (Gamon et al., 2016; Yingying et al., 2018). Alternative indices were however not tested in the case studies carried out as part of this thesis.

5.3 What drives variability in LSP?

Chapter 4.2 examines different drivers of mean-LSP at the sub-pixel level. The topography based MLR models primarily covering micro-climatic influences were able to explain most of the spatial variability observed in the SOS and LOS estimates from LSP which correspond well with previous studies by Chen and Pan, (2002) and Reaves et al., (2018). The use of popular and freely downloadable land cover maps such as CORINE though led to improvements in the topography based LSP models, but was not able to provide the best performing models. This was most probably due to the heterogeneity present in the land cover classes of CORINE maps (Doktor et al., 2009; Kosztra et al., 2014). The use of a proprietary habitat map that included information on land cover affected by disasters (windstorms), management (clear cut) and affected areas under regeneration further improved our understanding of the variability observed in LSP metrics. These insights are consistent with Norman et al., (2017), who reported phenological behaviour of land cover to be affected by vegetation type and extreme events such as wildfires and pest infestation. In agreement with Doktor et al., (2009) inclusion of additional predictors such as land cover information and forest stand data from LiDAR led to large improvements in the modelled LSP results for EOS, maxDOY, NDVImax and NDVIsum. The LSP-EOS however yielded the least explained variance (i.e. 37%) among all the modelled LSP metrics. The difficulty in the modelling EOS phases of vegetation has been discussed in previous studies that have incorporated drivers such as complex interactions between temperature, rainfall and photoperiod among different triggers (Estrella and Menzel, 2006; Meng et al., 2016; Xie et al., 2018, 2015b). The species specific dependence of EOS hypothesised in Richardson and O'Keefe, (2009) was corroborated in chapter 4.2, where the percentage of broadleaf species in the pixel was found to be one of the stronger drivers of variability in EOS. Analyses revealed improvements in modelled LSP when accounting for subpixel heterogeneity and inclusion of LiDAR based forest stand information (Chen et al., 2018; Hwang et al., 2011; Xie et al., 2018). In contrast to Hwang et al., (2011), chapter 4.2 reveals the importance of sub-pixel proportions of not only conifers but also broadleaves species in driving the spatial variability of LSP metrics. Since different species are known to respond to different drivers and conversely, similar triggers driving differential responses (Basler and Körner, 2014;

Burgess et al., 2018; Laube et al., 2014), the sub-pixel composition of land cover is critical in modelling and correctly interpreting drivers of LSP behaviour. Similar to Kraus et al., (2016), no significant influence of aspect on the LSP estimates was found. This is in contradiction to Xie et al., (2015a) and Reaves et al., (2018) who reported differences in the LSP observed in the north and south facing slopes. For NDVIsum and maxNDVI, the respective models revealed the maximum explained variance (> 80%). These indices are known to be comparatively less sensitive to outliers and methods of pre-processing. They are important measures of vegetation productivity, least insensitive to user bias and are hence the perfect candidates to study effects of biotic and abiotic drivers on vegetation (Berner et al., 2011; Heumann et al., 2007; Lumbierres et al., 2017; Wylie et al., 2008).

5.4 Climate change and phenology in the mountains

Studying differences in the seasonal variations of temperature are important as they can affect the phenological response of vegetation differently at different locations and in turn affect ecosystem functioning (Norman et al., 2017; Vandvik et al., 2018). Chapter 4.3 examines the spring-winter temperature driven phenological rates of forests in the pre-alpine (< 1000 metre elevation) and alpine region (> 1000 metre elevation) of the Bavarian Alps region. The influence of spring and winter temperatures on the SOS and EOS revealed differential effects on forest phenology. In comparison to pre-alpine regions, higher lapse rates of SOS were observed in the alpine areas, possibly due to longer duration of snow in the higher elevations (Asam et al., 2018). In agreement with Vitasse et al., (2017), the highest lapse rates in SOS were observed in years with cold spring with preceding warm winters. Previous studies have indicated the importance of winter temperatures along with the spring temperatures in driving spring timings in plants (Cook et al., 2012). Warm winters with a lack of chilling are known to delay the start of season in plants, yet warmer springs could expedite plant growth due to accumulation of heat (Laube et al., 2014; Wang et al., 2016). Therefore, it is also essential to evaluate the inter-annual seasonal temperature variations to obtain a synoptic overview of the complete plant growth cycle. Minimum difference in the LSP-SOS rates of pre-Alpine and Alpine regions was observed in years with both cold winters and spring. In general the pre-Alpine elevational rates of EOS were found to be higher than that of Alpine region. The LSP at lower elevations (pre-Alpine region) matched closely with the DWD based estimates of phenology. However, the DWD phenology at higher elevations (> 1000 meters) was difficult to analyse and validate due to uncertainties in interpolated data (due to limited/ varying observation sites for interpolation and the lack of detailed information on data processing)

(DWD, n.d.). This study provides important clues to drivers of inter-annual variability in phenological timings along climatic gradients.

6. Outlook

It is essential to understand both uncertainties and drivers of LSP to elucidate the effects of climate change on vegetation. This thesis evaluates various techniques of pre-processing satellite data and estimating LSP metrics. In agreement with previous studies, we find that such decisions (pre-processing and phenology estimation) are subjective and known to introduce bias into results. Therefore, a critical consideration is essential for selection of such methods. Additionally, it is essential to have high quality of input data (both remote sensing and ground based) to generate results with a greater degree of confidence. Inclusion of alternative and novel sources of data capturing such as LiDAR, drones or UAVs and close range camera (phenocams) can prove to be the essential bridge between space borne and ground observations. Remote sensing of phenology presents a promising future with missions such as Sentinel (from the European Union) that now provide high spatial and temporal resolution data. Use of field-based spectrometers mimicking spectral regions of space borne sensors could be used for calibrating models for detection of LSP (which was beyond the scope of this thesis). Applications of remote sensing indices other than NDVI, and microwave techniques for remote sensing (i.e. RADAR) for its all-weather visibility is also another avenue for research in the future.

7. References

Ahl, D.E., Gower, S.T., Burrows, S.N., Shabanov, N. V, Myneni, R.B., Knyazikhin, Y., 2006. Monitoring spring canopy phenology of a deciduous broadleaf forest using MODIS. Remote Sens. Environ. 104, 88–95. https://doi.org/10.1016/j.rse.2006.05.003

Asam, S., Callegari, M., Matiu, M., Fiore, G., Gregorio, L. De, Jacob, A., Menzel, A., Zebisch, M., Notarnicola, C., 2018. Relationship between Spatiotemporal Variations of Climate, Snow Cover and Plant Phenology over the Alps—An Earth Observation-Based Analysis. Remote Sens. 2018, Vol. 10, Page 1757 10, 1757. https://doi.org/10.3390/RS10111757

Atkinson, P.M., Dash, J., Jeganathan, C., 2011. Amazon vegetation greenness as measured by satellite sensors over the last decade. Geophys. Res. Lett. 38, n/a-n/a. https://doi.org/10.1029/2011GL049118

Badeck, F.W., Bondeau, A., Böttcher, K., Doktor, D., Lucht, W., Schaber, J., Sitch, S., 2004. Responses of spring phenology to climate change. New Phytol. https://doi.org/10.1111/j.1469-8137.2004.01059.x

Basler, D., Körner, C., 2014. Photoperiod and temperature responses of bud swelling and bud burst in four temperate forest tree species. Tree Physiol. 34, 377–388. https://doi.org/10.1093/treephys/tpu021

Beck, P.S.A., Atzberger, C., Høgda, K.A., Johansen, B., Skidmore, A.K., 2006. Improved monitoring of vegetation dynamics at very high latitudes: A new method using MODIS NDVI. Remote Sens. Environ. 100, 321–334. https://doi.org/10.1016/j.rse.2005.10.021

Bennet, K., Hope, D., 2018. PhenoCam network harnesses ‘big data’ to predict impact of warmer climate on ecosystem productivity and carbon cycling [WWW Document]. URL http://news.nau.edu/andrew-richardson-phenocam/#.XBpeOs8zbVo (accessed 12.19.18).

Berner, L.T., Beck, P.S.A., Bunn, A.G., Lloyd, A.H., Goetz, S.J., 2011. High-latitude tree growth and satellite vegetation indices: Correlations and trends in Russia and Canada (1982-2008). J. Geophys. Res. Biogeosciences 116, G01015. https://doi.org/10.1029/2010JG001475

Bradley, B.A., Jacob, R.W., Hermance, J.F., Mustard, J.F., 2007. A curve fitting procedure to derive inter-annual phenologies from time series of noisy satellite NDVI data. Remote Sens. Environ. 106, 137–145. https://doi.org/10.1016/j.rse.2006.08.002

Browning, D.M., Karl, J.W., Morin, D., Richardson, A.D., Tweedie, C.E., 2017. Phenocams bridge the gap between field and satellite observations in an arid grassland. Remote

Sens. in review, 1071. https://doi.org/10.3390/rs9101071

Brus, D.J., Hengeveld, G.M., Walvoort, D.J.J., Goedhart, P.W., Heidema, A.H., Nabuurs, G.J., Gunia, K., 2012. Statistical mapping of tree species over Europe. Eur. J. For. Res. 131, 145–157. https://doi.org/10.1007/s10342-011-0513-5

Buras, A., Zang, C., Menzel, A., 2017. Testing the stability of transfer functions. Dendrochronologia 42, 56–62. https://doi.org/10.1016/j.dendro.2017.01.005

Burgess, M.D., Smith, K.W., Evans, K.L., Leech, D., Pearce-Higgins, J.W., Branston, C.J., Briggs, K., Clark, J.R., Du Feu, C.R., Lewthwaite, K., Nager, R.G., Sheldon, B.C., Smith, J.A., Whytock, R.C., Willis, S.G., Phillimore, A.B., 2018. Tritrophic phenological match-mismatch in space and time. Nat. Ecol. Evol. 2, 970–975. https://doi.org/10.1038/s41559-018-0543-1

Cai, Z., Jönsson, P., Jin, H., Eklundh, L., 2017. Performance of smoothing methods for reconstructing NDVI time-series and estimating vegetation phenology from MODIS data. Remote Sens. 9, 1271. https://doi.org/10.3390/rs9121271

Chang, J., Ciais, P., Viovy, N., Soussana, J.F., Klumpp, K., Sultan, B., 2017. Future productivity and phenology changes in European grasslands for different warming levels: Implications for grassland management and carbon balance. Carbon Balance Manag. 12, 11. https://doi.org/10.1186/s13021-017-0079-8

Chen, X., Pan, W., 2002. Relationships among phenological growing season, time-integrated normalized difference vegetation index and climate forcing in the temperature region of Eastern China. Int. J. Climatol. 22, 1781–1792. https://doi.org/10.1002/joc.823

Chen, X., Wang, D., Chen, J., Wang, C., Shen, M., 2018. The mixed pixel effect in land surface phenology: A simulation study. Remote Sens. Environ. 211, 338–344. https://doi.org/10.1016/j.rse.2018.04.030

Chuine, I., Yiou, P., Viovy, N., Seguin, B., Daux, V., Ladurie, E.L.R., 2004. Grape ripening as a past climate indicator. Nature 432, 289–290. https://doi.org/10.1038/432289a

Clark, R.N., 1999. Spectroscopy of Rocks and Minerals, and Principles of Spectroscopy, in: Rencz., A.N. (Ed.), Remote Sensing for the Eartb Sciences: Manual of Remote Sensing. John Wiley & Sons, Inc.

Cleland, E.E., Chuine, I., Menzel, A., Mooney, H.A., Schwartz, M.D., 2007. Shifting plant phenology in response to global change. Trends Ecol. Evol. https://doi.org/10.1016/j.tree.2007.04.003

Clerici, N., Weissteiner, C.J., Gerard, F., 2012. Exploring the use of MODIS NDVI-based phenology indicators for classifying forest general habitat categories. Remote Sens. 4,

1781–1803. https://doi.org/10.3390/rs4061781

Cook, B.I., Wolkovich, E.M., Parmesan, C., 2012. Divergent responses to spring and winter warming drive community level flowering trends. Proc. Natl. Acad. Sci. 109, 9000–9005. https://doi.org/10.1073/pnas.1118364109

Core Team, R., 2014. R: A language and environment for statistical computing. Vienna, Austria: R Foundation for Statistical Computing; 2014.

Cornelius, C, Estrella, N., Franz, H., Menzel, A., 2013. Linking altitudinal gradients and temperature responses of plant phenology in the Bavarian Alps. Plant Biol. 15, 57–69. https://doi.org/10.1111/j.1438-8677.2012.00577.x

Cornelius, C., Estrella, N., Franz, H., Menzel, A., 2013. Linking altitudinal gradients and temperature responses of plant phenology in the Bavarian Alps. Plant Biol. 15, 57–69. https://doi.org/10.1111/j.1438-8677.2012.00577.x

Diez, J.M., Ibáñez, I., Miller-Rushing, A.J., Mazer, S.J., Crimmins, T.M., Crimmins, M.A., Bertelsen, C.D., Inouye, D.W., 2012. Forecasting phenology: From species variability to community patterns. Ecol. Lett. 15, 545–553. https://doi.org/10.1111/j.1461-0248.2012.01765.x

Doi, H., Gordo, O., Katano, I., 2008. Heterogeneous intra-annual climatic changes drive different phenological responses at two trophic levels. Clim. Res. 36, 181–190. https://doi.org/10.3354/cr00741

Doktor, D., Bondeau, A., Koslowski, D., Badeck, F.W., 2009. Influence of heterogeneous landscapes on computed green-up dates based on daily AVHRR NDVI observations. Remote Sens. Environ. 113, 2618–2632. https://doi.org/10.1016/j.rse.2009.07.020

Dupke, C., Bonenfant, C., Reineking, B., Hable, R., Zeppenfeld, T., Ewald, M., Heurich, M., 2017. Habitat selection by a large herbivore at multiple spatial and temporal scales is primarily governed by food resources. Ecography (Cop.). 40, 1014–1027. https://doi.org/10.1111/ecog.02152

DWD, n.d. Climate Data Center- German Meteorological Service [WWW Document]. URL https://cdc.dwd.de/portal/201810240858/index.html (accessed 11.26.18).

EEA, 2012. CLC 2012 — Copernicus Land Monitoring Service [WWW Document]. URL http://land.copernicus.eu/pan-european/corine-land-cover/clc-2012/view (accessed 6.26.17).

Eklundh, L., Jonsson, P., 2015. TIMESAT: A software package for time-series processing and assessment of vegetation dynamics, in: Kuenzer, C., Dech, S., Wagner, W. (Eds.), Remote Sensing and Digital Image Processing. Springer International Publishing, Cham,

pp. 141–158. https://doi.org/10.1007/978-3-319-15967-6_7

Elmore, A.J., Guinn, S.M., Minsley, B.J., Richardson, A.D., 2012. Landscape controls on the timing of spring, autumn, and growing season length in mid-Atlantic forests. Glob. Chang. Biol. 18, 656–674. https://doi.org/10.1111/j.1365-2486.2011.02521.x

Estay, S.A., Chavez, R., 2018. npphen: an R-package for non-parametric reconstruction of vegetation phenology and anomaly detection using remote sensing. bioRxiv 301143. https://doi.org/10.1101/301143

Estrella, N., Menzel, A., 2006. Responses of leaf colouring in four deciduous tree species to climate and weather in Germany. Clim. Res. 32, 253–267. https://doi.org/10.3354/cr032253

Filippa, G., Cremonese, E., Migliavacca, M., Galvagno, M., Forkel, M., Wingate, L., Tomelleri, E., Morra di Cella, U., Richardson, A.D., 2016. Phenopix: A R package for image-based vegetation phenology. Agric. For. Meteorol. 220, 141–150. https://doi.org/10.1016/j.agrformet.2016.01.006

Fisher, J.I., Mustard, J.F., 2007. Cross-scalar satellite phenology from ground, Landsat, and MODIS data. Remote Sens. Environ. 109, 261–273. https://doi.org/10.1016/j.rse.2007.01.004

Forkel, M., Carvalhais, N., Verbesselt, J., Mahecha, M.D., Neigh, C.S.R., Reichstein, M., 2013. Trend Change detection in NDVI time series: Effects of inter-annual variability and methodology. Remote Sens. 5, 2113–2144. https://doi.org/10.3390/rs5052113

Forkel, M., Migliavacca, M., Thonicke, K., Reichstein, M., Schaphoff, S., Weber, U., Carvalhais, N., 2015. Codominant water control on global interannual variability and trends in land surface phenology and greenness. Glob. Chang. Biol. 3414–3435. https://doi.org/10.1111/gcb.12950

Foster, T., Gonçalves, I.Z., Campos, I., Neale, C.M.., Brozović, N., 2019. Assessing landscape scale heterogeneity in irrigation water use with remote sensing and in situ monitoring. Environ. Res. Lett. 14. https://doi.org/10.1088/1748-9326/aaf2be

Frampton, W.J., Dash, J., Watmough, G., Milton, E.J., 2013. Evaluating the capabilities of Sentinel-2 for quantitative estimation of biophysical variables in vegetation. ISPRS J. Photogramm. Remote Sens. 82, 83–92. https://doi.org/10.1016/j.isprsjprs.2013.04.007

Fu, Y.H., Piao, S., Op de Beeck, M., Cong, N., Zhao, H., Zhang, Y., Menzel, A., Janssens, I.A., 2014. Recent spring phenology shifts in western Central Europe based on multiscale observations. Glob. Ecol. Biogeogr. 23, 1255–1263. https://doi.org/10.1111/geb.12210

Gallinat, A.S., Primack, R.B., Wagner, D.L., 2015. Autumn, the neglected season in climate change research. Trends Ecol. Evol. https://doi.org/10.1016/j.tree.2015.01.004

Gamon, J.A., Huemmrich, K.F., Wong, C.Y.S., Ensminger, I., Garrity, S., Hollinger, D.Y., Noormets, A., Peñuelas, J., 2016. A remotely sensed pigment index reveals photosynthetic phenology in evergreen conifers. Proc. Natl. Acad. Sci. 113, 13087–13092. https://doi.org/10.1073/pnas.1606162113

Garonna, I., De Jong, R., Stöckli, R., Schmid, B., Schenkel, D., Schimel, D., Schaepman, M.E., 2018. Shifting relative importance of climatic constraints on land surface phenology. Environ. Res. Lett. 13, 024025. https://doi.org/10.1088/1748-9326/aaa17b

Gill, A.L., Gallinat, A.S., Sanders-DeMott, R., Rigden, A.J., Short Gianotti, D.J., Mantooth, J.A., Templer, P.H., 2015. Changes in autumn senescence in northern hemisphere deciduous trees: A meta-analysis of autumn phenology studies. Ann. Bot. 116, 875–888. https://doi.org/10.1093/aob/mcv055

Giovanna, P., 2007. Origin and development of phenology as a science. Ital. J. Agrometeorol. 3, 24–29.

Glenn, E.P., Huete, A.R., Nagler, P.L., Nelson, S.G., 2008. Relationship between remotely-sensed vegetation indices, canopy attributes and plant physiological processes: What vegetation indices can and cannot tell us about the landscape. Sensors. https://doi.org/10.3390/s8042136

Grömping, U., 2006. Relative Importance for Linear Regression in R : The Package relaimpo. J. Stat. Softw. 17, 1–27. https://doi.org/10.18637/jss.v017.i01

Hamunyela, E., Verbesselt, J., Roerink, G., Herold, M., 2013. Trends in spring phenology of western European deciduous forests. Remote Sens. 5, 6159–6179. https://doi.org/10.3390/rs5126159

Helman, D., 2018. Land surface phenology: What do we really 'see' from space? Sci. Total Environ. https://doi.org/10.1016/j.scitotenv.2017.07.237

Heumann, B.W., Seaquist, J.W., Eklundh, L., Jönsson, P., 2007. AVHRR derived phenological change in the Sahel and Soudan, Africa, 1982-2005. Remote Sens. Environ. 108, 385–392. https://doi.org/10.1016/j.rse.2006.11.025

Hijmans, R.J., 2016. Geographic Data Analysis and Modeling. R package raster version 2.5-8. [WWW Document]. URL https://cran.r-project.org/web/packages/raster/index.html (accessed 10.4.17).

Holm, A.M., Cridland, S.W., Roderick, M.L., 2003. The use of time-integrated NOAA NDVI data and rainfall to assess landscape degradation in the arid shrubland of Western

Australia. Remote Sens. Environ. 85, 145–158. https://doi.org/10.1016/S0034-4257(02)00199-2

Hufkens, K., Basler, D., Milliman, T., Melaas, E.K., Richardson, A.D., 2018. An integrated phenology modelling framework in r. Methods Ecol. Evol. 9, 1276–1285. https://doi.org/10.1111/2041-210X.12970

Hufkens, K., Melaas, E.K., Mann, M.L., Foster, T., Ceballos, F., Robles, M., Kramer, B., 2019. Monitoring crop phenology using a smartphone based near-surface remote sensing approach. Agric. For. Meteorol. 265, 327–337. https://doi.org/S0168192318303484

Hwang, T., Song, C., Vose, J.M., Band, L.E., 2011. Topography-mediated controls on local vegetation phenology estimated from MODIS vegetation index. Landsc. Ecol. 26, 541–556. https://doi.org/10.1007/s10980-011-9580-8

Ide, R., Oguma, H., 2013. A cost-effective monitoring method using digital time-lapse cameras for detecting temporal and spatial variations of snowmelt and vegetation phenology in alpine ecosystems. Ecol. Inform. 16, 25–34. https://doi.org/10.1016/j.ecoinf.2013.04.003

IPG, n.d. The International Phenological Gardens of Europe [WWW Document]. URL http://ipg.hu-berlin.de/ (accessed 11.18.18).

Ivits, E., Cherlet, M., Mehl, W., Sommer, S., 2013. Ecosystem functional units characterized by satellite observed phenology and productivity gradients: A case study for Europe. Ecol. Indic. 27, 17–28. https://doi.org/10.1016/j.ecolind.2012.11.010

Jin, S., Sader, S.A., 2005. MODIS time-series imagery for forest disturbance detection and quantification of patch size effects. Remote Sens. Environ. 99, 462–470. https://doi.org/10.1016/j.rse.2005.09.017

Jönsson, P., Eklundh, L., 2004. TIMESAT - A program for analyzing time-series of satellite sensor data. Comput. Geosci. 30, 833–845. https://doi.org/10.1016/j.cageo.2004.05.006

Julien, Y., Sobrino, J.A., 2009. Global land surface phenology trends from GIMMS database. Int. J. Remote Sens. 30, 3495–3513. https://doi.org/10.1080/01431160802562255

Klosterman, S., Richardson, A.D., 2017. Observing spring and fall phenology in a deciduous forest with aerial drone imagery. Sensors (Switzerland) 17. https://doi.org/10.3390/s17122852

Kosztra, B., Arnold, S., Banko, G., Hazeu, G., Büttner, G., 2014. Proposal for enhancement of CLC nomenclature guidelines, EEA Technical Report.

Kraus, C., Zang, C., Menzel, A., 2016. Elevational response in leaf and xylem phenology reveals different prolongation of growing period of common beech and Norway spruce

under warming conditions in the Bavarian Alps. Eur. J. For. Res. 135, 1011–1023. https://doi.org/10.1007/s10342-016-0990-7

Kross, A., Fernandes, R., Seaquist, J., Beaubien, E., 2011. The effect of the temporal resolution of NDVI data on season onset dates and trends across Canadian broadleaf forests. Remote Sens. Environ. 115, 1564–1575. https://doi.org/10.1016/j.rse.2011.02.015

Kullman, L., 2010. Alpine flora dynamics - a critical review of responses to climate change in the Swedish Scandes since the early 1950s. Nord. J. Bot. 28, 398–408. https://doi.org/10.1111/j.1756-1051.2010.00812.x

Laube, J., Sparks, T.H., Estrella, N., Höfler, J., Ankerst, D.P., Menzel, A., 2014. Chilling outweighs photoperiod in preventing precocious spring development. Glob. Chang. Biol. 20, 170–182. https://doi.org/10.1111/gcb.12360

Leonelli, G., Pelfini, M., Cella, U.M. Di, Garavaglia, V., 2011. Climate warming and the recent treeline shift in the European alps: The role of geomorphological factors in high-altitude sites. Ambio 40, 264–273. https://doi.org/10.1007/s13280-010-0096-2

Lumbierres, M., Méndez, P., Bustamante, J., Soriguer, R., Santamaría, L., 2017. Modeling Biomass Production in Seasonal Wetlands Using MODIS NDVI Land Surface Phenology. Remote Sens. 9, 392. https://doi.org/10.3390/rs9040392

Luo, X., Chen, X., Xu, L., Myneni, R., Zhu, Z., 2013. Assessing performance of NDVI and NDVI3g in monitoring leaf unfolding dates of the deciduous broadleaf forest in Northern China. Remote Sens. 5, 845–861. https://doi.org/10.3390/rs5020845

Ma, X., Huete, A., Moran, S., Ponce-Campos, G., Eamus, D., 2015. Abrupt shifts in phenology and vegetation productivity under climate extremes. J. Geophys. Res. Biogeosciences 120, 2036–2052. https://doi.org/10.1002/2015JG003144

Massey, R., Sankey, T.T., Congalton, R.G., Yadav, K., Thenkabail, P.S., Ozdogan, M., Sánchez Meador, A.J., 2017. MODIS phenology-derived, multi-year distribution of conterminous U.S. crop types. Remote Sens. Environ. 198, 490–503. https://doi.org/10.1016/j.rse.2017.06.033

Meng, J., Li, S., Wang, W., Liu, Q., Xie, S., Ma, W., 2016. Mapping forest health using spectral and textural information extracted from SPOT-5 satellite images. Remote Sens. 8, 719. https://doi.org/10.3390/rs8090719

Menzel, A., 2002. Phenology: Its importance to the global change community: An editorial comment. Clim. Change 54, 379-385. https://doi.org/10.1023/A:1016125215496

Menzel, A., Fabian, P., 1999. Growing season extended in Europe. Nature 397, 659.

https://doi.org/10.1038/17709

Menzel, A., Jakobi, G., Ahas, R., Scheifinger, H., Estrella, N., 2003. Variations of the climatological growing season (1951-2000) in Germany compared with other countries. Int. J. Climatol. 23, 793–812. https://doi.org/10.1002/joc.915

Menzel, A., Sparks, T.H., Estrella, N., Roy, D.B., 2006. Altered geographic and temporal variability in phenology in response to climate change. Glob. Ecol. Biogeogr. 15, 498–504. https://doi.org/10.1111/j.1466-822X.2006.00247.x

Misra, G., Buras, A., Heurich, M., Asam, S., Menzel, A., 2018. LiDAR derived topography and forest stand characteristics largely explain the spatial variability observed in MODIS land surface phenology. Remote Sens. Environ. 218, 231–244. https://doi.org/10.1016/j.rse.2018.09.027

Misra, G., Buras, A., Menzel, A., 2016. Effects of Different Methods on the Comparison between Land Surface and Ground Phenology—A Methodological Case Study from South-Western Germany. Remote Sens. 8, 753. https://doi.org/10.3390/rs8090753

Myneni, R.B., Keeling, C.D., Tucker, C.J., Asrar, G., Nemani, R.R., 1997. Increased plant growth in the northern high latitudes from 1981 to 1991. Nature 386, 698–702. https://doi.org/10.1038/386698a0

Nagai, S., Nasahara, K.N., Inoue, T., Saitoh, T.M., Suzuki, R., 2016. Review: advances in in situ and satellite phenological observations in Japan. Int. J. Biometeorol. https://doi.org/10.1007/s00484-015-1053-3

Nagai, S., Nasahara, K.N., Muraoka, H., Akiyama, T., Tsuchida, S., 2010. Field experiments to test the use of the normalized-difference vegetation index for phenology detection. Agric. For. Meteorol. 150, 152–160. https://doi.org/10.1016/j.agrformet.2009.09.010

Norman, S., Hargrove, W., Christie, W., 2017. Spring and Autumn Phenological Variability across Environmental Gradients of Great Smoky Mountains National Park, USA. Remote Sens. 9, 407. https://doi.org/10.3390/rs9050407

Ovaskainen, O., Skorokhodova, S., Yakovleva, M., Sukhov, A., Kutenkov, A., Kutenkova, N., Shcherbakov, A., Meyke, E., Delgado, M. del M., 2013. Community-level phenological response to climate change. Proc. Natl. Acad. Sci. U. S. A. 110, 13434–9. https://doi.org/10.1073/pnas.1305533110

Panchen, Z.A., Primack, R.B., Gallinat, A.S., Nordt, B., Stevens, A.D., Du, Y., Fahey, R., 2015. Substantial variation in leaf senescence times among 1360 temperate woody plant species: Implications for phenology and ecosystem processes. Ann. Bot. 116, 865–873. https://doi.org/10.1093/aob/mcv015

Parmesan, C., Yohe, G., 2003. A globally coherent fingerprint of climate change impacts across natural systems. Nature 421, 37–42. https://doi.org/10.1038/nature01286

Peñuelas, J., 2009. Phenology feedbacks on climate change. Science 324, 887-888. https://doi.org/10.1126/science.1173004

Pettorelli, N., Schulte to Bühne, H., Tulloch, A., Dubois, G., Macinnis-Ng, C., Queirós, A.M., Keith, D.A., Wegmann, M., Schrodt, F., Stellmes, M., Sonnenschein, R., Geller, G.N., Roy, S., Somers, B., Murray, N., Bland, L., Geijzendorffer, I., Kerr, J.T., Broszeit, S., Leitão, P.J., Duncan, C., El Serafy, G., He, K.S., Blanchard, J.L., Lucas, R., Mairota, P., Webb, T.J., Nicholson, E., 2017. Satellite remote sensing of ecosystem functions: opportunities, challenges and way forward. Remote Sens. Ecol. Conserv. 4, 71–93. https://doi.org/10.1002/rse2.59

Pettorelli, N., Vik, J.O., Mysterud, A., Gaillard, J.-M., Tucker, C.J., Stenseth, N.C., 2005. Using the satellite-derived NDVI to assess ecological responses to environmental change. Trends Ecol. Evol. 20, 503–510. https://doi.org/10.1016/j.tree.2005.05.011

Reaves, V.C., Elmore, A.J., Nelson, D.M., McNeil, B.E., 2018. Drivers of spatial variability in greendown within an oak-hickory forest landscape. Remote Sens. Environ. 210, 422–433. https://doi.org/10.1016/j.rse.2018.03.027

Reed, B.C., Brown, J.F., VanderZee, D., Loveland, T.R., Merchant, J.W., Ohlen, D.O., 1994. Measuring phenological variability from satellite imagery. J. Veg. Sci. 5, 703–714. https://doi.org/10.2307/3235884

Richardson, A.D., Keenan, T.F., Migliavacca, M., Ryu, Y., Sonnentag, O., Toomey, M., 2013. Climate change, phenology, and phenological control of vegetation feedbacks to the climate system. Agric. For. Meteorol. 169, 156–173. https://doi.org/10.1016/j.agrformet.2012.09.012

Richardson, A.D., O'Keefe, J., 2009. Phenological differences between understory and overstory a case study using the long-term Harvard Forest records, in: Phenology of Ecosystem Processes: Applications in Global Change Research. Springer New York, New York, NY, pp. 87–117. https://doi.org/10.1007/978-1-4419-0026-5_4

Rodriguez-Galiano, V.F., Dash, J., Atkinson, P.M., 2015. Intercomparison of satellite sensor land surface phenology and ground phenology in Europe. Geophys. Res. Lett. 42, 2253–2260. https://doi.org/10.1002/2015GL063586

Rouse, R.W.H., Haas, J.A.W., Deering, D.W., 1974. Monitoring vegetation systems in the Great Plains with ERTS, in: NASA. Goddard Space Flight Center 3d ERTS-1 Symp. pp. 309–317.

Saleska, S.R., Didan, K., Huete, A.R., Da Rocha, H.R., 2007. Amazon forests green-up during 2005 drought. Science 318, 612. https://doi.org/10.1126/science.1146663

Samanta, A., Ganguly, S., Hashimoto, H., Devadiga, S., Vermote, E., Knyazikhin, Y., Nemani, R.R., Myneni, R.B., 2010. Amazon forests did not green-up during the 2005 drought. Geophys. Res. Lett. 37, n/a-n/a. https://doi.org/10.1029/2009GL042154

Schwartz, M.D., 2003. Phenology: An Integrative Environmental Science, Phenology: An Integrative Environmental Science, Tasks for Vegetation Science. Springer Netherlands, Dordrecht. https://doi.org/10.1007/978-94-007-0632-3

Schwartz, M.D., Reed, B.C., White, M.A., 2002. Assessing satellite-derived start-of-season measures in the conterminous USA. Int. J. Climatol. 22, 1793–1805. https://doi.org/10.1002/joc.819

Sparks, T.H., Carey, P.D., 1995. The Responses of Species to Climate Over Two Centuries: An Analysis of the Marsham Phenological Record, 1736-1947. J. Ecol. 83, 321. https://doi.org/10.2307/2261570

Spruce, J.P., Sader, S., Ryan, R.E., Smoot, J., Kuper, P., Ross, K., Prados, D., Russell, J., Gasser, G., McKellip, R., Hargrove, W., 2011. Assessment of MODIS NDVI time series data products for detecting forest defoliation by gypsy moth outbreaks. Remote Sens. Environ. 115, 427–437. https://doi.org/10.1016/j.rse.2010.09.013

Stöckli, R., Rutishauser, T., Dragoni, D., O'Keefe, J., Thornton, P.E., Jolly, M., Lu, L., Denning, A.S., 2008. Remote sensing data assimilation for a prognostic phenology model. J. Geophys. Res. Biogeosciences 113. https://doi.org/10.1029/2008JG000781

Tan, B., Morisette, J.T., Wolfe, R.E., Gao, F., Ederer, G.A., Nightingale, J., Pedelty, J.A., 2011. An enhanced TIMESAT algorithm for estimating vegetation phenology metrics from MODIS data, in: IEEE Journal of Selected Topics in Applied Earth Observations and Remote Sensing. pp. 361–371. https://doi.org/10.1109/JSTARS.2010.2075916

Tan, B., Woodcock, C.E., Hu, J., Zhang, P., Ozdogan, M., Huang, D., Yang, W., Knyazikhin, Y., Myneni, R.B., 2006. The impact of gridding artifacts on the local spatial properties of MODIS data: Implications for validation, compositing, and band-to-band registration across resolutions. Remote Sens. Environ. 105, 98–114. https://doi.org/10.1016/j.rse.2006.06.008

Tang, J., Körner, C., Muraoka, H., Piao, S., Shen, M., Thackeray, S.J., Yang, X., 2016. Emerging opportunities and challenges in phenology: A review. Ecosphere 7, e01436. https://doi.org/10.1002/ecs2.1436

Thackeray, S.J., Henrys, P.A., Hemming, D., Bell, J.R., Botham, M.S., Burthe, S., Helaouet,

P., Johns, D.G., Jones, I.D., Leech, D.I., Mackay, E.B., Massimino, D., Atkinson, S., Bacon, P.J., Brereton, T.M., Carvalho, L., Clutton-Brock, T.H., Duck, C., Edwards, M., Elliott, J.M., Hall, S.J.G., Harrington, R., Pearce-Higgins, J.W., Høye, T.T., Kruuk, L.E.B., Pemberton, J.M., Sparks, T.H., Thompson, P.M., White, I., Winfield, I.J., Wanless, S., 2016. Phenological sensitivity to climate across taxa and trophic levels. Nature 535, 241–245. https://doi.org/10.1038/nature18608

USGS, 2018. EarthExplorer - Home [WWW Document]. EarthExplorer. URL https://earthexplorer.usgs.gov/? (accessed 11.17.18).

Vandvik, V., Halbritter, A.H., Telford, R.J., 2018. Greening up the mountain. Proc. Natl. Acad. Sci. 115, 833–835. https://doi.org/10.1073/pnas.1721285115

Venables, W.N., Ripley, B.D., Venables, W.N. (William N.)., 2002. Modern applied statistics with S, 4th ed. Springer.

Verger, A., Filella, I., Baret, F., Peñuelas, J., 2016. Vegetation baseline phenology from kilometric global LAI satellite products. Remote Sens. Environ. 178, 1–14. https://doi.org/10.1016/j.rse.2016.02.057

Visser, M.E., Both, C., 2005. Shifts in phenology due to global climate change: The need for a yardstick. Proc. R. Soc. B Biol. Sci. https://doi.org/10.1098/rspb.2005.3356

Visser, M.E., Van Noordwijk, A.J., Tinbergen, J.M., Lessells, C.M., 1998. Warmer springs lead to mistimed reproduction in great tits (Parus major). Proc. R. Soc. B Biol. Sci. 265, 1867–1870. https://doi.org/10.1098/rspb.1998.0514

Vitasse, Y., Signarbieux, C., Fu, Y.H., 2017. Global warming leads to more uniform spring phenology across elevations. Proc. Natl. Acad. Sci. 115, 201717342. https://doi.org/10.1073/pnas.1717342115

Vrieling, A., Meroni, M., Darvishzadeh, R., Skidmore, A.K., Wang, T., Zurita-Milla, R., Oosterbeek, K., O'Connor, B., Paganini, M., 2018. Vegetation phenology from Sentinel-2 and field cameras for a Dutch barrier island. Remote Sens. Environ. 215, 517–529. https://doi.org/10.1016/j.rse.2018.03.014

Walther, G.R., Post, E., Convey, P., Menzel, A., Parmesan, C., Beebee, T.J.C., Fromentin, J.M., Hoegh-Guldberg, O., Bairlein, F., 2002. Ecological responses to recent climate change. Nature 416, 389–395. https://doi.org/10.1038/416389a

Wang, H., Ge, Q., Rutishauser, T., Dai, Y., Dai, J., 2015. Parameterization of temperature sensitivity of spring phenology and its application in explaining diverse phenological responses to temperature change. Sci. Rep. 5, 8833. https://doi.org/10.1038/srep08833

Wang, S., Yang, B., Yang, Q., Lu, L., Wang, X., Peng, Y., 2016. Temporal trends and spatial

variability of vegetation phenology over the Northern Hemisphere during 1982-2012. PLoS One 11, e0157134. https://doi.org/10.1371/journal.pone.0157134

White, K., Pontius, J., Schaberg, P., 2014. Remote sensing of spring phenology in northeastern forests: A comparison of methods, field metrics and sources of uncertainty. Remote Sens. Environ. 148, 97–107. https://doi.org/10.1016/j.rse.2014.03.017

White, M.A., de Beurs, K.M., Didan, K., Inouye, D.W., Richardson, A.D., Jensen, O.P., O'Keefe, J., Zhang, G., Nemani, R.R., van Leeuwen, W.J.D., Brown, J.F., de Wit, A., Schaepman, M., Lin, X., Dettinger, M., Bailey, A.S., Kimball, J., Schwartz, M.D., Baldocchi, D.D., Lee, J.T., Lauenroth, W.K., 2009. Intercomparison, interpretation, and assessment of spring phenology in North America estimated from remote sensing for 1982-2006. Glob. Chang. Biol. 15, 2335–2359. https://doi.org/10.1111/j.1365-2486.2009.01910.x

White, M.A., Thornton, P.E., Running, S.W., 1997. A continental phenology model for monitoring vegetation responses to interannual climatic variability. Global Biogeochem. Cycles 11, 217–234. https://doi.org/10.1029/97gb00330

Wulder, M.A., Loveland, T.R., Roy, D.P., Crawford, C.J., Masek, J.G., Woodcock, C.E., Allen, R.G., Anderson, M.C., Belward, A.S., Cohen, W.B., Dwyer, J., Erb, A., Gao, F., Griffiths, P., Helder, D., Hermosilla, T., Hipple, J.D., Hostert, P., Hughes, M.J., Huntington, J., Johnson, D.M., Kennedy, R., Kilic, A., Li, Z., Lymburner, L., McCorkel, J., Pahlevan, N., Scambos, T.A., Schaaf, C., Schott, J.R., Sheng, Y., Storey, J., Vermote, E., Vogelmann, J., White, J.C., Wynne, R.H., Zhu, Z., 2019. Current status of Landsat program, science, and applications. Remote Sens. Environ. 225, 127–147. https://doi.org/10.1016/j.rse.2019.02.015

Wylie, B.K., Zhang, L., Bliss, N., Ji, L., Tieszen, L.L., Jolly, W.M., 2008. Integrating modelling and remote sensing to identify ecosystem performance anomalies in the boreal forest, yukon river basin, Alaska. Int. J. Digit. Earth 1, 196–220. https://doi.org/10.1080/17538940802038366

Xie, Y., Ahmed, K.F., Allen, J.M., Wilson, A.M., Silander, J.A., 2015a. Green-up of deciduous forest communities of northeastern North America in response to climate variation and climate change. Landsc. Ecol. 30, 109–123. https://doi.org/10.1007/s10980-014-0099-7

Xie, Y., Wang, X., Silander, J.A., 2015b. Deciduous forest responses to temperature, precipitation, and drought imply complex climate change impacts. Proc. Natl. Acad. Sci. 112, 13585–13590. https://doi.org/10.1073/pnas.1509991112

Xie, Y., Wang, X., Wilson, A.M., Silander, J.A., 2018. Predicting autumn phenology: How deciduous tree species respond to weather stressors. Agric. For. Meteorol. 250–251, 127–137. https://doi.org/10.1016/j.agrformet.2017.12.259

Xin, Q., Olofsson, P., Zhu, Z., Tan, B., Woodcock, C.E., 2013. Toward near real-time monitoring of forest disturbance by fusion of MODIS and Landsat data. Remote Sens. Environ. 135, 234–247. https://doi.org/10.1016/j.rse.2013.04.002

Xu, L., Samanta, A., Costa, M.H., Ganguly, S., Nemani, R.R., Myneni, R.B., 2011. Widespread decline in greenness of Amazonian vegetation due to the 2010 drought. Geophys. Res. Lett. 38. https://doi.org/10.1029/2011GL046824

Yingying, X.I.E., Civco, D.L., Silander, J.A., 2018. Species-specific spring and autumn leaf phenology captured by time-lapse digital cameras. Ecosphere 9, e02089. https://doi.org/10.1002/ecs2.2089

Yu, H., Luedeling, E., Xu, J., 2010. Winter and spring warming result in delayed spring phenology on the Tibetan Plateau. Proc. Natl. Acad. Sci. 107, 22151–22156. https://doi.org/10.1073/pnas.1012490107

Zhang, X., Friedl, M., Tan, B., Goldberg, M., Yu, Y., 2012. Long-Term Detection of Global Vegetation Phenology from Satellite Instruments. Phenol. Clim. Chang. 297–320. https://doi.org/10.5772/39197

Zhang, X., Friedl, M.A., Schaaf, C.B., 2009. Sensitivity of vegetation phenology detection to the temporal resolution of satellite data. Int. J. Remote Sens. 30, 2061–2074. https://doi.org/10.1080/01431160802549237

8. Tables and figures

A. Acknowledgements

There hasn't been any other time in my life that has been so exciting and nerve-wrecking at the same time. These four years of PhD has probably shown it all – that life is full of surprises, some not so sweet ones, but there is always light at the end of the tunnel. Thank you Annette for bringing me to see this light. As my supervisor, you have not only helped me advance in my professional career with your timely comments on each piece of my work and writings but with your wisdom and experience, you helped me grow as a person. You even helped me find a comfortable housing which I now look back as being my "home".

I landed in Munich on a cold October morning and had it not been for Christian Schunk the journey from the airport to my temporary housing at Freising would not have been a happy memory today. Thank you, Eli and Nils for being the most wonderful "office mates" ever. Ye, thank you for making me fall in love with tea. Upasana, for being my Indian friend in the Chair. Renee, for being the first to help me figure out my ways in Freising. Wael for his funny and laid-back attitude. Thanks are also due to Sarah and Allan for being my mentors and helping me do better each time by providing timely and valuable suggestions. Discussions with you made my work more interesting. Marvin and Nicole, for being ever so ready with solutions to all my doubts-not just scientific ones but even with bureaucratic issues. Homa and Stefan, no amount of words are enough to express my gratitude for you. I have lost count of the number of emails, calls and message that I sent you days before my thesis submission. From helping me with translations to getting information from different offices, this submission would not have been possible without you. Thank you, Homa for waking up early to hand in my thesis at the doctoral office. This journey was also made easier by Brigette who has been the go to person for everything administrative-big or small. A big shout-out to you!!!.

A PhD, I believe is an amalgamation of hard work, loyalty, passion but also prayers and good wishes from my near and dear ones. I would like to thank my parents for their support and having faith in me even when I was not so sure of myself. Thank you Sourav, for your unflinching support. Your jokes about my student-life get me going through the hard times. My best friends- Aditya, Shakti and Adarsh, this journey would have been very different had it not been for you guys. You made me believe that one day my struggles would bear fruit. Our late night conversations (thanks to the time difference!) cheered me up on an otherwise

dull and tiresome day. Finally, thanks to my wife Rumia for being there all the while. Being a PhD student herself, she understood my trials and tribulations and never gave up on me.

B. Academic CV.

Curriculum Vitae

Gourav Misra

PERSONAL INFORMATION

Gourav Misra
gouravmisra@gmail.com; misra@wzw.tum.de
ORCID orcid.org/0000-0002-7973-8694

Sex Male | Date of birth 15/05/1988 | Nationality Indian

WORK EXPERIENCE

01/03/2018- present — Independent Consultant
- Remote sensing and GIS applications.

Business or sector Research

13/10/2014- 30/11/2017 — Research Associate
Professorship of Ecoclimatology, Technical University of Munich , Germany.
- Remote sensing of forest phenology under the Virtual Alpine Observatory (VAO) project.

Business or sector Research

06/06/2015- 27/06/2015 — Visiting Researcher
08/06/2016- 25/06/2016
Institute for Earth Observation, Eurac Research, Bolzano, Italy.
- Remote sensing of Alpine forest phenology.

Business or sector Research

19/08/2013- 30/09/2014 — Pre Doctoral Fellow
International Water Management Institute (IWMI), Colombo.
Duty Station: C/O. Dr. Tushaar Shah, Senior Fellow, IWMI, Anand-388001, India.
- Mapping of rain-fed and irrigated areas in Gujarat and Madhya Pradesh states of India using remote sensing and GIS techniques.
- Creating and maintaining GIS databases; and support for writing reports and journal publications.

Business or sector Research

14/05/2012- 14/11/2012 — Research Fellow
Punjab Remote Sensing Centre, Ludhiana, India.
- Study of bio-physical parameters of cotton crop and identification of cotton crop growing areas in Punjab, India.

Business or sector Research

EDUCATION AND TRAINING

10/2014- present — Ph.D. (*Dr. rer. nat)*
Professorship of Ecoclimatology, Technical University of Munich, Freising-85354.
- Studying the phenology of alpine vegetation with respect to changing climate using remote sensing techniques.

04/2012 — M.Sc. (Geoinformatics)
Faculty of ITC, University of Twente, The Netherlands.
- Distinction in thesis- "*Mapping Specific Crops and their Phenology: Multi-sensor and Temporal Approach*".
- Subjects- GIS, Remote Sensing, Mathematics, Programming in R, Databases-SQL and MS-Access, Photogrammetry, Image- Processing, Advanced Image- Analysis, etc.

05/2009 — B.Sc. (Agriculture)
Anand Agricultural University, Anand, India.
- Awarded distinction in B.Sc.
- Subjects- Agronomy, Horticulture & Forestry, Plant-physiology, Statistics, Agricultural-economics, Bio- Mathematics, Meteorology, etc.

Curriculum Vitae

Gourav Misra

RESEARCH INTERESTS

- Vegetation dynamics and phenology studies.
- Crop identification and irrigated area mapping.
- Time series analysis.
- Land use patterns and drivers.
- Climate change.

OTHER SKILLS

- Programming in R language for image processing and data analysis.
- Skilled in using remote sensing and GIS software like ERDAS Imagine, QGIS and ArcGIS.
- Database management using SQL and MS-Access.
- Experience in conducting field based studies and data collection.

PERSONAL SKILLS

Mother tongue(s): Odiya

Other language(s)

	UNDERSTANDING		SPEAKING		WRITING
	Listening	Reading	Spoken interaction	Spoken production	
English	C2	C2	C2	C2	C2
Hindi	C2	C2	C2	C2	C2

Levels: A1/A2: Basic user - B1/B2: Independent user - C1/C2 Proficient user

ADDITIONAL INFORMATION

Journal Publications

- Buras, A.; **Misra, G.**; Wimkling, M.; Sass-Klaassen, U,. Tundra land surface phenology heterogeneously mirrors glacier melt in South Norway. *(submitted; in review)*
- **Misra, G.**; Buras, A.; Heurich, M.; Sarah; A.; Menzel, A. LiDAR derived topography and forest stand characteristics largely explain the spatial variability observed in MODIS land surface phenology. Remote Sens. Environ 2018, 218, 231–244. **(part of Ph.D.)**
- **Misra, G.**; Buras, A.; Menzel, A. Effects of Different Methods on the Comparison between Land Surface and Ground Phenology- A Methodological Case Study from South-Western Germany. Remote Sensing 2016, 8, 753. **(part of Ph.D.)**
- Shah T., **Mishra, G.**, Kela, P., Chinnasamy, P. Madhya Pradesh's Irrigation Reform as a Model- Har Khet Ko Pani, Economic & Political Weekly 2016, Vol. 51.
- Chinnasamy, P.; **Misra, G.**; Shah, T.; Maheshwari, B.; Prathapar, S. Evaluating the effectiveness of water infrastructures for increasing groundwater recharge and agricultural production - A case study of Gujarat, India. Agricultural Water Management 2015, 158, 179–188.
- **Misra, G.**; Kumar, A.; Patel, N. R.; Zurita-Milla, R. Mapping a Specific Crop-A Temporal Approach for Sugarcane Ratoon. Journal of the Indian Society of Remote Sensing 2014, 42, 325–334.

Book Chapters

- **Misra, G.**; Misra, H.; Scott, C. A. Understanding Factors Influencing Hydro-climatic Risk and Human Vulnerability: Application of Systems Thinking in the Himalayan Region. In Climate Change, Glacier Response, and Vegetation Dynamics in the Himalaya; Springer International Publishing: Cham, 2016; pp. 251–267.

Curriculum Vitae

Gourav Misra

Symposiums/ Conferences

- **Misra, G.**; Buras, A.; Asam, S.; Menzel, A. Towards an improved Land Surface Phenology mapping using a new MODIS product: A case study of Bavarian Forest National Park. *Geophysical Research Abstracts EGU General Assembly* 2017, *19*, 2017–5158. (poster at EGU, Vienna, 24 April 2017)
- **Misra, G.**; Buras, A.; Asam, S.; Menzel, A. Mapping of Land Surface Phenology using a new MODIS product: A case study of Bavarian Forest National Park, Virtual Alpine Observatory Symposium, Bolzano, Italy, 28-30 March 2017.
- **Misra, G.**; Buras, A.; Menzel, A.; Management, E. Satellite based phenology detection of broadleaf forests in South-Western Germany. Geophysical Research Abstracts 2016, 18. (poster at EGU, Vienna, 18 April 2016)
- **Misra, G.**; Menzel, A. Satellite based phenology detection of broadleaf forests in south-western Germany. Virtual Alpine Observatory Symposium, Salzburg, 27-30 October 2015.
- **Misra, G.**; Kumar, A.; Patel, N. R.; Zurita-Milla, R.; Singh, A. Mapping specific crop- A multi sensor temporal approach. In International Geoscience and Remote Sensing Symposium (IGARSS); IEEE, 2012; pp. 3034–3037. (Oral presentation and symposium paper)

Courses studied

- Making Effective Scientific Presentations. TU Munich, 10/11- 20/11/2015.
- Advanced strategies for ecological data analysis. TU Munich, 25 /02- 13/05/2016.
- Statistics in DendRochRonology. TU Munich, 14 & 16/03/2016.

C. Re-prints of publications

This thesis consists of 2 accepted publications and one case study (to be submitted)

No restriction for reprints apply since:

1. Paper 1 (chapter 4.1) is open access.
2. Paper 2 (chapter 4.2) is allowed. Since the publisher allows authors to use full or part of the accepted article in their thesis and for non-commercial use. (please see: https://www.elsevier.com/about/policies/copyright/permissions, accessed: 17th January 2019)
3. Paper 3 (chapter 4.3) is an unpublished case study.

remote sensing

MDPI

Article

Effects of Different Methods on the Comparison between Land Surface and Ground Phenology—A Methodological Case Study from South-Western Germany

Gourav Misra [1,*], Allan Buras [1] and Annette Menzel [1,2]

[1] Ecoclimatology, Department of Ecology and Ecosystem Management, Freising, Technische Universität München, München 85354, Germany; buras@wzw.tum.de (A.B.); amenzel@wzw.tum.de (A.M.)

[2] Institute for Advanced Study, Garching, Technische Universität München, München 85748, Germany

* Correspondence: misra@wzw.tum.de; Tel.: +49-(0)-816-171-4748

Academic Editors: Geoffrey M. Henebry, Forrest M. Hoffman, Jitendra Kumar, Xiaoyang Zhang, Jose Moreno, Clement Atzberger and Prasad S. Thenkabail

Received: 27 June 2016; Accepted: 8 September 2016; Published: 13 September 2016

Abstract: Several methods exist for extracting plant phenological information from time series of satellite data. However, there have been only a few successful attempts to temporarily match satellite observations (Land Surface Phenology or LSP) with ground based phenological observations (Ground Phenology or GP). The classical pixel to point matching problem along with the temporal and spatial resolution of remote sensing data are some of the many issues encountered. In this study, MODIS-sensor's Normalised Differenced Vegetation Index (NDVI) time series data were smoothed using two filtering techniques for comparison. Several start of season (SOS) methods established in the literature, namely thresholds of amplitude, derivatives and delayed moving average, were tested for determination of LSP-SOS for broadleaf forests at a site in southwestern Germany using 2001–2013 time series of NDVI data. The different LSP-SOS estimates when compared with species-rich GP dataset revealed that different LSP-SOS extraction methods agree better with specific phases of GP, and the choice of data processing or smoothing strongly affects the LSP-SOS extracted. LSP methods mirroring late SOS dates, i.e., 75% amplitude and 1st derivative, indicated a better match in means and trends, and high, significant correlations of up to 0.7 with leaf unfolding and greening of late understory and broadleaf tree species. GP-SOS of early understory leaf unfolding partly were significantly correlated with earlier detecting LSP-SOS, i.e., 20% amplitude and 3rd derivative. Early understory SOS were, however, more difficult to detect from NDVI due to the lack of a high resolution land cover information.

Keywords: broadleaf forests; understory; phenology; start of season (SOS); leaf unfolding; match in LSP and GP

1. Introduction

Phenology, the science of periodic events in plant and animal life cycle, has been widely studied and well documented for many decades (e.g., [1–3]). It has been a core parameter for demonstrating and studying the impact of climate change on terrestrial ecosystems. However, the major drawback of traditional phenological observations (hereafter referred to as Ground Phenology (GP)) is the fact that they are labour intensive, localised and lacking global coverage, and cover only a limited number of species. The advent of modern remote sensing techniques provides a promising alternative and new opportunities for phenological studies [4], a departure from the traditional ground based observations

of phenology. In comparison to GP, remote sensing techniques provide a global coverage of data at various temporal and spatial scales, which can support the study of trends in phenology and its drivers.

Satellite based determination of vegetation phenology (hereafter referred to as Land Surface Phenology (LSP)) has been an active research area since the past two decades. Many studies have been conducted at global and local scales, which provide an ensemble of techniques and algorithms to handle varied spatial resolution and temporally discontinuous satellite data [5–10]. Though several methods exist for extracting phenological information or LSP from time series of satellite data, there have been only a few successful attempts to temporarily match GP with LSP [11–14]. Studies of such kind are known to be plagued with temporal and spatial resolution issues, where spatially continuous and pixel based or area averaged LSP-SOS have to be matched with spatially discontinuous and point-based, mostly species-specific GP. A further cause of mismatch in GP and LSP is the inherent difference in their respective definitions of phenology. GP is the visual interpretation of species-specific phenological phases such as bud-burst, leafing, flowering, etc., whereas LSP is defined in terms of area averaged intensity of dominant vegetation or canopy greenness and cover, including background such as soil and understory [6,15]. Moreover, the minute differences in phenology observed by ground volunteers might not be sufficient to produce changes in satellite measured reflectance of vegetation due to temporal and spectral limitations of satellite data [4,16]. Apart from differences in definition, LSP estimates are also known to be influenced by the methods used for corrections, smoothing, phenology detection [8,17], and the accuracy or homogeneity of land cover data analysed [18]. Despite the mentioned limitations, satellite data nevertheless may provide valuable and spatially continuous information about the LSP [19–21].

Among various available methods for determination of LSP, distinctions cannot be made to select a single best technique as such a decision would differ for various study areas, data and species studied [22–24]. Often various LSP-SOS have been matched with GP in form of leaf unfolding or a phenology index of vegetation [11–14] and past research has shown variability among various LSP measures. The selection of a LSP method for deriving or matching a specific GP event is therefore not so straightforward and more research is needed to attribute ecological meanings to various LSP-SOS methods [25].

Therefore, the central aim of this study is to test the hypothesis that different LSP-SOS correspond to specific GP-SOS observations. This is done by comparing and correlating various phases of GP with different measures of LSP obtained from two of many relevant smoothing algorithms (i.e., weighted Gaussian and Double Log) and using an ensemble of LSP-SOS detection methods established in the literature. Since GP and LSP have different definitions, an absolute match in terms of specific day of year is unlikely to occur. However, the general behaviour of trends in start of season from ground and satellite observations can be assumed to be fairly related, since both observe various starting points in the vegetation growth cycle [13,26]. Therefore in order to match GP and LSP, a three step validation was carried out as: (a) match in seasonality or mean onset dates; (b) match in climate change impacts in terms of temporal trends using linear regression techniques; and (c) match in inter-annual variation using correlations (see Section 2 for details).

In absence of reliable and high resolution land cover information, a successful match in LSP and GP might just be a matter of chance. In such a case there are higher chances of tracking species with similar behaviour, and it might be difficult to make any assumptions about the distribution of specific species in the study area as mentioned in Rodriguez-Galiano et al. [14]. In our study, GP-SOS are therefore used as reference points, and a higher correlation between LSP-SOS and GP-SOS only indicates the phenological similarity between pixel level LSP and species-specific GP during 2001–2013. This present study therefore calls for close scrutiny of studies comparing GP and LSP and addressing several important concerns. The first issue is the choice and reliability of data used, and compromising between spatial and temporal resolution of remote sensing data. The second is the choice of data processing and smoothing function used, which has to be decided according to data properties and can

affect the LSP estimates. The third important decision is regarding the ways of assessing the agreement between intrinsically different measures of SOS, i.e., GP and LSP.

2. Materials and Methods

2.1. Study Area and Data

The rural area east of Stuttgart (Figure 1) in the southwest of Germany covering an area of approximately 150 km^2 was selected for this study. The reason for choosing this particular site was the availability of a very detailed GP dataset. Data from various sources such as remote sensing Normalised Difference Vegetation Index (NDVI), land cover information (CORINE) and ground phenological data were used. The corresponding data sources are briefly described as below:

2.1.1. Remote Sensing Data

The Normalised Difference Vegetation Index (NDVI) data from the Moderate Resolution Imaging Spectrometer (MODIS) MOD13Q1 product was used for this study. These data are maximum value composites of 16 day and available at 231.65-m resolution. The NDVI and its corresponding pixel reliability information were downloaded from the MRT Web application of the United States Geological Survey website (https://mrtweb.cr.usgs.gov/) for 2001–2013.

2.1.2. Land Cover Data

The CORINE land cover (CLC) 2006 vector dataset was obtained from the European Environment Agency website [27] for determination of broadleaf forests in the study area. The CLC data for year 2006 has a reported 85% thematic and 100 m geometric accuracy.

2.1.3. Ground Phenological Data (GP)

The ground phenological (GP) observations for 2001–2013 were made at one single site east of Stuttgart, Germany, with surrounding agricultural areas and woods (48.73°N/9.26°E, elevation 410 m a.s.l.). Records were made by a highly dedicated naturalist, who also served as a phenological observer for the German Meteorological Service (DWD) for decades. He recorded the phenological development of numerous species 2–3 times a week following a permanent transect. Depending on the season and weather conditions, the entire transect took approximately 2–3 h by foot and a distance of 8–10 km was covered. For each species, onset dates of several phenological development stages were recorded. We used the phenophases leaf unfolding and forest greening-up of 8 and 13 common deciduous tree species, respectively, as well as leaf unfolding of 97 common understory species for our analysis. The leaf unfolding dates of 4 common conifer evergreen species were also included into the analyses (see Supplementary Figures S5 and S6 and Table S1 for complete details of GP). The leaf unfolding phase corresponds to the appearance of the first leaf (5%–10%) and the greening-up is the date when all leaves are out at their final size. This GP information was used for validation of the various satellite start of season estimates (LSP-SOS). Since the exact location of GP was not known, the GP was temporally linked with LSP (see Section 2.4 for details). From a limited ground survey in our study area, it was observed that the overstory of the forest stand marked as broadleaf species in CORINE cover were dominantly deciduous with presence of few conifer- evergreen tree species. The various GP observations were further grouped into understory comprising of Herbaceous Annuals, Herbaceous Perennials and Woody Perennials. The overstory species were grouped into coniferous- evergreen and deciduous species.

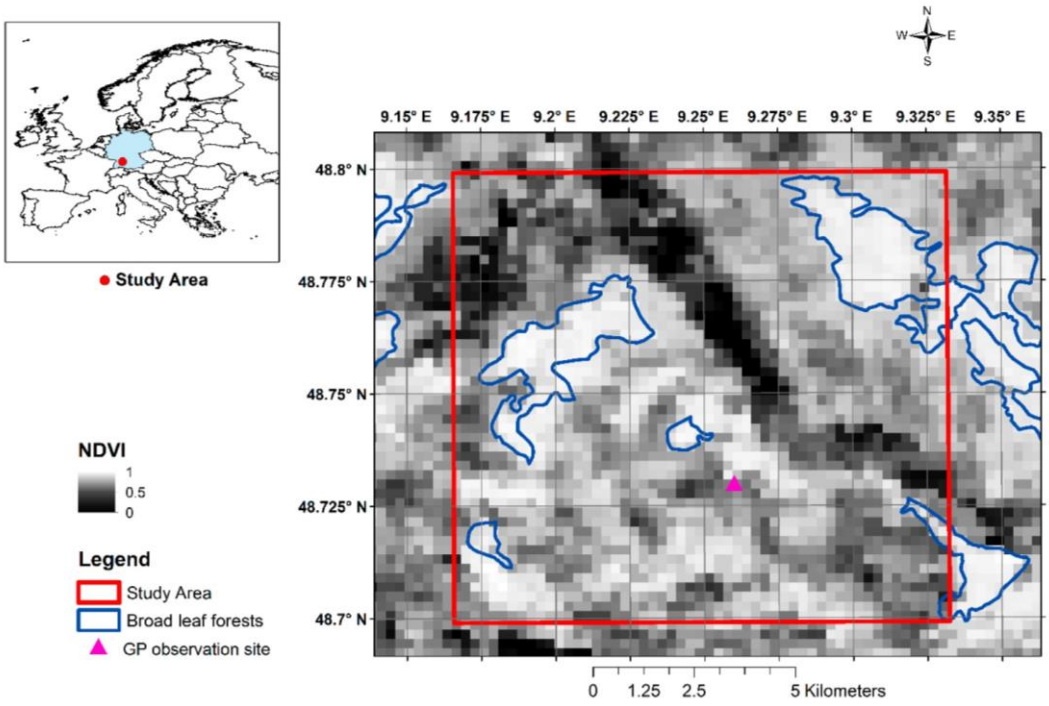

Figure 1. Study area and CORINE land cover map showing the distribution of broadleaf forests. (NDVI image is for day of the year (DOY) 145 in 2001). Inset: Location of study area in Germany.

2.2. Pre-Processing and Smoothing of Satellite Time Series Data

The times series of 16-day NDVI raster data from MODIS sensor for the years 2001–2013 were first layer stacked to obtain a time series of data for each pixel. The CORINE land cover mask was used to restrict the study to the broadleaf forests pixels only; 278 broadleaf forests pixels were finally assessed. In the NDVI time series of each pixel, data marked as good or marginal (in the corresponding pixel reliability information) were retained and those labelled as contaminated with snow or cloud or missing were removed. Thus, a raster stack of NDVI time series with reliable and uncontaminated values but with gaps was obtained. In order to create a complete NDVI time series, filling of gaps was done in two steps: (a) filling of winter gaps; and (b) linear interpolation of the remaining short gaps in 16-day data. The winter gaps of a pixel occurring in the months of December and January of each year were filled with the average of the available and uncontaminated winter NDVI from the same months in other years as in Beck et al. [7], Clerici et al. [28], and Forkel et al. [10]. Even though spurious NDVI values were removed, the time series still contained values supposed to be outliers due to high differences to the precedent and subsequent values. To cope with these "sudden spikes", a weighted Gaussian filter (the weighted Gaussian filter is explained in the Supplementary Material Equation (S1)) was applied to the time series. Deviations of raw NDVI from the Gaussian filtered data were z-transformed and values beyond two standard deviations were considered outliers and removed from the raw data, and replaced with the mean of the two neighbouring raw values. This outlier removed NDVI data were again smoothed using the weighted Gaussian filter. Alternatively, a double logistic smoothing function [7,29] was also applied to the outlier removed NDVI time series for testing one of the frequently used NDVI smoothing algorithms. In conclusion, the raw NDVI time series was initially filtered for obvious outliers using the Gaussian filter and then smoothed again using Gaussian or Double Log function to remove undetected outliers. A similar two-step process of outlier detection and consequently smoothing is also mentioned in [13,30]. All pixels in this study were treated in the same manner. An example of both smoothing methods is presented in Figure 2. The Gaussian and

Double Log smoothed NDVI time series were then spline and linearly interpolated to daily values, respectively. Different interpolations were used in order to retain much of the original shape of the 16-day smoothed NDVI for determination of LSP-SOS as described in Section 2.3.

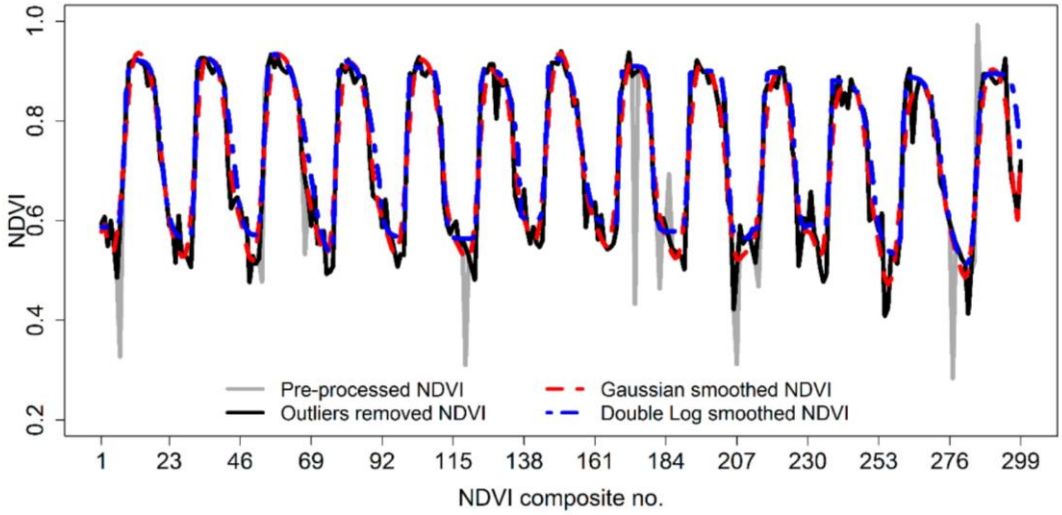

Figure 2. Illustration of smoothing of a pre-processed and outlier removed NDVI time series using Gaussian and Double Log functions. Note: In comparison to the Double Log smoothed NDVI, the Gaussian smoothed NDVI shows lower residuals in the winter troughs. The residuals in the non-winter period are almost similar for both the smoothing techniques.

2.3. Determination of Satellite Start of Season (LSP-SOS)

It has been observed by many researchers in the past [22,24,31,32] that different LSP-SOS derivation methods provide different results and therefore no single method can be claimed to best describe the phenology from satellite NDVI data. In this context Schwartz et al. [26] notes, "*though all (methods of LSP-SOS are) assessing the start of spring vegetation growth in some fashion, are effectively measuring different processes*". Hence, an ensemble of methods established in literature was used to determine several LSP-SOS in this study. The various start of season methods used for this study can be classified into three broad categories, namely thresholds of amplitude, delayed moving average (DMA) and rates of change (derivatives). The 20% [33,34], 50% [8,13,35], 60% and 75% [36] thresholds of amplitude determines the specific day of the year on which the smoothed NDVI time series crosses 20%, 50%, 60% and 75% of the NDVI amplitude of a given year. The delayed moving average [6,9,26,28] method used in this study is established from auto regressive moving average (ARMA) models that compare the NDVI time series with its moving average to determine the start of season. The derivatives, namely 1st [37–39], 2nd [38,40] and 3rd derivatives [32,38], determine the start of season as the date of the maximum increase in the respective NDVI derivative curve. As explained by Tan et al., 2011 [38], the local maxima of 1st derivative corresponds to the maximum rate of increase of green up phase, whereas, the local maxima of 2nd and 3rd derivative corresponds to the beginning of green up. In particular the SOS from 2nd derivative indicates the timing when the majority of pixel is turning green and 3rd derivative indicates where the change of green up rate is greatest (first flush of greenness on the ground). For ecological and detailed interpretation of these approaches, we refer to the cited literature.

2.4. Methods of Matching Satellite (LSP) and Ground (GP)-SOS

The objective of matching GP- and LSP-SOS was studied based on SOS obtained from a single regionally averaged NDVI time series as well as individual pixel SOS at native MODIS resolution of 231.65 m. The SOS from the regional averaged NDVI was compared with the SOS averaged from native resolution NDVI in order to check whether an spatially or regionally averaged NDVI could track the general behaviour of the local area phenology as mentioned in Atzberger et al. [41]. A three step validation between GP and LSP-SOS was carried out in this study as: (a) match in seasonality or mean onset dates; (b) match in climate change impacts (temporal trends) using linear regression analysis, where the slope of linear regression between time and SOS was used to compare the resulting trends; and (c) match in inter-annual variation of SOS using a Spearman's rank correlation measure. Correlations with $p < 0.05$ were considered to be significant for this study. Since the exact location and sub-pixel proportion of species was not known, each pixel in reality could be anything between a homogenous stand to a mixture of several species. Therefore each pixel LSP-SOS time series was correlated to each of the species-specific GP-SOS as mentioned in [13,14]. Our study uses specific GP-SOS records as reference points, and intends to show similarity in phenological behaviour of pixels (LSP) marked as broadleaf forests in CORINE land cover and species-specific GP during 2001–2013. The means and trends of LSP-SOS for individual pixels (analysis at native MODIS resolution of 231.65 m) were also checked for spatial dependence using a two-tailed correlation analysis. Finally, correlation strength among GP of species was also measured to examine the inter-species similarity with respect to inter-annual GP-SOS behaviour.

3. Results

3.1. Intra- and Inter-Annual Variability of LSP-SOS

Figure 2 shows the Gaussian and Double Log smoothed NDVI time series. It can be seen that the Gaussian filter was able to follow the winter troughs better than the Double Log function. In addition the variance of start of season dates and their annual means obtained from different methods was better described using the Gaussian smoothed NDVI (Figure 3). The different LSP-SOS methods showed more variability and differentiation when applied for the Gaussian smoothed series, whereas the Double Log did not differentiate well among the derivatives. Hence, the Gaussian smoothed time series is selected for further discussion in this paper (please refer to the Supplementary Figures S3 and S4 for Double Log smoothed results). The years 2007, 2009 and 2011 reveal relatively early mean LSP-SOS and on visual inspection they strongly correspond to the GP observations (see Supplementary Figure S5 for species specific GP-SOS time series). The year-to year variability in SOS reflects the different spring weather patterns. Overall the trends for LSP-SOS obtained from both smoothing methods show higher variability in the 2nd and 3rd derivatives, and lower variability for the 50%, 60% and 75% amplitudes and the 1st derivative (Figure 3). On average, the trends for 20% amplitude and 3rd derivative were positive, and the rest of the LSP-SOS methods provided negative trends, indicating an advance in onset over time.

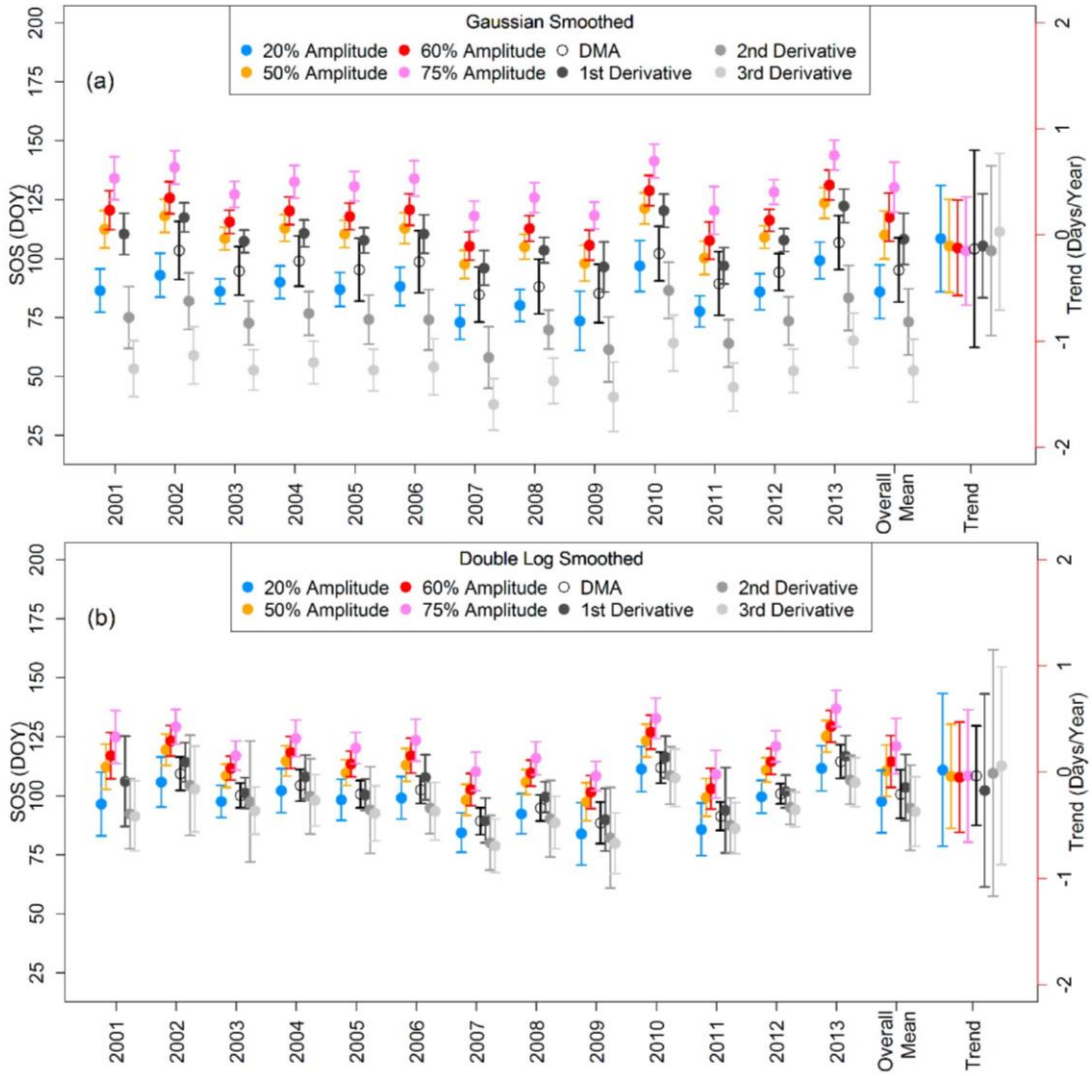

Figure 3. LSP-SOS from (**a**) Gaussian and (**b**) Double Log smoothed NDVI for broadleaf pixels using various methods (spatially averaged SOS for specific years as filled-coloured circles and one standard deviation as error bars). Overall mean is the mean SOS (2001–2013), which is a temporal and spatially averaged measure of LSP-SOS. The temporal trends in days/year (right y-axis) for all pixels' LSP-SOS are given as means and respective one standard deviation during 2001–2013. The year-to year variability in SOS reflects the different spring weather patterns.

3.2. Mean LSP-SOS and Their Trends

The spatial heterogeneity of LSP-SOS of broadleaf pixels in the study area is well captured in Figure 4a,b. The figure show the time averaged LSP-SOS (2001–2013) and the respective linear trends of the broadleaf pixels in the study area. However, no significant spatial correlation (at $p < 0.05$, two-tailed) was found between each mean LSP-SOS and its respective trends for any of the different methods.

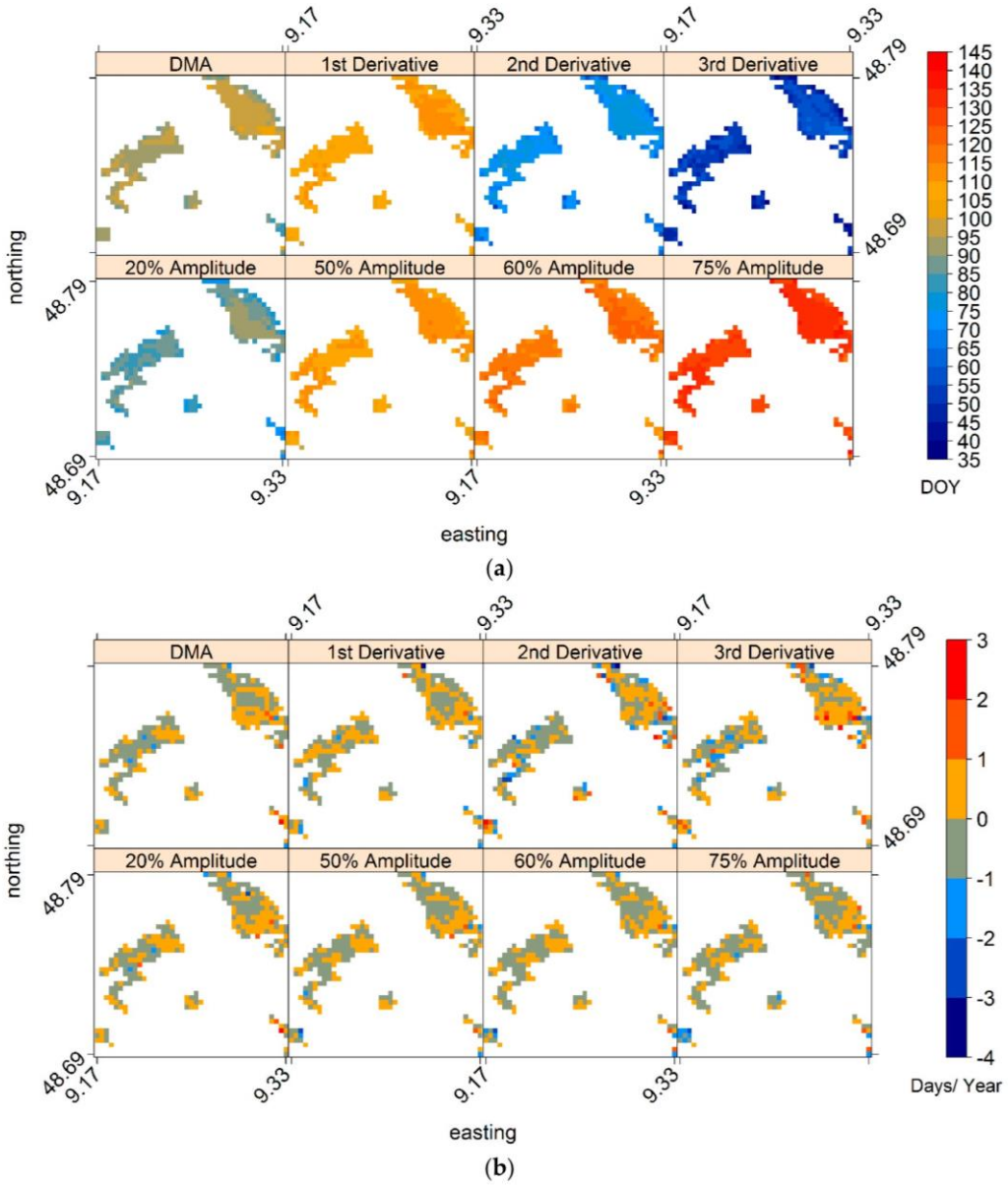

Figure 4. (**a**) Mean LSP-SOS (day of year) for the broadleaf pixels in the study area; (**b**) Linear trends of LSP-SOS (days/year) for the broadleaf pixels in the study area.

3.3. Comparison of Means and Trends of LSP-SOS and GP-SOS

The means and linear trends of GP and LSP were compared to analyse the effect of choosing different LSP-SOS extraction methods from NDVI (Figure 5). The various methods of LSP extraction revealed a wide range of SOS annual means and trends with major overlaps for both axes in particular for trends. Among all the methods of LSP-SOS extraction, the 20% amplitude, and 2nd and 3rd derivative SOS occur earliest in the calendar year and match better with the mean GP-SOS of understory species; however, there was a large disagreement in their respective observed mean trends. The other methods to determine LSP-SOS (50%, 60% and 75% of amplitude and 1st derivative) matched better with GP-SOS, both in trends and mean of broadleaf unfolding and greening, which occur in the later spring of the calendar year.

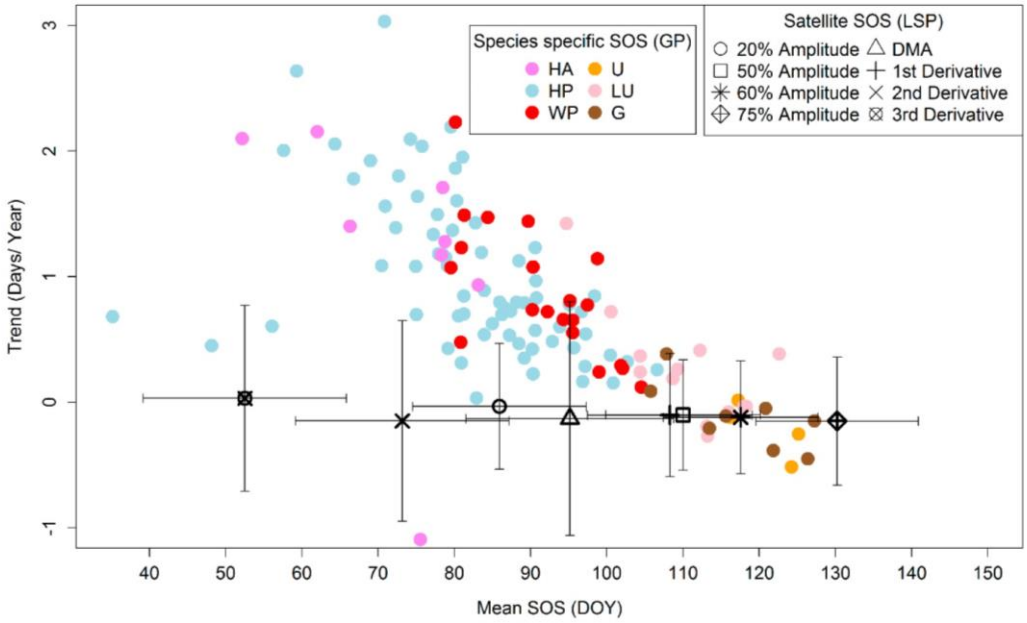

Figure 5. Comparison of LSP-SOS from Gaussian smoothed NDVI (mean LSP-SOS as special symbols in black and one standard deviation as error bars) and various species-specific GP-SOS (as filled and coloured circles, refer to Supplementary Table S1). Numbers are given in order of increasing mean SOS. Codes for GP: HA (herbaceous annuals), HP (herbaceous perennials) and WP (woody perennials) refer to understory leaf unfolding dates; U (Conifers leaf unfolding); LU (leaf unfolding) and G (greening) of broadleaf species (see Supplementary Table S1 for complete details of species-specific information).

3.4. Inter-Annual Variations of GP-SOS and LSP-SOS

The match in inter-annual variations of GP-SOS and LSP-SOS was assessed by non-parametric Spearman's rank correlation. Since the exact location and sub-pixel proportion of species was not known, each pixel LSP-SOS time series was correlated to each of the species-specific GP-SOS. Some of the species' SOS are higher correlated with specific methods of LSP extraction (see Supplementary Figure S2 for details). Figure 6 displays Spearman's rank correlations coefficients (at $p < 0.05$, one-tailed positive) between selected GP-SOS of understory/broadleaf species and selected LSP-SOS for all pixels in the study area. In general, leaf unfolding of understory species was found to be well correlated with LSP-SOS derived by methods covering the earlier part of the calendar year such as 20% amplitude and 3rd derivative, when the understory is believed to be dominant and the canopy cover of broadleaves is still minimal. LSP-SOS methods covering the later part of the year (i.e., 50% and 75% amplitude, and 1st derivative) strongly correlated with leaf unfolding and greening, when the canopy of the broadleaf tree species or overstory is mature and full.

GP-SOS of late understory species were better described by LSP-SOS methods providing onset dates of the later part of the year (namely 75% amplitude and 1st derivative). This behaviour of late understory phenology was similar to that of broadleaf phenology and was also mirrored in the correlations between the various species-specific GP in Figure 7. This correlation matrix revealed two phenological clusters, one for early understory and a second for late understory and broadleaf species. The early understory GP was, however, very different from the second cluster and was best (i.e., most significantly correlated pixels) described by early LSP-SOS methods such as 20% amplitude and 3rd derivative. For example, the raster maps in Figure 6 revealed higher significant correlations for: (1) early understory, i.e., *Myosotis sylvatica* (mean SOS = 70.5) with early LSP methods such as 20% amplitude and 3rd derivative; and (2) late understory, i.e., *Lathyrus niger* (mean SOS = 102.7) and broadleaf greening, i.e., *Fagus sylvatica* (mean SOS = 120.9) with 75% amplitude and 1st derivative.

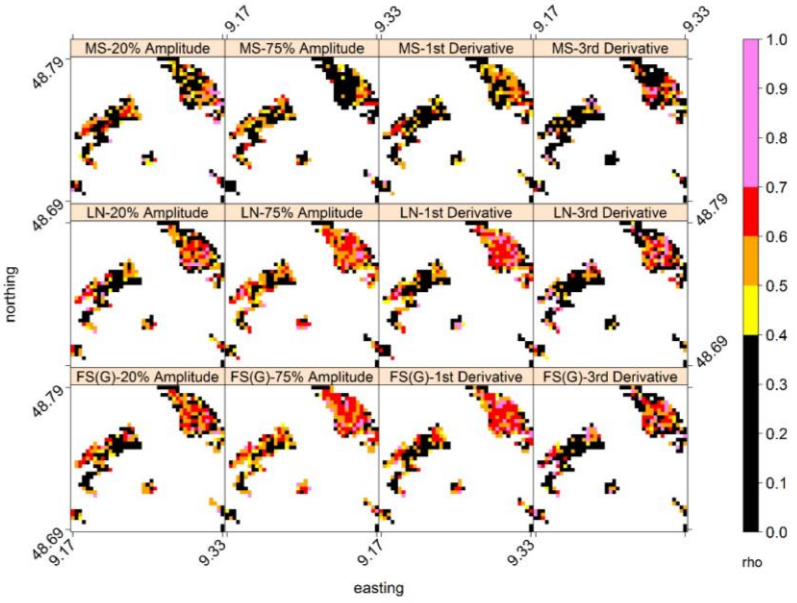

Figure 6. Maps showing Spearman's rank correlations ($p < 0.05$, one-tailed positive) between LSP-SOS and GP-SOS for selected understory and broadleaf tree species. MS, *Myosotis sylvatica* (leaf unfolding); LN, *Lathyrus niger* (leaf unfolding); and FG(G), *Fagus sylvatica* (greening), with mean SOS of 70.5, 102.7 and 120.9 day of year, and species ID/No. 12, 95 and 119, respectively. Note: The mean correlations of each species GP-SOS over the study area are shown in Figure S2 in supplement. Refer to Table S1 for details of GP-SOS.

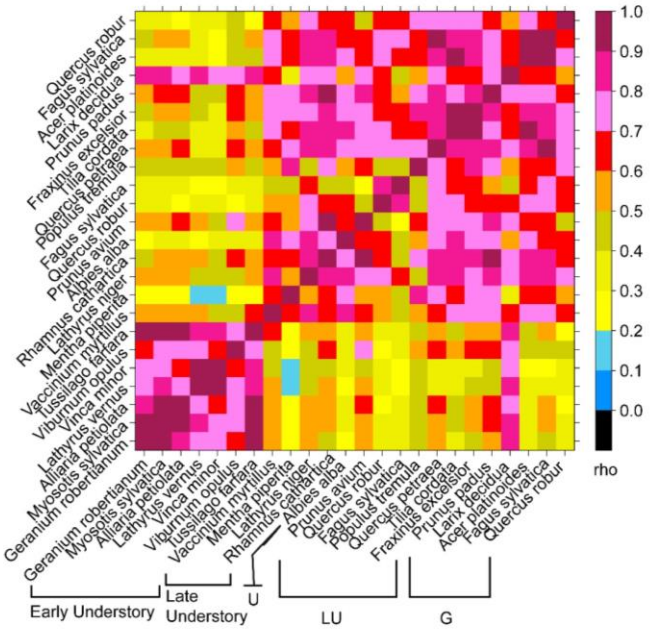

Figure 7. Spearman's rank correlation matrix for selected species-specific GP-SOS; the heatmap confirms that the phenology of many late understory species is highly correlated with broadleaf tree phenology. Note: Species are arranged in increasing order of their mean SOS; refer to Supplementary Table S1 for details of species-specific information.

3.5. Analyses Based on Spatially Averaged NDVI Time Series

The analyses of LSP-SOS at the native MODIS resolution of 231.65 m revealed the spatially heterogeneous behaviour of broadleaf pixels in the study area. Hence, an analysis at a regional scale was also undertaken by averaging the daily NDVI of the pixels. This spatially aggregated or regionally averaged NDVI time series was expected to capture the general phenological behaviour of the broadleaf pixels of the region. LSP-SOS by the different methods were then estimated from this averaged NDVI time series as described earlier. The annual LSP-SOS from this regionally-averaged NDVI time series strongly agreed with the annual averaged LSP-SOS obtained from the native MODIS scale with $R^2 = 0.99$ (Figure 8). The agreement was worse in the early part of the year when the NDVI is expected to be a mixture of understory, broadleaf and other background, e.g., soil.

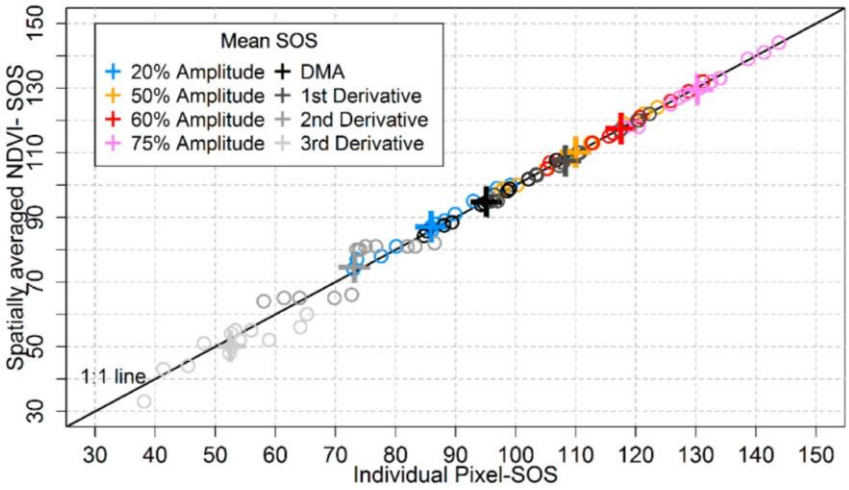

Figure 8. Comparison of LSP-SOS time series (day of year) obtained from spatially or regionally averaged NDVI for the broadleaf pixels in the study area (y-axis) and SOS averaged from single/individual pixels SOS (x-axis). Note: SOS time series as coloured unfilled circles and its mean as coloured crosses.

In order to analyse the match in inter-annual variability annual LSP-SOS from the spatially or regionally-averaged NDVI and GP-SOS time series were correlated by Spearman's rank correlations (Figure 9). Most of the significant and high coefficients (at $p < 0.05$, one-tailed positive) were revealed for broadleaf unfolding and greening. However, leaf unfolding of very few early understory species such as *Geranium robertianum*, *Myosotis sylvatica* and *Alliaria petiolata* displayed significant and high correlations for 20% amplitude method. Leaf unfolding of late understory as well as greening of broadleaf tree species showed significant and higher correlations with LSP-SOS by 75% amplitude or 1st derivative. This indicates that the choice of LSP method should be governed by the species and the phenophase under study.

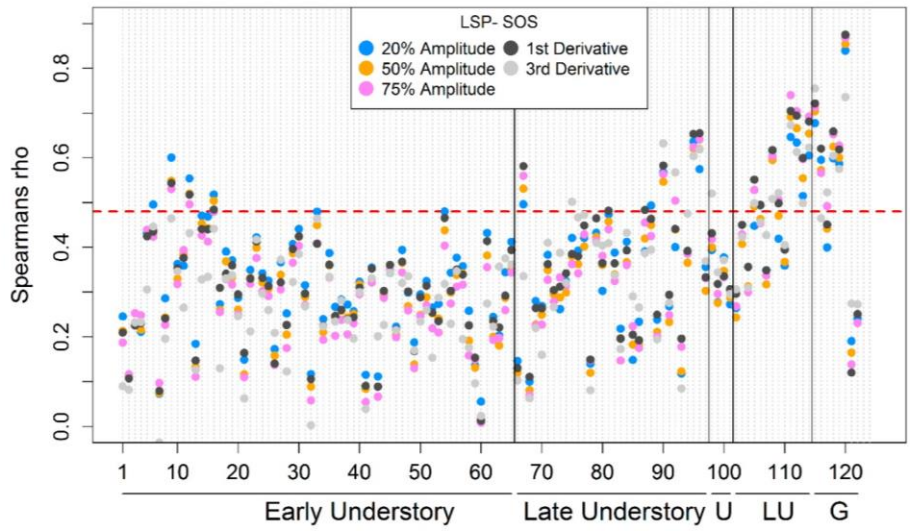

Figure 9. Spearman's rank correlation coefficients between GP-SOS and selected LSP-SOS based on a regionally averaged NDVI for broadleaf pixels during 2001–2013. Region above dotted horizontal red line comprises significant correlation coefficients, $p < 0.05$. Note: Species on the x-axis are grouped according to traits (Early Understory = leaf unfolding of early understory, Late Understory = leaf unfolding of late understory, U = leaf unfolding of conifers, LU = leaf unfolding of broadleaf species and G = greening of broadleaf species) and arranged in order of increasing mean GP-SOS; the x-labels are species ID number (see Supplementary Table S1 for complete details of GP).

4. Discussion

4.1. The Choice of Data Processing Technique

The smoothing of NDVI time series by two methods revealed considerable differences in the final smoothed NDVI (Figure 2) and eventually the LSP-SOS estimates from each method (Figure 3), as it has also been mentioned in Jönsson and Eklundh [17], White et al. [8] and Atkinson et al. [30]. Especially the winter troughs were better fitted by the Gaussian filter than the Double Log function (Figure 2). Since in the study area winters are not too long and continuous, the retention of winter troughs for broadleaf forests may still provide meaningful information. In addition, pre-processing before smoothing, e.g., outlier removal and gap filling of NDVI data, equally affect LSP-SOS estimates [28]. This indicates that each step of data processing and smoothing adds some uncertainty to the original data, and thus should be wisely decided by the researcher. The Double Log function used in this study was proposed by Beck et al. [7] for modelling of vegetation cycles in higher northern latitudes where the vegetation is completely inactive during the long winters. He therefore estimated the missing winter NDVI from the maximum value of first/last snow free winter NDVI values in the time series and then assumed it to be constant through all the winters. In another study by Tan et al. [38], first the growing season was defined by a minimum temperature threshold and values below this were removed, and connected by a line. Some studies substituted all gaps, winter or summer with the seasonal mean obtained from the time series [10,28,35]. However, in this present study winter and summer gaps were treated differently (see Section 2.2). The identification of outliers, their removal and subsequent filling is debatable, and has been handled by different authors in varied ways [13,17,28,42]. From a review of literature, the absence of agreement among researchers in gap filling is evident and this disagreement persists in the other steps of data handling. Since several ways have been proposed to handle noisy data, the choice of data processing should therefore be governed by the properties of the data, amount of noise and the area under study.

4.2. Mean of LSP- and GP-SOS

The inter-annual pattern of mean LSP-SOS (Figure 3) obtained from both the smoothing methods matched strongly with the GP-SOS records (see Supplementary Figure S5). The years 2007, 2009 and 2011 indicate a relatively early mean SOS for the majority of species, where these years also show higher preseason (March–April) temperatures, confirming the temperature dependence of vegetation SOS [1,2,43]. This general match in inter-annual pattern of mean SOS obtained from different LSP methods and GP was also reported by Schwartz et al. [26]. For the sake of brevity, the results from the Gaussian smoothed NDVI time series are discussed here forth (refer to Supplementary Figures S3 and S4 for results of Double Log smoothing results). The various mean LSP-SOS estimates (Figure 5 and Supplementary Figure S1) indicate that each method corresponds to a particular region of the seasonal NDVI growth curve and therefore mirrors specific seasonal occurring GP-SOS observations. In this present study, among all the methods of LSP-SOS extraction, a few such as 20% amplitude, 2nd and 3rd derivative SOS that occur earliest in the calendar year, and match better with the mean GP-SOS of understory species. The other methods of LSP-SOS (50%, 60% and 75% of amplitude and 1st derivative) match very strongly with mean GP-SOS of broadleaf unfolding and greening, and occur later part in the year.

4.3. Trends in LSP- and GP-SOS

In this study, the GP-SOS observations reveal a positive trend for understory, i.e., leaf unfolding of understory species occurring later over the last 13 years, and a weaker positive and even some negative (earlier) trends for broadleaf species which were observed in later spring (Figure 5). In contrast, although LSP-SOS dates spread over the whole spring season depending on the method applied as found by Studer et al. [12], Hird and McDermid [44] and White et al. [8], their temporal trends were quite uniform indicating almost no change over the study period. In contrast to Fu et al. [24] who reported stronger advancing trends of GP-SOS than of LSP-SOS (2000–2011) in central Europe, our study for southwestern Germany (2001–2013) sees for early season events stronger advancing of LSP-SOS than of GP-SOS of understory species.

It is therefore important to attribute specific LSP methods to specific GP, as also noted by some previous studies [25,26]. In general, the earliest LSP-SOS dates based on 2nd and 3rd derivative equally revealed positive trends for 42% and 52% of the pixels, respectively. The last LSP-SOS dates, i.e., based on the 60% and 75% amplitude, revealed negative trends for 59% and 63% of pixels, respectively. On average, trends for 20% amplitude and 3rd derivative were positive and the rest of the LSP-SOS methods revealed negative trends. The largest mismatches in trends from GP-SOS and LSP-SOS (2nd, 3rd derivatives and 20% amplitude) occurred in the early part of the year, i.e., the early understory leaf unfolding occurring before the 90th day of the year.

4.4. Inter- and Intra-Annual Variability in LSP- and GP-SOS

The correlation analyses between GP-SOS and LSP-SOS confirmed these findings, since GP-SOS of specific species matched better with specific LSP-SOS methods (Supplementary Figure S2). Different categories of GP, i.e., early understory, late understory and broadleaf species dictated the different best performing LSP method. The early understory species (e.g., *Geranium robertianum*, *Myosotis sylvatica*, *Alliaria petiolata*) were better correlated with the earliest detected LSP-SOS method such as the 3rd derivative and 20% amplitude. Alternatively, leaf unfolding of broadleaf species (e.g., *Fagus sylvatica*, *Quercus petraea*, *Fraxinus excelsior*) and greening (e.g., *Fagus sylvatica*, *Quercus robur*, *Prunus padus*) significantly corresponded to the later detected LSP-SOS methods such as the 75% amplitude and 1st derivative. The understory species with late GP-SOS (*Vinca minor*, *Lathyrus niger* and *Rhamnus cathartica*), however, were significantly related to LSP-SOS based on the 75% amplitude and 1st derivative. This similarity in the phenological behaviour of late understory and broadleaf species was also revealed by the two clusters obtained from correlation analysis between

GP-SOS observations comprising two phenologically similar clusters, first for early understory and second for late understory and broadleaf species. In addition, we also correlated GP-SOS and LSP-SOS with mean SOS and trends of corresponding pixels (not shown). Although no clear pattern was observed, there was an indication of earlier LSP-SOS mirroring early understory GP-SOS and the later LSP-SOS pixels corresponding strongly with broadleaf phenology.

In general, the inter-annual variability in GP-SOS decreased as the season progressed in time (Supplementary Figure S6), which also corresponds well to LSP-SOS based on the different methods operating in the various regions of the NDVI curve (Figure 3). Apart from the mean GP-SOS and its trends, the early detecting LSP-SOS in form of 20% amplitude and 3rd derivative were also able to capture the high inter-annual variability of early species GP-SOS (understory) occurring before 90th day of the year (Supplementary Figure S6). These early species are limited by the frost period and hence show higher response to temperature fluctuations and therefore a higher inter-annual variability in their SOS [45,46]. The lower correlations of early understory species' GP-SOS with LSP-SOS could be due to the short time series of data or may be due to artefacts introduced in smoothing of early season NDVI. In comparison, species with later GP-SOS, however, had lower variability in their SOS, which was also evident in the corresponding LSP-SOS such as 75% amplitude and 1st derivative. The broadleaf species with later GP-SOS showing higher correlations with the mentioned LSP-SOS (75% amplitude and 1st derivative) can be classified as either climax or intermediate species according to their successional strategy [47].

As discussed before, previous research has provided a variety of LSP-SOS methods for detection of start of season, which in turn has been analysed for matching with GP. However, our study clearly demonstrates that specific LSP methods are tightly linked to specific GP phases. Our study also indicates that in order to match LSP estimates with GP, a complete knowledge of the species composition of the landscape is required. Since in heterogeneous landscapes the satellite green-up might actually capture the understory green-up that occurs several weeks earlier than broadleaf overstory greening. In absence of detailed land cover information, it is difficult to attribute the changes in NDVI profile (for estimating LSP-SOS) to changes in either overstory or understory [4,18].

4.5. Does the Regionally Averaged NDVI Capture the General Behaviourof Local Area Phenology?

To tackle the issue of heterogeneity of LSP at individual pixel level and due to the lack of detailed ground-truth information for each pixel, the pixel based NDVI was averaged to a daily measure for the broadleaf pixels in the study area. It was expected to capture the general trend of the broadleaf forests' phenology, though losing the specific behaviour of the pixels. The LSP-SOS obtained from this regionally averaged-NDVI was found to have a strong linearity ($R^2 = 0.99$) with the averaged LSP-SOS obtained from individual pixels (Figure 8). The maximum departure in the LSP-SOS pairs occurred in the early part of the calendar year, which covers understory growth period. Here, the NDVI is expected to be a contribution of understory and/or dormant overstory and/or background (e.g., soil). The positive trends for the early understory in the pixel based LSP-SOS were lost in the LSP-SOS obtained from averaged NDVI. As mentioned earlier we emphasize the importance of having a reliable land cover classification at high resolution for both understory and broadleaf forests. In absence of such reliable land cover information, the uncertainty in NDVI is higher, especially in the earlier part of year and thus also increasing the uncertainty in the LSP-SOS extracted. However, in the later part of the year, when the broadleaf canopy is mature and full, the uncertainty in NDVI is expected to decrease since NDVI predominantly provides broadleaf canopy reflectance, though the information about specific species within the pixel would still be lacking. The correlation measure of the regionally-averaged NDVI SOS and the species-specific GP-SOS yield similar results as with the pixel level-native resolution LSP-SOS. In general, it was observed that GP of early understory species were highly correlated with earliest LSP methods such as 20% amplitude or 3rd derivative, whereas the GP of late understory and broadleaf were strongly correlated with later occurring LSP methods such as 75% amplitude or

1st derivative (Figure 9). There were, however, only a few species of early understory corresponding to LSP-SOS, indicating the general difficulty in detecting their phenology.

4.6. Detecting Specific GP in NDVI Curves

The success in matching LSP-SOS with GP is most likely linked as whether the understory species can be seen as typical for the broadleaf forest communities. Then, their phenology of explicitly covering the spring gap before full canopy maturity is adjusted to the climax species' phenology and therefore might be mirrored in the respective NDVI curves. Additionally, the possibility of finding an important phenological event in the interpolated period of NDVI would only increase the uncertainty of LSP-SOS estimates along with the sub-pixel heterogeneity issue [28,42]. For example, bud break, the first noticeable swelling of the buds is traditionally a phase recorded in GP but is reportedly undetectable in LSP. Definitively, phenological phases such as bud break are a too small feature or event to produce detectable changes in the NIR band of satellite sensor [4]. The mixing of bud burst signals with pre-existing understory might also be another reason for the poor detection of early phenophases of broadleaf species. Fisher and Mustard [15] indicate this in their study where inter-annual behaviour of LSP-SOS obtained from 50% amplitude of NDVI indicated a stronger linear relationship with GP records of greening of 75% of leaves than with 50% bud break. Soudani et al. [42] also reported a better performance of the inflection point of the fitted NDVI curve or late LSP-SOS with the start of onset of greening in 90% of trees, whereas the day of minimum NDVI or earlier LSP-SOS showed higher agreement with the earlier phase of onset of greening i.e., in 10% of trees. As pointed out by Nagai et al [48] NDVI thresholds may also be used to detect spring phenology of broad-leaved forests. However, our results suggest that an overall threshold may not account for the vegetation type specific differences of spring phenology. Though earlier research has reported a better agreement of some specific LSP methods with some GP phases, but none of them had systematically tested the performance of various LSP methods with a variety of GP observations. Hence, our paper reveals some of the characteristics of commonly used LSP estimation methods, their variability and its agreement with GP observations. Since there seems to be a fair indication of correspondence of specific GP-SOS to specific LSP-SOS, we therefore suggest that the 20% amplitude and 3rd derivatives are the best measures of early understory SOS; and 75% amplitude and 1st derivative to best correspond with broadleaf SOS. However, these results need to be tested further with improved data resolution and at different sites.

5. Conclusions

This paper aimed at studying the LSP of broadleaf forests and to assess its agreement with a rich set of GP observations for specific species. The problem of attributing or matching pixel based LSP estimates to GP of specific species is one of the important underlying limitations of this paper and many similar studies. A variety of available LSP-SOS estimation methods were tested and revealed an inherent uncertainty associated with the initial processing and smoothing of data, estimation of LSP-SOS and finally the validation with GP. Therefore, this study reveals and discusses some of the limitations of LSP studies from remote sensing data.

It was found that the agreement between GP and LSP method is governed by the species and phenophase under study. Broadleaf species and late understory occurring after the 90th day of the year reveal stronger significant correlation ($p < 0.05$) with late detected LSP methods such as 75% amplitude and 1st derivative, whereas early understory reveal stronger significant correlation ($p < 0.05$) with early detected LSP methods like 20% amplitude and 3rd derivative. There were several mismatches either in mean SOS or trends or both when comparing GP of species and LSP, which accentuate the need for detailed studies with data quality of highest order. The limitations of using a 13-year length satellite NDVI time series also have to be considered. Past studies and our analyses indicate the importance of a reliable land cover map both for understory and broadleaves, in order to improve our understanding of phenology from LSP and relate it to GP. Even though the results from this study are specific to a

small area and a specific GP dataset, it nonetheless provides vital insights into problems of matching LSP estimates with GP observations. We therefore recommend careful analyses of LSP methods and land use cover of the study area for future studies and redoing similar analyses in other regions.

Supplementary Materials: The following are available online at www.mdpi.com/2072-4292/8/9/753/s1, Equation (S1) Weighted Gaussian filter, Figure S1: Gaussian smoothing results-I, Figure S2: Gaussian smoothing results-II, Figure S3: Double Log smoothing results-I, Figure S4: Double Log smoothing results-II, Figure S5: Time series of GP-SOS-I, Figure S6: Time series of GP-SOS-II and Table S1: showing Mean-SOS and trends of species-specific GP and their ID numbers (No.).

Acknowledgments: The authors would like to thank the MODIS team and the CORINE land cover team for making the data freely available. This study was funded by the Virtual Alpine Observatory project of the Bavarian State Ministry of the Environment and Consumer Protection (VAO II TP II/01 TUS01UFS-67090).

Author Contributions: Gourav Misra and Annette Menzel conceptualized the design of the study. Gourav Misra carried out the data processing with support from Allan Buras and wrote the manuscript. All authors contributed to the interpretation of results and editing of the manuscript.

Conflicts of Interest: The authors declare no conflict of interest. The founding sponsors had no role in the design of the study; in the collection, analyses, or interpretation of data; in the writing of the manuscript, and in the decision to publish the results.

References

1. Menzel, A.; Fabian, P. Growing season extended in Europe. *Nature* **1999**, *397*, 659.
2. Menzel, A.; Sparks, T.H.; Estrella, N.; Koch, E.; Aasa, A.; Ahas, R.; Alm-KüBler, K.; Bissolli, P.; Braslavská, O.; Briede, A.; et al. European phenological response to climate change matches the warming pattern. *Glob. Chang. Biol.* **2006**, *12*, 1969–1976. [CrossRef]
3. Schwartz, M.D. *Phenology: An Integrative Environmental Science*; Tasks for Vegetation Science; Springer Netherlands: Dordrecht, The Netherlands, 2013.
4. Badeck, F.W.; Bondeau, A.; Böttcher, K.; Doktor, D.; Lucht, W.; Schaber, J.; Sitch, S. Responses of spring phenology to climate change. *New Phytol.* **2004**, *162*, 295–309. [CrossRef]
5. Lloyd, D. A phenological classification of terrestrial vegetation cover using shortwave vegetation index imagery. *Int. J. Remote Sens.* **1990**, *11*, 2269–2279. [CrossRef]
6. Reed, B.C.; Brown, J.F.; VanderZee, D.; Loveland, T.R.; Merchant, J.W.; Ohlen, D.O. Measuring phenological variability from satellite imagery. *J. Veg. Sci.* **1994**, *5*, 703–714. [CrossRef]
7. Beck, P.S.A.; Atzberger, C.; Høgda, K.A.; Johansen, B.; Skidmore, A.K. Improved monitoring of vegetation dynamics at very high latitudes: A new method using MODIS NDVI. *Remote Sens. Environ.* **2006**, *100*, 321–334. [CrossRef]
8. White, M.A.; de BEURS, K.M.; Didan, K.; Inouye, D.W.; Richardson, A.D.; Jensen, O.P.; O'Keefe, J.; Zhang, G.; Nemani, R.R.; van Leeuwen, W.J.D.; et al. Intercomparison, interpretation, and assessment of spring phenology in North America estimated from remote sensing for 1982–2006. *Glob. Chang. Biol.* **2009**, *15*, 2335–2359. [CrossRef]
9. Ivits, E.; Cherlet, M.; Mehl, W.; Sommer, S. Ecosystem functional units characterized by satellite observed phenology and productivity gradients: A case study for Europe. *Ecol. Indic.* **2013**, *27*, 17–28. [CrossRef]
10. Forkel, M.; Migliavacca, M.; Thonicke, K.; Reichstein, M.; Schaphoff, S.; Weber, U.; Carvalhais, N. Codominant water control on global interannual variability and trends in land surface phenology and greenness. *Glob. Chang. Biol.* **2015**, 3414–3435. [CrossRef] [PubMed]
11. Fisher, J.; Mustard, J.; Vadeboncoeur, M. Green leaf phenology at Landsat resolution: Scaling from the field to the satellite. *Remote Sens. Environ.* **2006**, *100*, 265–279. [CrossRef]
12. Studer, S.; Stöckli, R.; Appenzeller, C.; Vidale, P.L. A comparative study of satellite and ground-based phenology. *Int. J. Biometeorol.* **2007**, *51*, 405–414. [CrossRef] [PubMed]
13. Hamunyela, E.; Verbesselt, J.; Roerink, G.; Herold, M. Trends in spring phenology of Western European deciduous forests. *Remote Sens.* **2013**, *5*, 6159–6179. [CrossRef]
14. Rodriguez-Galiano, V.F.; Dash, J.; Atkinson, P.M. Intercomparison of satellite sensor land surface phenology and ground phenology in Europe: Inter-annual comparison and modelling. *Geophys. Res. Lett.* **2015**, *42*, 2253–2260. [CrossRef]

15. Fisher, J.I.; Mustard, J.F. Cross-scalar satellite phenology from ground, Landsat, and MODIS data. *Remote Sens. Environ.* **2007**, *109*, 261–273. [CrossRef]
16. White, K.; Pontius, J.; Schaberg, P. Remote sensing of spring phenology in northeastern forests: A comparison of methods, field metrics and sources of uncertainty. *Remote Sens. Environ.* **2014**, *148*, 97–107. [CrossRef]
17. Jönsson, P.; Eklundh, L. TIMESAT—A program for analyzing time-series of satellite sensor data. *Comput. Geosci.* **2004**, *30*, 833–845. [CrossRef]
18. Doktor, D.; Bondeau, A.; Koslowski, D.; Badeck, F.-W. Influence of heterogeneous landscapes on computed green-up dates based on daily AVHRR NDVI observations. *Remote Sens. Environ.* **2009**, *113*, 2618–2632. [CrossRef]
19. Myneni, R.B.; Keeling, C.D.; Tucker, C.J.; Asrar, G.; Nemani, R.R. Increased plant growth in the northern high latitudes from 1981 to 1991. *Nature* **1997**, *386*, 698–702. [CrossRef]
20. Tucker, C.J.; Slayback, D.A.; Pinzon, J.E.; Los, S.O.; Myneni, R.B.; Taylor, M.G. Higher northern latitude normalized difference vegetation index and growing season trends from 1982 to 1999. *Int. J. Biometeorol.* **2001**, *45*, 184–190. [CrossRef] [PubMed]
21. Han, Q.; Luo, G.; Li, C. Remote sensing-based quantification of spatial variation in canopy phenology of four dominant tree species in Europe. *J. Appl. Remote Sens.* **2013**, *7*, 073485. [CrossRef]
22. Curnel, Y.; Oger, R. Agrophenology indicators from remote sensing: state of the art. In Proceedings of the ISPRS Archives XXXVI-8/W48 Workshop Proceedings: Remote Sensing Support to Crop Yield Forecast and Area Estimates, Stresa, Italy, 30 November–1 December 2006.
23. Henebry, G.M.; de Beurs, K.M. Remote sensing of land surface phenology: A prospectus. In *Phenology: An Integrative Environmental Science*; Springer Netherlands: Dordrecht, The Netherlands, 2013; pp. 385–411.
24. Fu, Y.H.; Piao, S.; Op de Beeck, M.; Cong, N.; Zhao, H.; Zhang, Y.; Menzel, A.; Janssens, I.A. Recent spring phenology shifts in western Central Europe based on multiscale observations: Multiscale observation of spring phenology. *Glob. Ecol. Biogeogr.* **2014**, *23*, 1255–1263. [CrossRef]
25. Eklundh, L.; Jönsson, P. *TIMESAT: A Software Package for Time-Series Processing and Assessment of Vegetation Dynamics*; Kuenzer, C., Dech, S., Wagner, W., Eds.; Springer International Publishing: Cham, Switzerland, 2015; pp. 141–158.
26. Schwartz, M.D.; Reed, B.C.; White, M.A. Assessing satellite-derived start-of-season measures in the conterminous USA. *Int. J. Climatol.* **2002**, *22*, 1793–1805. [CrossRef]
27. Corine Land Cover 2006 Seamless Vector Data—European Environment Agency. Available online: http://www.eea.europa.eu/data-and-maps/data/clc-2006-vector-data-version-3 (accessed on 5 June 2016).
28. Clerici, N.; Weissteiner, C.J.; Gerard, F. Exploring the use of MODIS NDVI-Based phenology indicators for classifying forest general habitat categories. *Remote Sens.* **2012**, *4*, 1781–1803. [CrossRef]
29. Elmore, A.J.; Guinn, S.M.; Minsley, B.J.; Richardson, A.D. Landscape controls on the timing of spring, autumn, and growing season length in mid-Atlantic forests. *Glob. Chang. Biol.* **2012**, *18*, 656–674. [CrossRef]
30. Atkinson, P.M.; Jeganathan, C.; Dash, J.; Atzberger, C. Inter-comparison of four models for smoothing satellite sensor time-series data to estimate vegetation phenology. *Remote Sens. Environ.* **2012**, *123*, 400–417. [CrossRef]
31. Sakamoto, T.; Yokozawa, M.; Toritani, H.; Shibayama, M.; Ishitsuka, N.; Ohno, H. A crop phenology detection method using time-series MODIS data. *Remote Sens. Environ.* **2005**, *96*, 366–374. [CrossRef]
32. Gonsamo, A.; Chen, J.M.; D'Odorico, P. Deriving land surface phenology indicators from CO_2 eddy covariance measurements. *Ecol. Indic.* **2013**, *29*, 203–207. [CrossRef]
33. Jönsson, P.; Eklundh, L. *TIMESAT—A Program for Analyzing Time-Series of Satellite Sensor Data Users Guide for TIMESAT 2.3*; Malmö and LundTime: Lund, Sweden, 2007.
34. van Leeuwen, W.J.D. Monitoring the effects of forest restoration treatments on post-fire vegetation recovery with MODIS multitemporal data. *Sensors* **2008**, *8*, 2017–2042. [CrossRef]
35. Bradley, B.A.; Jacob, R.W.; Hermance, J.F.; Mustard, J.F. A curve fitting procedure to derive inter-annual phenologies from time series of noisy satellite NDVI data. *Remote Sens. Environ.* **2007**, *106*, 137–145. [CrossRef]
36. Richardson, A.D.; Andy Black, T.; Ciais, P.; Delbart, N.; Friedl, M.A.; Gobron, N.; Hollinger, D.Y.; Kutsch, W.L.; Longdoz, B.; Luyssaert, S.; et al. Influence of spring and autumn phenological transitions on forest ecosystem productivity. *Philos. Trans. R. Soc. B Biol. Sci.* **2010**, *365*, 3227–3246. [CrossRef] [PubMed]

37. Zhang, X.; Friedl, M.A.; Schaaf, C.B.; Strahler, A.H.; Hodges, J.C.F.; Gao, F.; Reed, B.C.; Huete, A. Monitoring vegetation phenology using MODIS. *Remote Sens. Environ.* **2003**, *84*, 471–475. [CrossRef]
38. Tan, B.; Morisette, J.T.; Wolfe, R.E.; Gao, F.; Ederer, G.A.; Nightingale, J.; Pedelty, J.A. An enhanced TIMESAT Algorithm for estimating vegetation phenology metrics from MODIS data. *IEEE J. Sel. Top. Appl. Earth Obs. Remote Sens.* **2011**, *4*, 361–371. [CrossRef]
39. Wang, X.; Piao, S.; Xu, X.; Ciais, P.; Macbean, N.; Myneni, R.B.; Li, L. Has the advancing onset of spring vegetation green-up slowed down or changed abruptly over the last three decades? *Glob. Ecol. Biogeogr.* **2015**, *24*, 621–631. [CrossRef]
40. Xu, H.; Twine, T.; Yang, X. Evaluating remotely sensed phenological metrics in a dynamic ecosystem model. *Remote Sens.* **2014**, *6*, 4660–4686. [CrossRef]
41. Atzberger, C.; Klisch, A.; Mattiuzzi, M.; Vuolo, F. Phenological metrics derived over the european continent from NDVI3g data and MODIS Time series. *Remote Sens.* **2013**, *6*, 257–284. [CrossRef]
42. Soudani, K.; le Maire, G.; Dufrêne, E.; François, C.; Delpierre, N.; Ulrich, E.; Cecchini, S. Evaluation of the onset of green-up in temperate deciduous broadleaf forests derived from Moderate Resolution Imaging Spectroradiometer (MODIS) data. *Remote Sens. Environ.* **2008**, *112*, 2643–2655. [CrossRef]
43. Richardson, A.D.; Bailey, A.S.; Denny, E.G.; Martin, C.W.; O'Keefe, J. Phenology of a northern hardwood forest canopy. *Glob. Chang. Biol.* **2006**, *12*, 1174–1188. [CrossRef]
44. Hird, J.N.; McDermid, G.J. Noise reduction of NDVI time series: An empirical comparison of selected techniques. *Remote Sens. Environ.* **2009**, *113*, 248–258. [CrossRef]
45. Wang, H.; Ge, Q.; Rutishauser, T.; Dai, Y.; Dai, J. Parameterization of temperature sensitivity of spring phenology and its application in explaining diverse phenological responses to temperature change. *Sci. Rep.* **2015**. [CrossRef] [PubMed]
46. Cornelius, C.; Estrella, N.; Franz, H.; Menzel, A. Linking altitudinal gradients and temperature responses of plant phenology in the Bavarian Alps. *Plant Biol.* **2013**, *15*, 57–69. [CrossRef] [PubMed]
47. Laube, J.; Sparks, T.H.; Estrella, N.; Höfler, J.; Ankerst, D.P.; Menzel, A. Chilling outweighs photoperiod in preventing precocious spring development. *Glob. Chang. Biol.* **2014**, *20*, 170–182. [CrossRef] [PubMed]
48. Nagai, S.; Nasahara, K.N.; Muraoka, H.; Akiyama, T.; Tsuchida, S. Field experiments to test the use of the normalized-difference vegetation index for phenology detection. *Agric. For. Meteorol.* **2010**, *150*, 152–160. [CrossRef]

Remote Sensing of Environment 218 (2018) 231–244

Contents lists available at ScienceDirect

Remote Sensing of Environment

journal homepage: www.elsevier.com/locate/rse

LiDAR derived topography and forest stand characteristics largely explain the spatial variability observed in MODIS land surface phenology

Gourav Misra[a,*], Allan Buras[a,1], Marco Heurich[b,c], Sarah Asam[d,2], Annette Menzel[a,e]

[a] Ecoclimatology, Department of Ecology and Ecosystem Management, Technical University of Munich, 85354 Freising, Germany
[b] Department of Conservation and Research, Bavarian Forest National Park, Zoology, Freyunger Str. 2, 94481 Grafenau, Germany
[c] Faculty of Environment and Natural Resources, University of Freiburg, Tennenbacher Straße 4, 79106 Freiburg, Germany
[d] Institute for Earth Observation, Eurac Research, Viale Druso, 1, 39100 Bolzano, Italy
[e] Institute for Advanced Study, Technical University of Munich, 85748 Garching, Germany

ARTICLE INFO

Keywords:
NDVI
LiDAR
Land cover
Phenology
Modelling
Spatial variability
Forest stand characteristics
Mountains
Bavarian Forest National Park

ABSTRACT

In the past, studies have successfully identified climatic controls on the temporal variability of the land surface phenology (LSP). Yet we lack a deeper understanding of the spatial variability observed in LSP within a land cover type and the factors that control it. Here we make use of a high resolution LiDAR based dataset to study the effect of subpixel forest stand characteristics on the spatial variability of LSP metrics based on MODIS NDVI. Multiple linear regression techniques (MLR) were applied on forest stand information and topography derived from LiDAR as well as land cover information (i.e. CORINE and proprietary habitat maps for the year 2012) to predict average LSP metrics of the mountainous Bavarian Forest National Park, Germany. Six different LSP metrics, i.e. start of season (SOS), end of season (EOS), length of season (LOS), NDVI integrated over the growing season (NDVIsum), maximum NDVI value (NDVImax) and day of maximum NDVI (maxDOY) were modelled in this study. It was found that irrespective of the land cover, the mean SOS, LOS and NDVIsum were largely driven by elevation. However, inclusion of detailed forest stand information improved the models considerably. The EOS however was more complex to model, and the subpixel percentage of broadleaf forests and the slope of the terrain were found to be more strongly linked to EOS. The explained variance of the NDVImax improved from 0.45 to 0.71 when additionally considering land cover information, which further improved to 0.84 when including LiDAR based subpixelforest stand characteristics. Since completely homogenous pixels are rare in nature, our results suggest that incorporation of subpixel forest stand information along with land cover type leads to an improved performance of topography based LSP models. The novelty of this study lies in the use of topography, land cover and subpixel vegetation characteristics derived from LiDAR in a stepwise manner with increasing level of complexity, which demonstrates the importance of forest stand information on LSP at the pixel level.

1. Introduction

Phenology, the science of annual recurring events in organisms, has been studied and manually recorded for centuries, e.g. the observations of Japanese cherry blossoms started in the 9th century (Nagai et al., 2016). Since the changing climate is known to affect species in various degrees, such long term records provide insights into the life cycle of organisms and their adaptation strategies (Thackeray et al., 2016). The study of temporal and spatial variations of phenology is therefore particularly important in assessing threats to key species interactions affecting the stability of whole ecosystems. Phenology has been extensively studied to elucidate the impact of climate change on biota (Cleland et al., 2007; Menzel et al., 2006; Parmesan and Yohe, 2003) based on various data types such as in situ observations of species' phenology including citizen science initiatives, remote sensing indices, as well as measurement of carbon fluxes and isotopes (Gonsamo et al., 2017; Menzel and Fabian, 1999; Walther et al., 2002; White et al., 2009).

In the last few decades, remote sensing based detection of vegetation phenology or Land Surface Phenology (LSP) has gained

* Corresponding author.
E-mail address: misra@wzw.tum.de (G. Misra).
[1] Currently at Forest Ecology and Forest Management, Wageningen University and Research, Droevendaalsesteg 3a, PB 6708 Wageningen, The Netherlands.
[2] Currently at German Remote Sensing Data Center (DFD), German Aerospace Center (DLR), 82234 Wessling, Germany.

https://doi.org/10.1016/j.rse.2018.09.027
Received 31 March 2018; Received in revised form 3 August 2018; Accepted 30 September 2018

considerable attention due to its ease in data acquisition with very little time lag. Unlike traditional methods of surveying, remote sensing based platforms provide repetitive coverage of the earth at multiple spatial scales, allowing the analysis of important events in the vegetation cycles over large areas. Remote sensing based studies of vegetation dynamics have therefore been used to map land cover, to report trends in phenology, to detect disturbances (i.e. fire, wind throws and pests) as well as to assess ecosystem productivity (Di-Mauro et al., 2014; Matiu et al., 2017; Myneni et al., 1997; Simonetti et al., 2015).

Despite several advantages when compared to classical i.e. ground based phenological approaches, LSP studies face certain limitations and require specialized knowledge to process and interpret time series of remote sensing data adequately. Apart from choosing from multiple options of data selection and processing, there is no optimal method to derive LSP (Cai et al., 2017). Therefore studies have used multiple approaches/methods to process remote sensing data and to estimate LSP interchangeably (Eklundh and Jonsson, 2015; Hird and McDermid, 2009; Studer et al., 2007; White et al., 1997). The start of season (SOS), end of season (EOS), and length of season (LOS) and other phenological metrics have been computed in various ways including fixed thresholds, amplitudes and rate of change of curvature (derivatives), with each method providing a different estimate (Misra et al., 2016; Nagai et al., 2010; Soudani et al., 2008). Studies suggest a large variability among different LSP measures (Schwartz et al., 2002; Shang et al., 2017; Studer et al., 2007), which might however be explicitly used for estimating different phenological phases (Fisher and Mustard, 2007; Misra et al., 2016; Soudani et al., 2008) or to differentiate understory from tree canopy (Badeck et al., 2004; Misra et al., 2016; Rautiainen et al., 2012; Richardson and O'Keefe, 2009). The ecological meaning of many LSP estimates is therefore still not very clear and requires further investigation (Eklundh and Jonsson, 2015; Nagai et al., 2016).

Additionally, studies frequently lack clarity in validating LSP estimates with ground phenology (GP) observations (Duncan et al., 2015; Hanes et al., 2014). In this regard, pixel based LSP has been linked with species based GP and the limitations of this approach have been discussed (Han et al., 2013; Rodriguez-Galiano et al., 2015a; Studer et al., 2007). Apart from the difficulty in detecting a single date from the NDVI time series to report SOS or the even more prolonged EOS period (Gallinat et al., 2015; Stöckli et al., 2008), errors in estimation of LSP have also been reported to be affected by flowering and retention of withered leaves which are a species specific characteristic (Nakaji et al., 2011). Most importantly, mixing of land cover with in a pixel presents challenges in correlating GP data. More specifically, GP data are based on visual observation of phenological events of single plant species on the ground which are correlated with LSP estimates based on changes observed in the spectral reflectance of vegetation mixtures within the pixel. Since completely pure and homogenous pixels of forest tree species with 100% fractional cover are rare and difficult to identify in medium to coarse resolution remote sensing data, data on the mixing of land cover and vegetation types that occurs in the pixel from which the LSP is estimated seems important (Fisher and Mustard, 2007; Liang et al., 2011), especially when drivers of the observed temporal and spatial variability in LSP are to be analyzed. Variability in LSP has been linked to different climatic factors, geo-location (latitude, longitude and elevation) and general land use types (with discrete classes) so far, but has not considered the effect of subpixel composition of vegetation (Koster et al., 2014; Luo and Yu, 2017; S. Wang et al., 2016; Y. Wang et al., 2016; Wang et al., 2017; Y. Zhang et al., 2017). In this context, the lack of subpixel information has certain drawbacks such as reporting an underestimation of green-up dates and overestimation of dormancy dates in coarser resolution data as observed in studies on the effect of different pixel sizes on LSP (Klosterman et al., 2014; S. Wang et al., 2016; Y. Wang et al., 2016; Zhao et al., 2012).

Since the uncertainty in LSP estimates increases in the absence of sub pixel land cover information (Doktor et al., 2009; Liang et al., 2011), the importance of high resolution land cover cannot be ignored. It is therefore essential to understand the uncertainties associated with LSP estimated from readily available and popular medium to coarse resolution data sets since high resolution datasets are not always readily accessible. In this regard a few recent studies have reported LSP to be linearly or logarithmically varying across scales, with earlier greening pixels driving the SOS more strongly than later pixels (Peng et al., 2017; X. Zhang et al., 2017). Even though previous studies (Cho et al., 2017; Fuller, 1999) have reported the influence of the percentage of general canopy cover or fractional cover on LSP, the effect of subpixel based detailed forest stand information on LSP needs further investigation. Hwang et al. (2011) found that apart from topographical variables, the minimum Leaf Area Index (indicating the evergreen proportion of the pixel) significantly influenced the LSP, too. However, their study was restricted to broadleaf dominated pixels and mainly used topographical predictors to explain variability in LSP. The effect of mixed pixel on LSP was simulated by Chen et al. (2018) through varying fractional cover of two different end members that revealed considerable effects of the proportions of sub pixel land cover or species on the estimated LSP metrics. Subpixel information on land cover mixing is also important to attribute changes in LSP behavior to its real cause i.e. climatic or land cover changes (Chen et al., 2018; Doktor et al., 2009; Helman, 2018; Xie et al., 2015b).Though limited research exists on effects of mixed pixels on LSP and uncertainty in LSP can be better estimated using information on homogeneity of pixels, an intensive investigation is however required in this field in to understand the role of class mixing on the LSP of complex landscapes. For this purpose, high resolution LiDAR and hyperspectral data may provide valuable insights for mapping species at the subpixel level (Branson et al., 2018) and understanding the LSP estimates obtained from medium to coarse resolution remote sensing data. Apart from land cover type and homogeneity of pixels, LSP is also known to be affected by events such as snow, droughts, fire and pest infestation (Gessner et al., 2015; Kobayashi et al., 2016; Norman et al., 2017; Studer et al., 2007; Xie et al., 2015b). Therefore, besides high quality remote sensing data, research has also indicated the importance of not only detailed but also up-to-date land cover information in LSP studies (Badeck et al., 2004; Doktor et al., 2009; Misra et al., 2016; Norman et al., 2017; S. Wang et al., 2016; Y. Wang et al., 2016).

To overcome this knowledge gap, we here assess here the effects of land cover information and subpixel forest stand characteristics on the estimated pixel based mean LSP (2002–2015) of the mountainous Bavarian Forest National Park (BFNP) in Germany. High resolution LiDAR data was aggregated at Moderate Resolution Imaging Spectrometer (MODIS) pixel resolution (250 m) to various measures describing forest stand characteristics and was then compared to two other land cover products (the freely available CORINE and proprietary habitat maps for the BFNP) regarding their ability to improve topography based LSP models. A 4-day maximum value composite Normalized Difference Vegetation Index (NDVI) dataset covering the years 2002–2015 from the MODIS sensor was used in this study since a shorter compositing period is known to be more robust in estimating LSP (Brown and de Beurs, 2008; Kross et al., 2011). Since inter-annual NDVI variations are driven by climatic anomalies (Schultz and Halpert, 1993; Zeng et al., 2013), we assume that the 14-year mean values of phenological metrics represent the site or pixel specific climatic averaged signal. Therefore, temporal deviations from this mean MODIS pixel LSP would be the result of yearly weather conditions, whereas spatial variations in the pixel means may be traced back both to the spatial variability in topography reflecting site specific mean climatic conditions and in the characteristics of the forest stands. We hence hypothesize that the models predicting mean LSP increase in the explanatory power when incorporating high resolution forest stand information. In this study, we set forth to understand the spatial variability observed in the mean LSP metrics of the BFNP region. The central research questions of this study are:

1. Does sub pixel based information on forest stand characteristics improve the prediction of LSP based metrics?
2. Which variables are most important for understanding the spatial variability of LSP metrics?

2. Materials and methods

2.1. Study area and data

2.1.1. Study area

The study area of 24,222 ha comprises the whole Bavarian Forest National Park (BFNP) which is a protected and extensively monitored forest area in southeastern Germany (49°3′19″N, 13°12′9″E). It is situated at the border to the Czech Republic. The area is mountainous, with elevations between 600 and 1453 m a.s.l, the mean annual temperature varies between 7.5 °C in the valleys and 2 °C along the ridges and at higher elevations. Mean annual precipitation ranges between 830 and 2230 mm, of which a considerable amount occurs as snowfall (Heurich et al., 2010).

Three major forest types exist within the BFNP along the elevation gradient, dominated by Norway spruce (*Picea abies* L.) and European beech (*Fagus sylvatica* L.) (Cailleret et al., 2014). A summary of the dominant vegetation is presented in Table 1. Since the mid-1980s, the forests of the BFNP have been affected by wind throws and subsequent spruce bark beetle (*Ips typographus* L.) infestation resulting in large amounts of dead wood and consecutively regenerating mixed forest stands (Lausch et al., 2011; Zeppenfeld et al., 2015).

2.1.2. Land cover data

The freely available CORINE (COoRdination of INformation on the Environment) land cover map at 250 m resolution for the year 2012 was downloaded from the Copernicus Land Monitoring Service of the European Environment Agency (EEA, 2012). The CORINE maps have been optimized for the entire European region and hence consist of generalized land cover classes i.e. broadleaf, conifer, mixed forest, transitional woodlands, pasture, arable land, urban areas and water bodies. A more detailed proprietary habitat map of the BFNP was also provided by the BFNP administration. This land cover habitat map is based on visual interpretation of digital color infrared images acquired in August 2012 using a DMC camera. The flight height was 1900 m, leading to a spatial resolution of 20 cm. On this basis nine different land cover classes were identified namely urban, clear-cut, conifer, broadleaf, meadow, mixed forest, dead wood-lying, dead wood-regenerating and water (Dupke et al., 2017). Fig. 1 shows the CORINE and habitat land cover maps (resampled at 250 m resolution) of BFNP for the year 2012.

2.1.3. LiDAR data

Full-waveform LiDAR data were acquired in June 2012 using a Riegl LMS-680i scanner under leaf-on conditions. The system was run at an altitude of 650 m with a pulse repetition rate of 350 KHz resulting in a nominal point density of around 30 points per m^2. During the preprocessing steps, a decomposition of the LiDAR waveforms using Gaussian functions and a correction of the intensity values according to Reitberger et al. (2009) was used. Single dead and living trees were detected by a 3D-segmentation, whereas, tree species were identified using a supervised maximum likelihood classification technique with an accuracy of 95%, considering mean intensity in entire tree, mean distances of layer points to tree trunk, mean pulse widths of single and first reflections of the entire tree segment and ratio of number of single reflection to multiple reflections within an individual tree polygon (Yao et al., 2012). After that a two-step procedure for classification with linear regression and an active learning approach to distinguish living and dead trees based on the properties of the LiDAR point cloud and aerial images was applied (Polewski et al., 2016). The land cover information from LiDAR data mostly consists of information on forests types since the landscape in BFNP is dominated by forests. The LiDAR based digital terrain model at 1 m resolution was also obtained for mapping the topography of the study area.

2.1.4. MODIS- NDVI data

A 4-day Maximum Value Composite (MVC) of MODIS NDVI product was used for this study. The 4-day NDVI time series for 2002–2015 were derived from the daily MOD09GQ Terra product at 250 m resolution (Survey, 2015) for all vegetated areas. From this surface reflectance product, the bands in the red (0.62–0.67 μm) and near infrared (0.84–0.88 μm) spectrum were extracted for the calculation of NDVI. They were used in conjunction with the daily MOD09GA product which includes geometry information (solar and sensor zenith and azimuth angles) as well as scene acquisition quality flags at 1 km spatial resolution (Vermote and Wolfe, 2015). In a first step, the 1 km resolution bands were oversampled, all necessary bands were stacked, and non-vegetated areas were masked based on the CORINE land cover classification for the reference year 2012. The vegetated area of the CORINE and BFNP habitat maps reveal a high degree of overlap (> 95%) and only differ in the type of vegetation, hence the choice of land cover map for masking did not make much difference. Processing and interpretation of time series of daily MODIS data is complicated by the variation of its footprint on consecutive days that may lead to false variability in spectral signatures. Therefore, a MVC method has been suggested in literature to minimize noise in the data (Jin and Sader, 2005; Tan et al., 2006; Xin et al., 2013). Subsequently, the 4-day MVC were generated omitting pixels of poor observation, geometry and quality. Pixels with topographically corrected sun and sensor zenith angles higher than 70° and 80° respectively were omitted. No further steps were taken to address the BRDF effects. On average, 2.8% of all pixels of the daily input images had to be excluded due to bad geometry conditions, and 75.4% of the pixels had to be masked due to bad quality (cloud, aerosol, or snow contamination) derived from the MODIS product quality flags. Nevertheless, this 4-day NDVI MVC increased the temporal sampling of valid data points in comparison to the MOD13 16-day NDVI product. In addition to the NDVI values layer, two other layers containing the pixel-wise quality flag information as well as the day of the year (DOY) of the respective selected maximum value were generated for each dataset. Lastly, the NDVI raster datasets were reprojected from the original Sinusoidal projection to the geographic Latitude/Longitude projection (WGS84 ellipsoid, EPSG:4326) and then used for estimating different land surface phenology metrics (see Section 2.2.1).

All datasets i.e. the two land cover maps (CORINE and habitat maps) and the digital terrain model from LiDAR were resampled to MODIS pixel resolution of 250 m by applying a mode function and

Table 1
Dominant vegetation along the elevation gradient in the BFNP.

Elevation	Dominant vegetation
a) Bottom of valleys (~600–700 m); often characterized by cold air pockets in course of inversions.	Norway spruce (*Picea abies*), mountain ash and birch (*Betula pendula*, *Betula pubescens*).
b) Hill slopes (600–1100 m)	Mixed montane forests with Norway Spruce (*Picea abies*), silver fir (*Abies alba*), sycamore maple (*Acer pseudoplatanus*) and European beech (*Fagus sylvatica*)
c) > 1100 m	Sub-alpine spruce forests with Norway spruce (*Picea abies*) and mountain ash (*Sorbus aucuparia*)

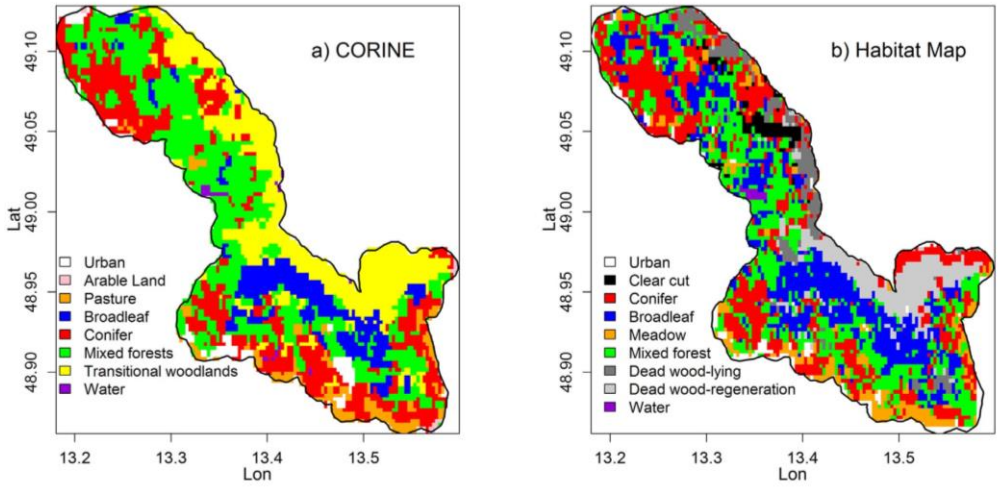

Fig. 1. a) CORINE land cover map for year 2012 and b) the detailed habitat map of the Bavarian National Forest Park. There is high degree of overlap in the vegetated areas, however the transitional woodlands in CORINE are classified as clear cut, deadwood-lying and dead wood-regeneration in habitat map.

Table 2
List of all pixel based response and predictor variables (used in multiple linear regressions). Predictor variables except CORINE and Habitat are based on LiDAR data (see Sections 2.1.3 and 2.2.2), the LSP response variables represent averaged values from MODIS NDVI over the period 2002–2015.

S/No.	Variable	Description	Unit
Response			
1.	SOS	Mean day of the year when 50% of seasonal amplitude is reached in spring (start of season).	Day of year
2.	EOS	Mean day of the year (DOY) when 50% of seasonal amplitude is reached in autumn (end of season).	Day of year
3.	LOS	Mean of length of season in days calculated as EOS – SOS.	Day of year
4.	NDVImax	Mean of maximum NDVI value or maximum greenness (Duchemin et al., 1999).	Unitless
5.	maxDOY	Mean day of year when maximum NDVI value is registered.	Day of year
6.	NDVIsum	Mean of seasonally integrated NDVI obtained by adding the daily values between two troughs of the NDVI time series or the gross primary productivity (Berner et al., 2011).	Unitless
Predictors			
1.	Lat	Latitude	Degree
2.	Lon	Longitude	Degree
3	Slope	Slope	Degree
4.	Aspect	Aspect calculated as folded aspect (McCune and Keon, 2002)	Degree
5.	Elevation	Elevation	m a.s.l
6.	Heat Load	Potential incident solar radiation (McCune and Keon, 2002)	MJ/cm^2/yr
7.	Tree Height	Average tree height	m
8.	Crown Volume	Average crown volume	m^3
9.	Crown Area	Total crown area	m^2
10.	Conifer %	Percentage of crown area of conifer trees	Percentage
11.	Broadleaf %	Percentage of crown area of broadleaf trees	Percentage
12.	No. of Trees	Total number of trees	
13.	Shannon's Entropy	$SE = \Sigma_{i=1}{}^{n}Pi.\ln(Pi)$; where Pi is the proportion of the *ith* species in the pixel and n is the number of species in the pixel (Muller et al., 2000).	Unitless
14.	Habitat	Classes of proprietary habitat map of the study area for the year 2012	Factor
15.	CORINE	Classes of CORINE land use land cover for year 2012.	Factor

calculating the zonal mean respectively, before any further data processing.

2.1.5. Ground phenological observations

Both the German Meteorological Service (DWD) and International Phenological Gardens (IPG) run phenological networks for ground survey based information. Information for DWD sites is available at Freyung Schönbrunn (775 m a.s.l.), Neureichenau (770 m a.sl.) and Großer Arber (1436 m a.s.l.), and IPG site at Waldhaeuser (956 m a.s.l). Collection of ground phenological data for mountainous regions such as the BFNP is challenging because of difficult accessibility and lack of volunteer observers. Though all the sites are not located exactly in the BFNP, they are within a 10 km radius of the study area and therefore they may very well depict the phenological conditions at different elevations inside the BFNP. Dates of leaf unfolding and leaf fall of broadleaf species (i.e. *Fagus sylvatica and Sorbus aucuparia*) were collected as day of the year events. Similarly, dates of May shoot for start of season were obtained for conifer species (*Picea abies*) during the years 2002–2015.

2.2. Data preparation

2.2.1. NDVI data processing and estimation of LSP measures

The MODIS NDVI dataset consisting of 1254 raster layers for the period 2002–2015 were stacked in chronological order to obtain a raster time series. The NDVI time series for each pixel was then

screened for local outliers, gap filled and smoothed using a Gaussian smoothing function as described in Misra et al. (2016). The NDVI values from the 4 day MVC were then set to their actual dates as recorded in the DOY layer and were linearly interpolated between available observations to daily values assuming a continuous plant growth behavior over a limited time of four days, in order to enable day-exact LSP metric calculation using a threshold approach. Since the uncertainty and mismatch in LSP measures and GP is well documented (Hmimina et al., 2013; Misra et al., 2016; Verger et al., 2016), we calculated various phenological metrics as suggested in the literature to cover the entire period of seasonal vegetation activity. Phenological metrics such as start of the season (SOS), end of the season (EOS), length of the season (LOS), seasonal maximum NDVI value (NDVImax), day of season maximum NDVI (maxDOY) and integrated seasonal NDVI (NDVIsum) were calculated (Gessner et al., 2015; Heumann et al., 2007; Misra et al., 2016; Spruce et al., 2011). In this study we focus on SOS, EOS and LOS calculated using the 50% amplitude method (see Table 2 for definitions of various LSP metrics). The 50% amplitude method is widely applied over a variety of ecosystems and was shown to be most consistent in extracting phenological metrics from time series of NDVI (Hamunyela et al., 2013; S. Wang et al., 2016; White et al., 1997; White et al., 2009). These metrics were then averaged to estimate the corresponding mean LSP of the BFNP for the years 2002–2015 (see Section 3.2 and Fig. 3 for maps).

2.2.2. Aggregating LiDAR data at MODIS resolution

The LiDAR data available in the form of a spatial point database was overlaid on an empty MODIS raster grid and summarized to calculate several pixel based indices such as total crown area, average crown volume, average tree height, number of trees in pixel, percentage crown area of conifers and broadleaf trees. This summarized forest stand information was then exported to a raster format comparable to MODIS using rasterize function in R. The digital terrain model from LiDAR was used for calculating various topographical variables such as elevation, slope and aspect using the terrain function available in the raster package (Hijmans, 2016) of the R programming language. The heat load or the incoming solar radiation for the pixels was calculated as explained in McCune and Keon (2002) and the species measure of diversity aka Shannon's Entropy (SE) was calculated according to Muller et al. (2000) (see Section 3.1 and, Fig. 3 and Supplement Fig. S1 for maps). The response variables based on LSP measures as well as predictor variables derived from two land cover maps and from LiDAR data were used in multiple linear regressions (see Table 2).

2.2.3. Statistical analyses

The SOS and EOS dates from MODIS LSP were separated by tree type, i.e. conifers and broadleaf areas using the habitat map. Their time series were compared to by species (conifer/*Picea abies*, broadleaf/*Fagus sylvatica*, *Sorbus aucuparia*) and season (SOS/leaf unfolding and EOS/leaf fall).

Next, we computed multiple linear regressions (MLR) to obtain a better understanding of the LSP metrics with regards to the different predictors already listed in Table 2. Since, strongly collinear predictors are known to cause problems in regression models, we used a stepwise Variance Inflation Factors (VIF) function to remove such predictors from the set of independent variables (vifstep function in usdm package in R (Naimi, 2017)). VIF_i provides a measure of the proportion of variance that the ith predictor shares with other predictors in the model. A $VIF_i > 10$ is considered to be a collinearity problem in the model (Naimi et al., 2014). This means that the estimated variance of the ith predictor is 10 times higher than what it would have been if it was linearly independent of other predictors (O'Brien, 2007). Therefore, predictors with VIF > 10 were removed from the multiple linear regression analyses (see supplement Fig. S2 for the output of the vifstep function). Additionally, a non-parametric Kruskal-Wallis test was carried out for multiple comparisons of LSP according to habitat classes to test whether differences existed between classes, followed by a posthoc Dunn's test (using Kruskal.test (Core Team, 2014) and dunn.test (Dinno, 2016) functions in R) to reveal the classes that show significant differences in their mean LSP. The correlation strength (Spearman's rank correlation) between various pairs of predictors and response variables was also checked after the VIF procedure and plotted as a heat map to represent the strength of interrelationships.

MLR analyses (see also Archetti et al., 2013; Kariyeva and van Leeuwen, 2011; Matthews and Mazer, 2016; Stoner et al., 2016) were computed to model mean LSP metrics using topography, land cover and LiDAR based forest characteristics as the predictors following a stepwise procedure. Since LSP is known to be affected by variations in topography due to differences in thermal accumulation (Cornelius et al., 2013; Kraus et al., 2016; Menzel et al., 2003; Tansey et al., 2017; Yu et al., 2016), we carry out multiple linear regression (MLR) analyses with mean LSP as response and topography as predictor being the initial model. Subsequently, land cover in the form of CORINE and detailed habitat maps of BFNP, as well as LiDAR based forest stand information were added to the topography model to evaluate improvements in the explained variance. Interactions between specific predictors i.e. land cover and LiDAR based forest stand information was also allowed in the MLR analyses. A stepwise BIC function (stepAIC function in MASS package in R (Venables et al., 2002), with k = log(n) for BIC) was applied to select the models with the best predictors, such that the resulting BIC was minimized. The relative importance of the independent variables for the best models was also calculated (using calc.relimp function in relaimpo package in R) and normalized to sum to 1 as suggested by (Grömping, 2006). The recommended lmg (Lindeman, Merenda and Gold) metric was used to report the relative importance as it defines the importance of a predictor as the averaged contribution to R^2 (coefficient of determination) across all possible orderings. It is known to account for both direct effects and effects adjusted for other independent variables while decomposing the modelled R^2 (Grömping, 2006; Johnson and LeBreton, 2004). It is not yet possible to calculate the relative importance for models with interactions using the available function in R and hence lmg is not reported for these cases. Finally, to account for possibly instable model parameters, all model parameters were bootstrapped in a similar manner as explained in (Buras et al., 2017). That is, over 1000 iterations calibration data were randomly split in two sub-sets to estimate model parameters (slopes, intercept, R^2), respectively. Differences of the sub-set parameters were expressed as ratios, and the bootstrapped ratio estimates were tested for similarity to the value of one (indicating stability of parameters) using empirical cumulative distribution functions (Buras et al., 2017). All data preparation, analyses and plotting of figures for this study was carried out in the R programming environment (Core Team, 2014).

3. Results

3.1. Agreement between LSP and GP

Fig. 2 shows the comparison between the LSP i.e. SOS and EOS from MODIS sensor and the leaf unfolding and leaf fall dates from ground survey during the period 2002–2015. Even though an exact match between LSP and GP dates is not expected due to reasons already discussed in the introduction, there is a high correlation between the time series of both datasets ($R^2 > 0.70$).The elevation dependent delay in the SOS and the advancement of EOS is also clearly evident from the distributions of phenological dates of both conifers and broadleaf species.

3.2. Variation in LSP and predictor variables

Spatial patterns of SOS strongly resembled topographical variations of the Bavarian forest, mostly being related to elevation with later onset of spring in higher elevations (Fig. 3a compared to Fig. S1). Mean

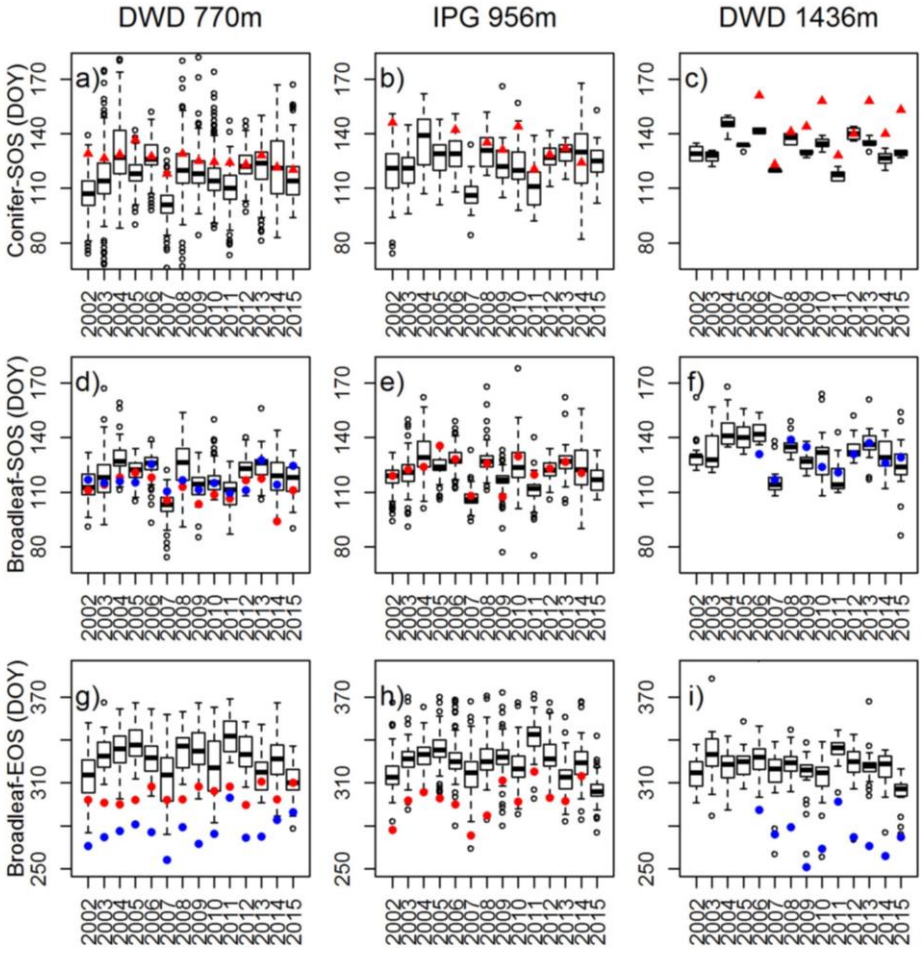

Fig. 2. Comparison between LSP and GP of conifers (a,b,c) and broadleaf (d,e,f,g,h,i) at different elevations. The red and blue filled circles are GP of Fagus sylvatica and Sorbus aucuparia respectively, whereas, the red filled triangle is GP of Picea abies. Subplots (a,d,g) and (c,f,i) show GP from DWD sites at 770 m and 1436 m elevation respectively, and the corresponding boxplots of LSP filtered for broadleaf and conifer species at 750–800 m and > 1200 m elevation. Similarly, subplots (b,e,h) show GP from IPG site at 956 m elevation and the boxplots for LSP filtered for broadleaf and conifer species at 925–975 m elevation. Note: the GP information during 2015 and 2002–2005 was unavailable at IPG 956 m and DWD 1436 m sites. (For interpretation of the references to color in this figure legend, the reader is referred to the web version of this article.)

spring onsets in lowest elevations of 700 m a.s.l were observed around DOY 80 whereas on the mountain peaks (~1400 m a.s.l.) around DOY 160. However, the EOS patterns (Fig. 3b) did not seem to be related to elevation nor any other explanatory variables. EOS of a few pixels (< 1% in the study area), most of which were conifers or dead trees, was determined later than DOY 365, thus already in the next calendar year. Since the length of the growing season (LOS, Fig. 3c) is only partly driven by SOS, it was only moderately linked to elevation. NDVImax and NDVIsum revealed a spatial heterogeneity, which appeared to be related to elevation and forest stand characteristics (Fig. 3e–f compared to Figs. S1 and 4c-d-e). The conifers in the frost affected valleys (Fig. 4a) and the broadleaves (Fig. 4b) in the mid-mountain ranges can be clearly seen in the spatial maps. The areas affected by storms and bark beetle infestation are characterized by lower values of average tree height, average crown volume and the number of trees in the pixels (see Fig. 4c-d-e). Land cover classes also had a significant effect on the different LSP-metrics at the 95% confidence level according to Kruskal Wallis and the post-hoc Dunn's test (supplement Table S3 and Fig. 5). Fig. 5 revealed the various classes to have significantly different mean LSP, with broadleaf trees having a significantly later EOS and higher NDVImax, and the conifers having a longer LOS and a later maxDOY as compared to other land cover classes.

3.3. Collinearity and interdependency

Among the explanatory variables, only total crown area was removed due to strong collinearity with percentage of broadleaf (see Fig. S2). However, some of the retained explanatory variables still expressed relatively high correlations among each other (Supplement Fig. S4). When relating response variables to the independent predictor variables, it was obvious that elevation had a strong effect on SOS, LOS, and NDVIsum. Moreover, NDVImax and NDVIsum were strongly related to LiDAR based forest stand characteristics such as tree height, crown volume, percentage of conifers and broadleaved trees as well as the number of trees within the pixel (Fig. S4). Significantly differing effects of LiDAR information were observed on the different LSP metrics in

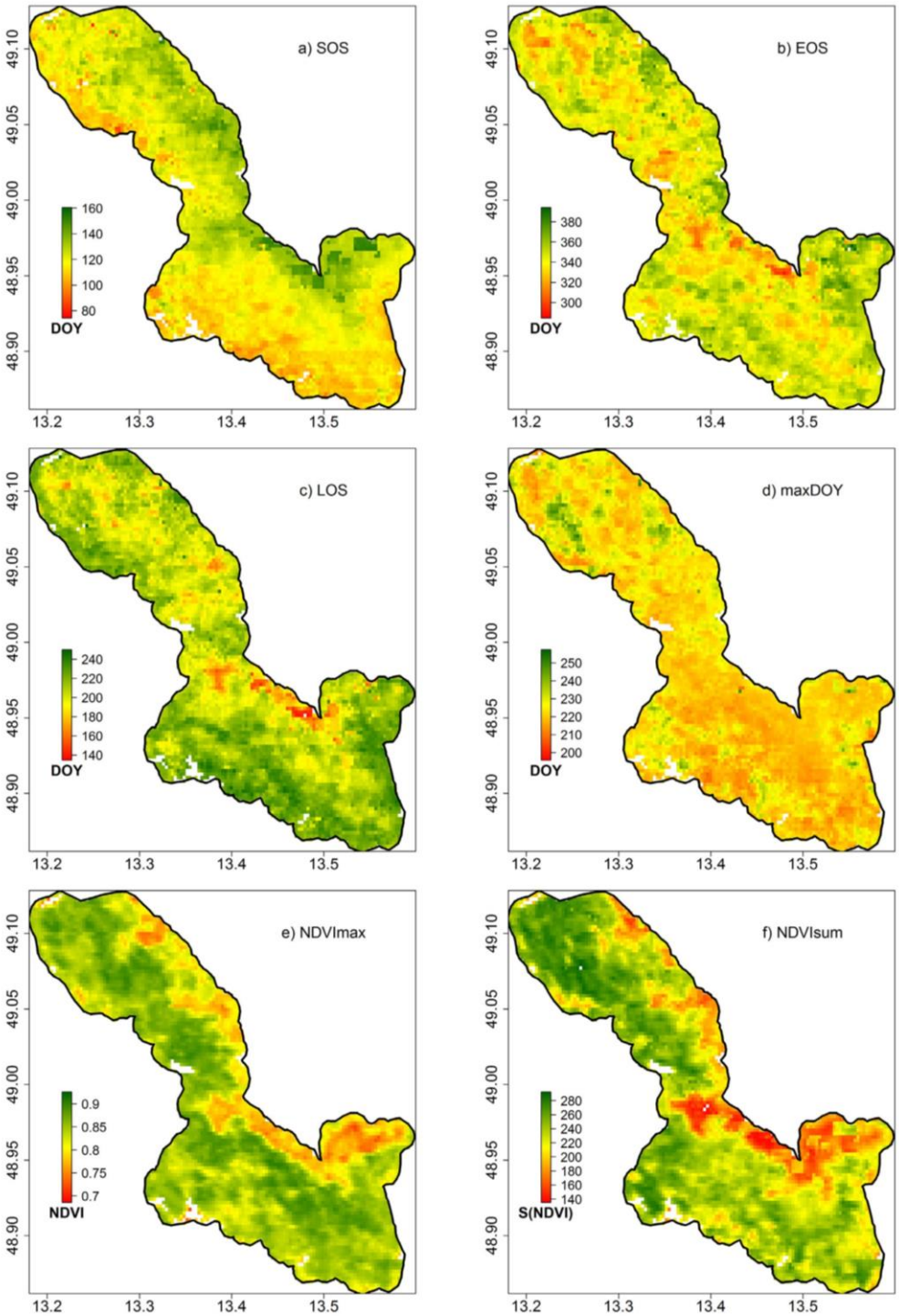

Fig. 3. Mean LSP metrics calculated from MODIS NDVI time series data for the period 2002–2015 in the Bavarian Forest National Park. The variability in different LSP measures is clearly evident from the maps, especially the elevation dependence of a) SOS and, the land cover driven e) NDVImax and f) NDVIsum.

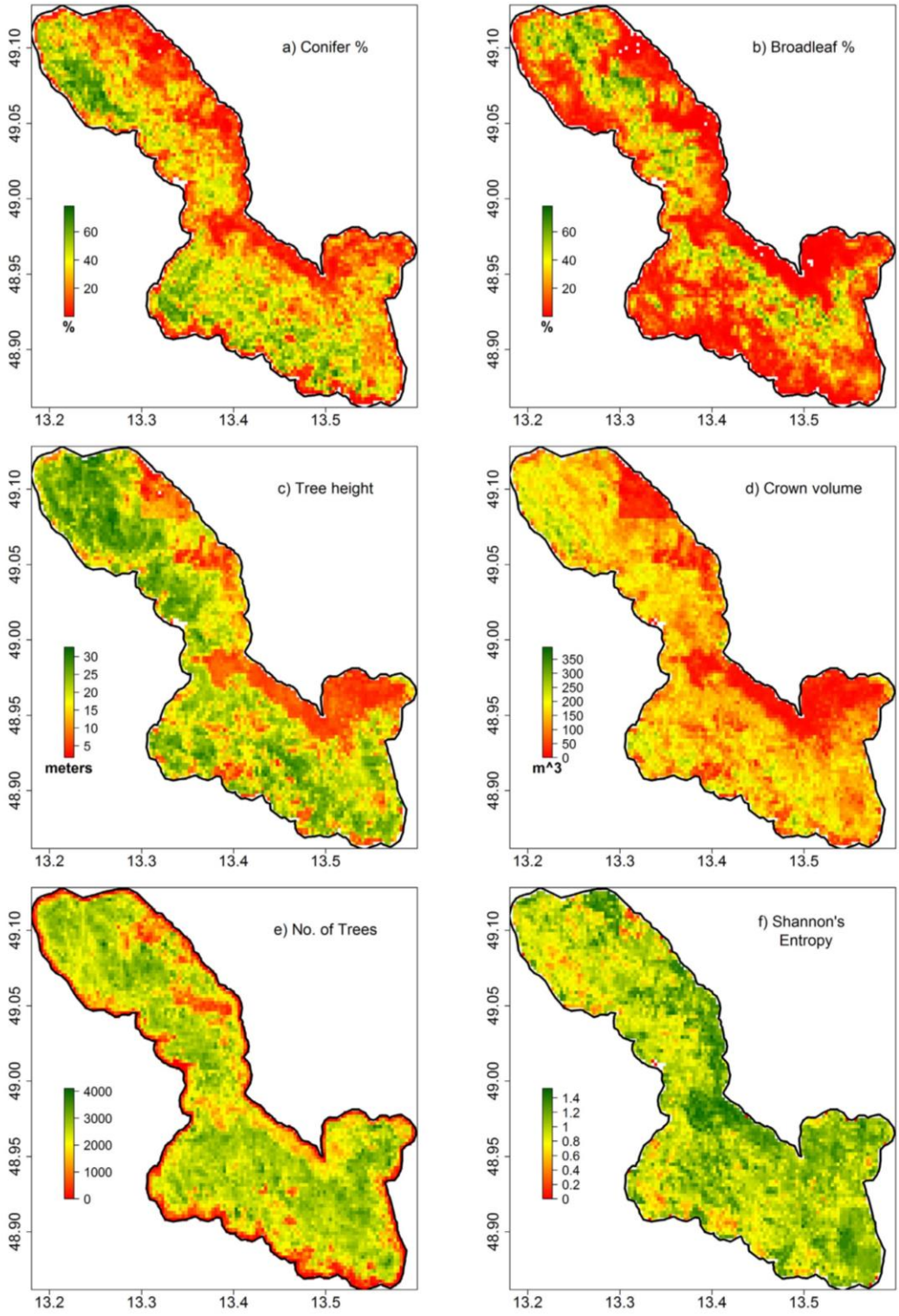

Fig. 4. Important LiDAR derived predictor variables aggregated at MODIS resolution.

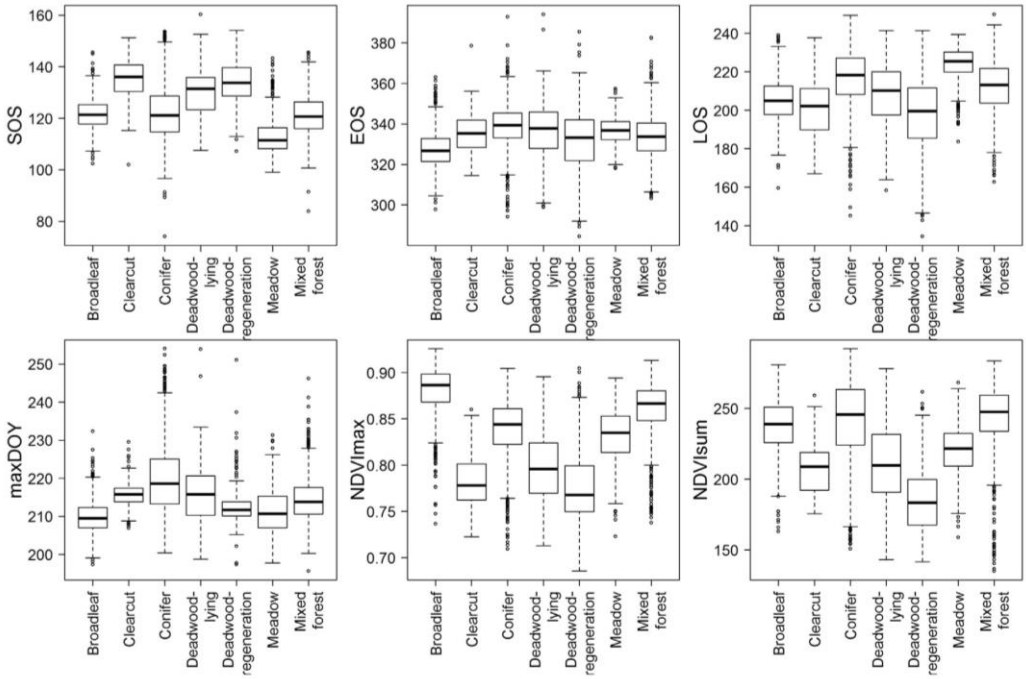

Fig. 5. Averaged annual phenological metrics (years 2002–2015) for the BFNP grouped by habitat classes. The different habitats reveal significant differences in LSP metrics, except for SOS of conifer, broadleaf and mixed forest; EOS of clearcut, deadwood-lying and meadow; LOS of clearcut and dead-regeneration; maxDOY of clearcut and deadwood-lying; NDVImax of clearcut and deadwood-regeneration; and NDVIsum of clearcut and deadwood-lying classes. (see Table S3 in supplement for significance of differences in class means of LSP metrics, the Kruskal-Wallis tests were significant at $p < 0.001$).

dependence of land cover class, which indicated the possibility of interactions between LiDAR and land cover information (Fig. 6 and Supplement Figs. S5–S6).

3.4. Model comparison

The topography based models were able to explain between 17% (EOS) and 62% (SOS) of LSP variability (Table 3). The SOS, LOS, NDVImax as well as NDVIsum exhibited higher predictive powers and were more strongly linked to elevation among the topographical variables. When adding land-cover information (CORINE and habitat) as well as LiDAR based forest stand characteristics independently, the model performance improved significantly for all LSP-parameters with R^2 ranging from 0.29 (EOS) to 0.78 (NDVIsum and NDVImax, see Table 3). CORINE and habitat almost equally improved the model fit except for NDVImax and NDVIsum for which CORINE seemed to better fitting information. Finally, allowing for interactions between LiDAR and other two land-cover information significantly improved the performance of all models (Table 3), with explained variances ranging from 0.36 for EOS to 0.84 for NDVImax. The results of bootstrapping analyses (see Section 2.2.3) revealed stable models for all phenological metrics, except the two interaction models for EOS and LOS, and the Topo+ (CORINE∗LiDAR) models for maxDOY, NDVImax and NDVIsum. The relative importance of variables and the results of the best LSP models i.e. with minimum BIC are shown in supplement Tables S7 and S8 respectively. The coefficients of the models reveal the relationship between the respective LSP metrics and its predictors. For e.g. the direct relationship between SOS and MaxDOY with elevation is clearly evident, whereas, the inverse relationship between EOS and LOS with elevation and proportion of broadleaf in pixel (Broadleaf %) is also revealed. The Broadleaf % also affects different LSP metrics differently, where it directly affects NDVIsum and has an inverse relationship with maxDOY.

4. Discussion

In this study we modelled 2002–2015 mean values from six different LSP metrics for 5141 pixels within the BFNP. For this purpose, we used a higher temporal resolution MODIS NDVI data set to derive LSP metrics, and prepared topographical and stand variables aggregated from a LiDAR database as well as two land cover maps in order to explain spatial variations in LSP. MLR analyses with land cover information, i.e. the freely available CORINE and proprietary habitat maps along with LiDAR information on forest stand improved the explained variances of the topography based LSP models. Inclusion of LiDAR information on forest stand characteristics along with a land cover map and allowing for interactions between them was the best option to represent subpixel dynamics that drive intra-class variability in LSP.

4.1. Topography and land cover drives the spatial variability of mean LSP

Our analyses revealed a clear dependency of mean LSP metrics on topography, particularly for SOS, LOS and NDVIsum (Figs. 3 and 6). The strongest topographical driver of LSP was elevation (Fig. 6 and Table 3). For instance, we observed a delay in SOS and a weak advance in EOS of 3.7 days and −0.65 days respectively with every 100 m increase in elevation, confirming previous studies (Hwang et al., 2011; Norman et al., 2017; Richardson et al., 2006). SOS in most species is dominantly driven by air temperature along the elevation gradient (Cornelius et al., 2013; Hwang et al., 2011; Stöckli et al., 2008). In agreement with Kraus et al. (2016), little to no influence of aspect on

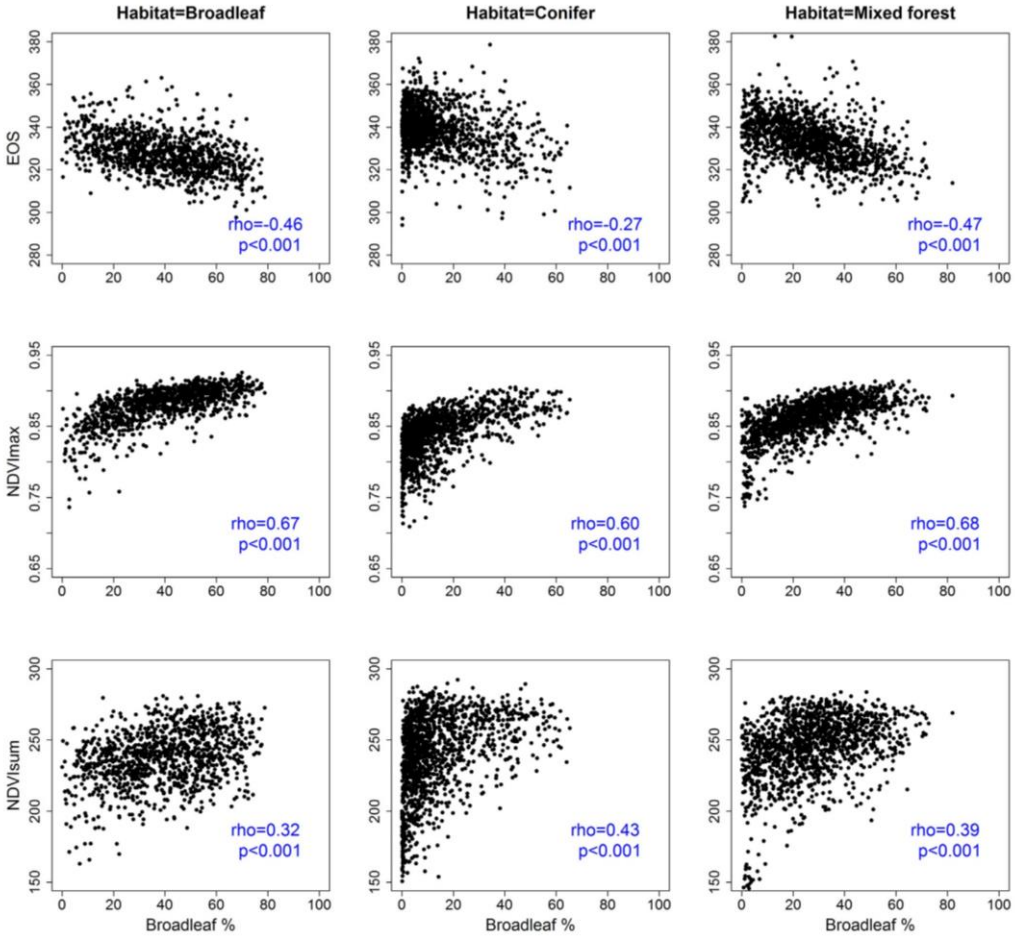

Fig. 6. Relationship between selected mean LSP metrics and percentage of broadleaf in different habitat classes (Spearman correlation coefficients (rho) and its corresponding p values are shown in the subplots). The LiDAR based subpixel information (here percentage of broadleaf) clearly shows an impact on the intra-class variability of LSP.

LSP was found in our study area. Previous studies have however reported the influence of aspect on the LSP behavior due to the difference in radiation received in the south and north facing slopes (Reaves et al., 2018; Xie et al., 2015a). A plausible explanation for the absence of this effect in our study could be that other factors override possible effects of aspect on LSP variability. These factors could be related to the contribution of conifers and broadleaves in mixed forests, an overriding effect of elevation, as well as the temperature inversion in the valleys, which frequently experience late-spring and early autumn frost (Schuster et al., 2014a, 2014b).

Besides topography, land cover characteristics as derived from the habitat map revealed a significant effect on mean LSP variability (Fig. 5) which has also been reported in previous studies for instance using bio-geographical units (Doktor et al., 2009; Ivits et al., 2013; Norman et al., 2017; Rodriguez-Galiano et al., 2015b). Inclusion of either CORINE or Habitat information led to similar improvements in the topography only models, and hence they could be used interchangeably. The effect of forest stand characteristics on LSP metrics however was more pronounced when considering LiDAR-based subpixel information and their interactions (Fig. 6). Consequently, LiDAR based information on the forest stand characteristics revealed highest or comparably high explained variances in LSP-models, confirming that it provides additional information in comparison to the categorical land cover maps.

The better performance of LiDAR based models is likely to be explained by the fact that LiDAR provides information rich subpixel information compared to the categorical land cover maps. That is, land cover maps were not able to resolve the varying proportions of tree types in general, and more specifically the proportion of conifers and broadleaves within each class (see Fig. 6). This information however plays an important role, since these proportions have a significant and land-cover class dependent effect on LSP variability (Fig. 6 and Table 3). As a consequence, LSP models allowing for interactions between LiDAR and land cover maps revealed the highest explained variance for all considered LSP metrics. It is therefore important to consider the subpixel composition of vegetation as similar climatic drivers are known to influence species phenology differently, and conversely different species responding to different triggers (Körner and Basler, 2010; Xie et al., 2015a). Our results also agree with Doktor et al. (2009), who found LSP variability to be not only driven by interannual weather conditions but also to be affected by the deciduous fraction of pixels. For example, in their study, an earlier SOS similar to that of

Table 3
Results of multiple linear regression models of LSP metrics (response variables SOS, EOS, LOS, maxDOY, NDVImax, NDVIsum) for different model types (groups of explanatory variables). Topography model version includes topographical variables (latitude, longitude, slope, elevation, aspect as well as heat load), +CORINE/+ Habitat comprises Topography as well as CORINE and Habitat land cover classes respectively, +LiDAR comprises Topography as well as various stand characteristics (tree height, crown volume, Conifer %, Broadleaf %, number of trees, Shannon's Entropy). The respective best multiple linear regression models were selected in a stepwise procedure based on minimum BIC. The Adj.R^2 and the p-values for bootstrapping analyses in also shown for the respective models (refer Tables S7–8 for detailed results). The models with the minimum BIC are shown in bold.

LSP	Model	Adj. R^2	BIC	p-Value (Bootstrapping)
SOS	Topography	0.62	18,275	0.95
	+CORINE	0.64	18,058	0.78
	+Habitat	0.65	17,898	0.90
	+LiDAR	0.64	18,038	0.90
	+CORINE * LiDAR	0.65	17,934	0.30
	+Habitat * LiDAR	**0.67**	**17,754**	0.10
EOS	Topography	0.17	24,300	0.95
	+CORINE	0.24	23,951	0.22
	+Habitat	0.25	23,826	0.13
	+LiDAR	0.29	23,531	0.90
	+CORINE * LiDAR	0.35	23,314	< 0.001***
	+Habitat * LiDAR	**0.36**	**23,180**	< 0.001***
LOS	Topography	0.42	25,314	0.94
	+CORINE	0.45	25,090	0.73
	+Habitat	0.47	24,876	0.50
	+LiDAR	0.48	24,758	0.95
	+CORINE * LiDAR	0.53	24,468	< 0.001***
	+Habitat * LiDAR	**0.55**	**24,206**	< 0.05*
maxDOY	Topography	0.19	19,689	0.98
	+CORINE	0.31	18,900	0.53
	+Habitat	0.33	18,750	0.32
	+LiDAR	0.34	18,638	0.94
	+CORINE * LiDAR	0.41	18,296	< 0.001***
	+Habitat * LiDAR	**0.42**	**18,172**	0.43
NDVImax	Topography	0.45	−3499	0.94
	+CORINE	0.71	−38,174	0.28
	+Habitat	0.64	−37,224	0.96
	+LiDAR	0.78	−39,063	0.95
	+CORINE * LiDAR	**0.84**	**−40,992**	< 0.001***
	+Habitat * LiDAR	0.82	−40,629	0.30
NDVIsum	Topography	0.61	30,121	0.95
	+CORINE	0.72	28,490	0.42
	+Habitat	0.68	29,169	0.96
	+LiDAR	0.78	27,293	0.94
	+CORINE * LiDAR	0.80	26,931	< 0.001***
	+Habitat * LiDAR	**0.80**	**26,904**	0.112

grasslands was observed as the non-deciduous fraction increased in the pixels. This is particularly interesting when using frequently considered land cover maps such as the CORINE for LSP studies, where the broadleaf forest class is defined as pixels with minimum 30% crown cover and 75% of planting pattern. As a consequence, pixels defined accordingly could at worst still contain 70% non-broadleaf (Doktor et al., 2009; Kosztra et al., 2014). Depending on the relative contribution of such pixels, existing land cover maps might not sufficiently be able to describe the observed spatial variability in LSP. This problem could however be addressed in the future through the use of newer higher resolution satellite data, e.g. as derived from the Sentinel mission from the European Space Agency (ESA, 2016).

Although elevation was revealed as the most important predictor in the various LSP models, we found EOS to be driven more strongly by LiDAR based percentage of broadleaves in the pixels and slope (Table 3). This is reasonable since the proportion of broadleaf trees would also determine the extent of leaf coloration in the pixels i.e. most conifers do not show distinct leaf coloration and hence have a different EOS than broadleaf trees. Typically EOS has been cited to be driven by complex factors, showing non-linear relationships with elevation and to be more tightly linked to light than temperature (Hwang et al., 2011; Stöckli et al., 2008). Xie et al. (2015b) studied a set environmental factors affecting dormancy in deciduous forests and reported cold, frost and heat stress to induce earlier EOS, and moderate-heat and drought stress to delay EOS. Previous research also discussed the difficulty in modelling EOS in vegetation (Estrella and Menzel, 2006; Schuster et al., 2014a, 2014b), which unlike the SOS is less abrupt, and might span a prolonged period, sometimes taking weeks from leaf coloring to complete abscission and hence making it comparatively difficult to observe (Gallinat et al., 2015; Stöckli et al., 2008). Our analyses thus provide vital insights into one of the least understood aspects of LSP (i.e. EOS) and suggests it to be partly spatially driven by subpixel characteristics of forest stand characteristics along with topography.

The NDVImax and the NDVIsum provided the maximum explained variance among the LSP metrics (Table 3). These phenological metrics have been used to quantify ecosystem productivity, post-disaster ecosystem resilience and detection of pest infestation (Berner et al., 2011; Spruce et al., 2011; Wylie et al., 2008). Metrics such as NDVImax, NDVIsum and maxDOY are measures of overall productivity or biomass and timing of maximum availability of vegetation respectively, and are cited to be highly correlated to various ecosystem characteristics such as species richness, migratory and feeding behavior of herbivores (Heumann et al., 2007; Pettorelli et al., 2005). They are known to be robust to outliers and data processing methods, and also correspond better with ground observations (Lumbierres et al., 2017). Such integrated measures of LSP that are not based on specific dates of the year, which are less influenced by user bias might therefore be considered more suitable for tracking climatic effects and phenologically similar pixels in remote sensing data. Hence, these metrics were also included in this study to evaluate the spatial variability in LSP. Since, LSP metrics such as NDVImax are liable to change over time in pixels undergoing land cover disturbances, we have used categorical information from a habitat map to model influence of different land cover types (some of which are undergoing changes such as clear cut, dead wood-lying and dead wood-regenerating) on LSP.

Bootstrapping analyses revealed the different models for SOS to be stable. The inclusion of LiDAR based information on forest stand characteristics still provided additional insight. However, some instability was found in the interaction models for the other phenological metrics. Such instabilities should in future investigations be accounted for using more complex modelling analyses such as random forest models, however care must be taken as such methods can create the impression of a black box if not properly understood (Palczewska et al., 2014).

Previous studies considering land cover effect on LSP have often included oly generic information on land cover classes that might not be able to describe the mixing of different classes and their status (vegetation under stress or undergoing different succession patterns after disturbance, etc.) that is known to affect LSP (Fisher and Mustard, 2007; Helman, 2018; Norman et al., 2017; Spruce et al., 2011; S. Wang et al., 2016). Here, high resolution data from multi spectral sensors along with LiDAR can help identify species and species-specific attributes (Bolton et al., 2018; Fassnacht et al., 2016; Immitzer et al., 2018; Pu and Landry, 2012; Yao et al., 2012) that could improve our understanding on the effect of mixing of classes on LSP at the subpixel level. In our current study, inclusion of LiDAR based information on forest stand helped improve models explaining variability in LSP in the BFNP that shows a complex topography and an even more complex vegetation pattern. Thus, the novelty of this study lies in the use of subpixel vegetation characteristics from LiDAR data that demonstrates the importance of land cover as well as subscale level information in the expression of LSP at the pixel level. Building upon previous studies (Dinno, 2016; Archetti et al., 2013; Klosterman et al., 2014; Nakaji et al., 2011; Schwartz et al., 2002) and our analyses, we therefore strongly recommend incorporating detailed land cover maps and information regarding vegetation characteristics along with disturbances

in LSP models to better account for vegetation composition variability, ideally supplemented with high resolution LiDAR measurements.

4.2. Limitations and outlook

The mismatch in LSP and GP dates as seen in our study is a well-known problem in literature (Misra et al., 2016; Stöckli et al., 2008; Verger et al., 2016). The uncertainties in estimating EOS are larger than other phenophases due its complex and less understood nature (Gallinat et al., 2015; Hwang et al., 2011; Reaves et al., 2018; Stöckli et al., 2008). However, matching of GP and LSP, and choosing the best method is an issue of ongoing debate and beyond the scope of this study, we therefore use commonly cited methods to extract LSP and discuss the variability observed in them.

Certain limitations of our study need to be noted regarding the temporal averaging of LSP measures. Long term variability in LSP measures has not been included for simplicity since frequent or major changes in climatic drivers (i.e. temperature and precipitation) were not expected within the study period (2002–2015). Subsequent studies may find a way to take temporal factors into account for more complex modelling of LSP. Our results however provide a clear improvement in the understanding of land cover and its subpixel heterogeneity that drives spatial variability in mean LSP.

We have to stress, that the acquisition of LiDAR based information is very time consuming and labor intensive, particularly concerning the in-situ measurements as well as the post-processing. Once the data are obtained, they may allow for improving models explaining spatial LSP-variability by up to 112% in explained variance (EOS-model in Table 3), however for SOS the improvement was as low as 8%. Thus, it seems to be a case sensitive decision whether to incorporate LiDAR ground truth information in LSP-models. For EOS, NDVImax and maxDOY it seems meaningful to take the effort in order to extend our knowledge on these yet hardly understood LSP metrics (Gallinat et al., 2015; Stöckli et al., 2008).

5. Conclusions

This study shows the importance of high resolution land cover and forest stand information for understanding the spatial variability of mean LSP. Consequently, detailed land cover information can help to, I) understand the phenology of vegetation cover or forests better and II) link variability or anomalies in LSP to sub pixel information or disturbances. In our study we found significant differences in the mean LSP of the different land cover classes. Even though previous studies have reported the influence of percentage of general canopy cover or fractional cover on LSP, our study is unique as it uses detailed LiDAR information to model the effect of subpixel forest stand information on the mean LSP. We therefore recommend including up-to-date land cover information to better understand the variability in the estimated LSP.

The use of detailed land cover and LiDAR based rich information on forest stand provided crucial insights into the subscale dynamics of vegetation type, proportion and condition that drive intra-class variability in LSP. Improvements in the modelled results of the less understood EOS and the infrequently discussed NDVImax and maxDOY metrics were observed through inclusion of high resolution LiDAR based information on forest stand. Our study builds on previous research on topography and vegetation fractional cover driven variability of LSP, and justifies use of fine scale details of forest stand to understand the real drivers of spatial variability in LSP.

As a surrogate for the labor-intensive LiDAR measures, data-inherent features such as trends and temporal variability may be taken into consideration, since they directly reflect the specificity of each single pixel and may allow for a meaningful aggregation of pixels with similar features (Bajocco et al., 2015; Ivits et al., 2013). This however needs to be evaluated in a direct comparison between such methods and LiDAR based forest stand information. Moreover, our results hold valid for our study area but we highly recommend further studies and replications in areas with different climate, vegetation cover, and consequently phenology to confirm these results.

Acknowledgments

The authors would like to thank the MODIS team and the CORINE land cover team for making the data freely available. This study was funded by the Virtual Alpine Observatory project of the Bavarian Ministry of the Environment and Consumer Protection (VAO II TP II/01 TUS01UFS-67090).

Appendix A. Supplementary data

Supplementary data to this article can be found online at https://doi.org/10.1016/j.rse.2018.09.027.

References

Archetti, M., Richardson, A.D., O'Keefe, J., Delpierre, N., 2013. Predicting climate change impacts on the amount and duration of autumn colors in a new England Forest. PLoS One 8, e57373. https://doi.org/10.1371/journal.pone.0057373.

Badeck, F.W., Bondeau, A., Böttcher, K., Doktor, D., Lucht, W., Schaber, J., Sitch, S., 2004. Responses of spring phenology to climate change. New Phytol. https://doi.org/10.1111/j.1469-8137.2004.01059.x.

Bajocco, S., Dragoz, E., Gitas, I., Smiraglia, D., Salvati, L., Ricotta, C., 2015. Mapping forest fuels through vegetation phenology: the role of coarse-resolution satellite time-series. PLoS One 10, e0119811. https://doi.org/10.1371/journal.pone.0119811.

Berner, L.T., Beck, P.S.A., Bunn, A.G., Lloyd, A.H., Goetz, S.J., 2011. High-latitude tree growth and satellite vegetation indices: correlations and trends in Russia and Canada (1982–2008). J. Geophys. Res. Biogeosci. 116, G01015. https://doi.org/10.1029/2010JG001475.

Bolton, D.K., White, J.C., Wulder, M.A., Coops, N.C., Hermosilla, T., Yuan, X., 2018. Updating stand-level forest inventories using airborne laser scanning and Landsat time series data. Int. J. Appl. Earth Obs. Geoinf. 66, 174–183. https://doi.org/10.1016/j.jag.2017.11.016.

Branson, S., Wegner, J.D., Hall, D., Lang, N., Schindler, K., Perona, P., 2018. From Google Maps to a fine-grained catalog of street trees. ISPRS J. Photogramm. Remote Sens. 135, 13–30. https://doi.org/10.1016/j.isprsjprs.2017.11.008.

Brown, M.E., de Beurs, K.M., 2008. Evaluation of multi-sensor semi-arid crop season parameters based on NDVI and rainfall. Remote Sens. Environ. 112, 2261–2271. https://doi.org/10.1016/j.rse.2007.10.008.

Buras, A., Zang, C., Menzel, A., 2017. Testing the stability of transfer functions. Dendrochronologia 42, 56–62. https://doi.org/10.1016/j.dendro.2017.01.005.

Cai, Z., Jönsson, P., Jin, H., Eklundh, L., 2017. Performance of smoothing methods for reconstructing NDVI time-series and estimating vegetation phenology from MODIS data. Remote Sens. 9, 1271. https://doi.org/10.3390/rs9121271.

Cailleret, M., Heurich, M., Bugmann, H., 2014. Reduction in browsing intensity may not compensate climate change effects on tree species composition in the Bavarian Forest National Park. For. Ecol. Manag. 328, 179–192. https://doi.org/10.1016/j.foreco.2014.05.030.

Chen, X., Wang, D., Chen, J., Wang, C., Shen, M., 2018. The mixed pixel effect in land surface phenology: a simulation study. Remote Sens. Environ. 211, 338–344. https://doi.org/10.1016/j.rse.2018.04.030.

Cho, M.A., Ramoelo, A., Dziba, L., 2017. Response of land surface phenology to variation in tree cover during green-up and senescence periods in the semi-arid savanna of Southern Africa. Remote Sens. 9, 689. https://doi.org/10.3390/rs9070689.

Cleland, E.E., Chuine, I., Menzel, A., Mooney, H.A., Schwartz, M.D., 2007. Shifting plant phenology in response to global change. Trends Ecol. Evol. https://doi.org/10.1016/j.tree.2007.04.003.

Core Team, R., 2014. R: A Language and Environment for Statistical Computing. R Foundation for Statistical Computing, Vienna, Austria, pp. 2014.

Cornelius, C., Estrella, N., Franz, H., Menzel, A., 2013. Linking altitudinal gradients and temperature responses of plant phenology in the Bavarian Alps. Plant Biol. (Stuttg.) 15 (Suppl. 1), 57–69. https://doi.org/10.1111/j.1438-8677.2012.00577.x.

Di-Mauro, B., Fava, F., Busetto, L., Crosta, G.F., Colombo, R., 2014. Post-fire resilience in the Alpine region estimated from MODIS satellite multispectral data. Int. J. Appl. Earth Obs. Geoinf. 32, 163–172. https://doi.org/10.1016/j.jag.2014.04.010.

Dinno, Alexis, 2016. Dunn's test of multiple comparisons using rank sums - R package version, 132 [WWW document]. https://cran.r-project.org/web/packages/dunn.test/index.html, Accessed date: 4 October 2017.

Doktor, D., Bondeau, A., Koslowski, D., Badeck, F.W., 2009. Influence of heterogeneous landscapes on computed green-up dates based on daily AVHRR NDVI observations. Remote Sens. Environ. 113, 2618–2632. https://doi.org/10.1016/j.rse.2009.07.020.

Duchemin, B., Goubier, J., Courrier, G., 1999. Monitoring phenological key stages and cycle duration of temperate deciduous forest ecosystems with NOAA/AVHRR data. Remote Sens. Environ. 67, 68–82. https://doi.org/10.1016/S0034-4257(98)00067-4.

Duncan, J.M.A., Dash, J., Atkinson, P.M., 2015. The potential of satellite-observed crop phenology to enhance yield gap assessments in smallholder landscapes. Front. Environ. Sci. 3 (56). https://doi.org/10.3389/fenvs.2015.00056.

Dupke, C., Bonenfant, C., Reineking, B., Hable, R., Zeppenfeld, T., Ewald, M., Heurich, M., 2017. Habitat selection by a large herbivore at multiple spatial and temporal scales is

primarily governed by food resources. Ecography 40, 1014–1027. https://doi.org/10.1111/ecog.02152. (Cop.).
EEA, 2012. CLC 2012 — copernicus land monitoring service [WWW Document]. http://land.copernicus.eu/pan-european/corine-land-cover/clc-2012/view, Accessed date: 26 June 2017.
Eklundh, L., Jonsson, P., 2015. TIMESAT: a software package for time-series processing and assessment of vegetation dynamics. In: Kuenzer, C., Dech, S., Wagner, W. (Eds.), Remote Sensing and Digital Image Processing. Springer International Publishing, Cham, pp. 141–158. https://doi.org/10.1007/978-3-319-15967-6_7.
ESA, 2016. Copernicus. Observing the Earth [WWW Document]. ESA websitehttp://www.esa.int/Our_Activities/Observing_the_Earth/Copernicus/Overview4, Accessed date: 17 October 2017.
Estrella, N., Menzel, A., 2006. Responses of leaf colouring in four deciduous tree species to climate and weather in Germany. Clim. Res. 32, 253–267. https://doi.org/10.3354/cr032253.
Fassnacht, F.E., Latifi, H., Stereńczak, K., Modzelewska, A., Lefsky, M., Waser, L.T., Straub, C., Ghosh, A., 2016. Review of studies on tree species classification from remotely sensed data. Remote Sens. Environ. 186, 64–87. https://doi.org/10.1016/j.rse.2016.08.013.
Fisher, J.I., Mustard, J.F., 2007. Cross-scalar satellite phenology from ground, Landsat, and MODIS data. Remote Sens. Environ. 109, 261–273. https://doi.org/10.1016/j.rse.2007.01.004.
Fuller, D.O., 1999. Canopy phenology of some mopane and miombo woodlands in eastern Zambia. Glob. Ecol. Biogeogr. 8, 199–209. https://doi.org/10.1046/j.1365-2699.1999.00130.x.
Gallinat, A.S., Primack, R.B., Wagner, D.L., 2015. Autumn, the neglected season in climate change research. Trends Ecol. Evol. https://doi.org/10.1016/j.tree.2015.01.004.
Gessner, U., Knauer, K., Kuenzer, C., Dech, S., 2015. Land surface phenology in a West African Savanna: impact of land use, land cover and fire. In: Remote Sensing Time Series. Springer, Cham, pp. 203–223. https://doi.org/10.1007/978-3-319-15967-6_10.
Gonsamo, A., D'Odorico, P., Chen, J.M., Wu, C., Buchmann, N., 2017. Changes in vegetation phenology are not reflected in atmospheric CO_2 and 13C/12C seasonality. Glob. Chang. Biol. https://doi.org/10.1111/gcb.13646.
Grömping, U., 2006. Relative importance for linear regression in R: the package relaimpo. J. Stat. Softw. 17, 1–27. https://doi.org/10.18637/jss.v017.i01.
Hamunyela, E., Verbesselt, J., Roerink, G., Herold, M., 2013. Trends in spring phenology of western European deciduous forests. Remote Sens. 5, 6159–6179. https://doi.org/10.3390/rs5126159.
Han, Q., Luo, G., Li, C., 2013. Remote sensing-based quantification of spatial variation in canopy phenology of four dominant tree species in Europe. J. Appl. Remote. Sens. 7 (73485). https://doi.org/10.1117/1.JRS.7.073485.
Hanes, J.M., Liang, L., Morisette, J.T., 2014. Land surface phenology. In: Biophysical Applications of Satellite Remote Sensing. Springer Remote Sensing/Photogrammetry, pp. 236. https://doi.org/10.1007/978-3-642-25047-7.
Helman, D., 2018. Land surface phenology: what do we really "see" from space? Sci. Total Environ. https://doi.org/10.1016/j.scitotenv.2017.07.237.
Heumann, B.W., Seaquist, J.W., Eklundh, L., Jönsson, P., 2007. AVHRR derived phenological change in the Sahel and Soudan, Africa, 1982–2005. Remote Sens. Environ. 108, 385–392. https://doi.org/10.1016/j.rse.2006.11.025.
Heurich, M., Beudert, B., Rall, H., Křenová, Z., 2010. National parks as model regions for interdisciplinary long-term ecological research: The Bavarian forest and Šumavá national parks underway to transboundary ecosystem research. In: Long-Term Ecological Research: Between Theory and Application. Springer, Dordrecht, pp. 327–344. https://doi.org/10.1007/978-90-481-8782-9_23.
Hijmans, R.J., 2016. Geographic data analysis and modeling. R package raster version 2.5-8. [WWW document]. https://cran.r-project.org/web/packages/raster/index.html, Accessed date: 4 October 2017.
Hird, J.N., McDermid, G.J., 2009. Noise reduction of NDVI time series: an empirical comparison of selected techniques. Remote Sens. Environ. 113, 248–258. https://doi.org/10.1016/j.rse.2008.09.003.
Hmimina, G., Dufrêne, E., Pontailler, J.Y., Delpierre, N., Aubinet, M., Caquet, B., de Grandcourt, A., Burban, B., Flechard, C., Granier, A., Gross, P., Heinesch, B., Longdoz, B., Moureaux, C., Ourcival, J.M., Rambal, S., Saint André, L., Soudani, K., 2013. Evaluation of the potential of MODIS satellite data to predict vegetation phenology in different biomes: an investigation using ground-based NDVI measurements. Remote Sens. Environ. 132, 145–158. https://doi.org/10.1016/j.rse.2013.01.010.
Hwang, T., Song, C., Vose, J.M., Band, L.E., 2011. Topography-mediated controls on local vegetation phenology estimated from MODIS vegetation index. Landsc. Ecol. 26, 541–556. https://doi.org/10.1007/s10980-011-9580-8.
Immitzer, M., Böck, S., Einzmann, K., Vuolo, F., Pinnel, N., Wallner, A., Atzberger, C., 2018. Fractional cover mapping of spruce and pine at 1 ha resolution combining very high and medium spatial resolution satellite imagery. Remote Sens. Environ. 204, 690–703. https://doi.org/10.1016/j.rse.2017.09.031.
Ivits, E., Cherlet, M., Mehl, W., Sommer, S., 2013. Ecosystem functional units characterized by satellite observed phenology and productivity gradients: a case study for Europe. Ecol. Indic. 27, 17–28. https://doi.org/10.1016/j.ecolind.2012.11.010.
Jin, S., Sader, S.A., 2005. MODIS time-series imagery for forest disturbance detection and quantification of patch size effects. Remote Sens. Environ. 99, 462–470. https://doi.org/10.1016/j.rse.2005.09.017.
Johnson, J.W., LeBreton, J.M., 2004. History and use of relative importance indices in organizational research. Organ. Res. Methods 7, 238–257. https://doi.org/10.1177/1094428104266510.
Kariyeva, J., van Leeuwen, W.J.D., 2011. Environmental drivers of NDVI-based vegetation phenology in Central Asia. Remote Sens. 3, 203–246. https://doi.org/10.3390/rs3020203.
Klosterman, S.T., Hufkens, K., Gray, J.M., Melaas, E., Sonnentag, O., Lavine, I., Mitchell, L., Norman, R., Friedl, M.A., Richardson, A.D., 2014. Evaluating remote sensing of deciduous forest phenology at multiple spatial scales using PhenoCam imagery. Biogeosciences 11, 4305–4320. https://doi.org/10.5194/bg-11-4305-2014.
Kobayashi, H., Yunus, A.P., Nagai, S., Sugiura, K., Kim, Y., Van Dam, B., Nagano, H., Zona, D., Harazono, Y., Bret-Harte, M.S., Ichii, K., Ikawa, H., Iwata, H., Oechel, W.C., Ueyama, M., Suzuki, R., 2016. Latitudinal gradient of spruce forest understory and tundra phenology in Alaska as observed from satellite and ground-based data. Remote Sens. Environ. 177, 160–170. https://doi.org/10.1016/j.rse.2016.02.020.
Körner, C., Basler, D., 2010. Phenology under global warming. Science. https://doi.org/10.1126/science.1186473. (80-.).
Koster, R.D., Walker, G.K., Collatz, G.J., Thornton, P.E., 2014. Hydroclimatic controls on the means and variability of vegetation phenology and carbon uptake. J. Clim. 27, 5632–5652. https://doi.org/10.1175/JCLI-D-13-00477.1.
Kosztra, B., Arnold, S., Banko, G., Hazeu, G., Büttner, G., 2014. Proposal for Enhancement of CLC Nomenclature Guidelines, EEA Technical Report.
Kraus, C., Zang, C., Menzel, A., 2016. Elevational response in leaf and xylem phenology reveals different prolongation of growing period of common beech and Norway spruce under warming conditions in the Bavarian Alps. Eur. J. For. Res. 135, 1011–1023. https://doi.org/10.1007/s10342-016-0990-7.
Kross, A., Fernandes, R., Seaquist, J., Beaubien, E., 2011. The effect of the temporal resolution of NDVI data on season onset dates and trends across Canadian broadleaf forests. Remote Sens. Environ. 115, 1564–1575. https://doi.org/10.1016/j.rse.2011.02.015.
Lausch, A., Fahse, L., Heurich, M., 2011. Factors affecting the spatio-temporal dispersion of *Ips typographus* (L.) in Bavarian Forest National Park: a long-term quantitative landscape-level analysis. For. Ecol. Manag. 261, 233–245. https://doi.org/10.1016/j.foreco.2010.10.012.
Liang, L., Schwartz, M.D., Fei, S., 2011. Validating satellite phenology through intensive ground observation and landscape scaling in a mixed seasonal forest. Remote Sens. Environ. 115, 143–157. https://doi.org/10.1016/j.rse.2010.08.013.
Lumbierres, M., Méndez, P., Bustamante, J., Soriguer, R., Santamaría, L., 2017. Modeling biomass production in seasonal wetlands using MODIS NDVI land surface phenology. Remote Sens. 9, 392. https://doi.org/10.3390/rs9040392.
Luo, Z., Yu, S., 2017. Spatiotemporal variability of land surface phenology in China from 2001–2014. Remote Sens. 9, 65. https://doi.org/10.3390/rs9010065.
Matiu, M., Bothmann, L., Steinbrecher, R., Menzel, A., 2017. Monitoring succession after a non-cleared windthrow in a Norway spruce mountain forest using webcam, satellite vegetation indices and turbulent CO_2 exchange. Agric. For. Meteorol. 244–245, 72–81. https://doi.org/10.1016/j.agrformet.2017.05.020.
Matthews, E.R., Mazer, S.J., 2016. Historical changes in flowering phenology are governed by temperature × precipitation interactions in a widespread perennial herb in western North America. New Phytol. 210, 157–167. https://doi.org/10.1111/nph.13751.
McCune, B., Keon, D., 2002. Equations for potential annual direct incident radiation and heat load. J. Veg. Sci. 13, 603–606. https://doi.org/10.1111/j.1654-1103.2002.tb02087.x.
Menzel, A., Fabian, P., 1999. Growing season extended in Europe. Nature 397, 659. https://doi.org/10.1038/17709.
Menzel, A., Jakobi, G., Ahas, R., Scheifinger, H., Estrella, N., 2003. Variations of the climatological growing season (1951–2000) in Germany compared with other countries. Int. J. Climatol. 23, 793–812. https://doi.org/10.1002/joc.915.
Menzel, A., Sparks, T.H., Estrella, N., Koch, E., Aasa, A., Ahas, R., Alm-Kübler, K., Bissolli, P., Braslavská, O., Briede, A., Chmielewski, F.M., Crepinsek, Z., Curnel, Y., Dahl, åSlöG, Defila, C., Donnelly, A., Filella, Y., Jatczak, K., MåGe, F., Mestre, A., Nordli, øYvind, Peñuelas, J., Pirinen, P., Remišová, V., Scheifinger, H., Striz, M., Susnik, A., Van Vliet, A.J.H., Wielgolaski, F.-E., Zach, S., Zust, A., 2006. European phenological response to climate change matches the warming pattern. Glob. Chang. Biol. 12, 1969–1976. https://doi.org/10.1111/j.1365-2486.2006.01193.x.
Misra, G., Buras, A., Menzel, A., 2016. Effects of different methods on the comparison between land surface and ground phenology—a methodological case study from South-Western Germany. Remote Sens. 8, 753. https://doi.org/10.3390/rs8090753.
Muller, S., Ammer, C., Nosslein, S., 2000. Analyses of stand structure as a tool for silvicultural decisions - a case study in a *Quercus petraea - Sorbus torminalis* stand. Forstw. Cbl. 119, 32–42.
Myneni, R.B., Keeling, C.D., Tucker, C.J., Asrar, G., Nemani, R.R., 1997. Increased plant growth in the northern high latitudes from 1981 to 1991. Nature 386, 698–702. https://doi.org/10.1038/386698a0.
Nagai, S., Nasahara, K.N., Muraoka, H., Akiyama, T., Tsuchida, S., 2010. Field experiments to test the use of the normalized-difference vegetation index for phenology detection. Agric. For. Meteorol. 150, 152–160. https://doi.org/10.1016/j.agrformet.2009.09.010.
Nagai, S., Nasahara, K.N., Inoue, T., Saitoh, T.M., Suzuki, R., 2016. Review: advances in in situ and satellite phenological observations in Japan. Int. J. Biometeorol. https://doi.org/10.1007/s00484-015-1053-3.
Naimi, B., 2017. usdm: uncertainty analysis for species distribution models-CRAN - package usdm [WWW document]. https://cran.r-project.org/web/packages/usdm/index.html, Accessed date: 4 October 2017.
Naimi, B., Hamm, N.A.S., Groen, T.A., Skidmore, A.K., Toxopeus, A.G., 2014. Where is positional uncertainty a problem for species distribution modelling? Ecography 37, 191–203. https://doi.org/10.1111/j.1600-0587.2013.00205.x. (Cop.).
Nakaji, T., Oguma, H., Hiura, T., 2011. Ground-based monitoring of the leaf phenology of deciduous broad-leaved trees using high resolution NDVI camera images. J. Agric. Meteorol. 67, 65–74. https://doi.org/10.2480/agrmet.67.2.3.
Norman, S., Hargrove, W., Christie, W., 2017. Spring and Autumn phenological variability across environmental gradients of Great Smoky Mountains National Park, USA. Remote Sens. 9, 407. https://doi.org/10.3390/rs9050407.
O'Brien, R.M., 2007. A caution regarding rules of thumb for variance inflation factors. Qual. Quant. 41, 673–690. https://doi.org/10.1007/s11135-006-9018-6.
Palczewska, A., Palczewski, J., Marchese Robinson, R., Neagu, D., 2014. Interpreting random forest classification models using a feature contribution method. In: Bouabana-Tebibel, T., Rubin, S. (Eds.), Integration of Reusable Systems. Springer, Cham, pp. 193–218. https://doi.org/10.1007/978-3-319-04717-1_9.

Parmesan, C., Yohe, G., 2003. A globally coherent fingerprint of climate change impacts across natural systems. Nature 421, 37–42. https://doi.org/10.1038/nature01286.
Peng, D., Zhang, X., Zhang, B., Liu, L., Liu, X., Huete, A.R., Huang, W., Wang, S., Luo, S., Zhang, X., Zhang, H., 2017. Scaling effects on spring phenology detections from MODIS data at multiple spatial resolutions over the contiguous United States. ISPRS J. Photogramm. Remote Sens. 132, 185–198. https://doi.org/10.1016/J.ISPRSJPRS.2017.09.002.
Pettorelli, N., Vik, J.O., Mysterud, A., Gaillard, J.-M., Tucker, C.J., Stenseth, N.C., 2005. Using the satellite-derived NDVI to assess ecological responses to environmental change. Trends Ecol. Evol. 20, 503–510. https://doi.org/10.1016/j.tree.2005.05.011.
Polewski, P., Yao, W., Heurich, M., Krzystek, P., Stilla, U., 2016. Combining active and semisupervised learning of remote sensing data within a Renyi entropy regularization framework. IEEE J. Sel. Top. Appl. Earth Obs. Remote Sens. 9, 2910–2922. https://doi.org/10.1109/JSTARS.2015.2510867.
Pu, R., Landry, S., 2012. A comparative analysis of high spatial resolution IKONOS and WorldView-2 imagery for mapping urban tree species. Remote Sens. Environ. 124, 516–533. https://doi.org/10.1016/j.rse.2012.06.011.
Rautiainen, M., Heiskanen, J., Korhonen, L., 2012. Seasonal changes in canopy leaf area index and MODIS vegetation products for a boreal forest site in central Finland. Boreal Environ. Res. 17, 72–84.
Reaves, V.C., Elmore, A.J., Nelson, D.M., McNeil, B.E., 2018. Drivers of spatial variability in greendown within an oak-hickory forest landscape. Remote Sens. Environ. 210, 422–433. https://doi.org/10.1016/j.rse.2018.03.027.
Reitberger, J., Schnörr, C., Krzystek, P., Stilla, U., 2009. 3D segmentation of single trees exploiting full waveform LIDAR data. ISPRS J. Photogramm. Remote Sens. 64, 561–574. https://doi.org/10.1016/j.isprsjprs.2009.04.002.
Richardson, A.D., O'Keefe, J., 2009. Phenological differences between understory and overstory a case study using the long-term Harvard Forest records. In: Phenology of Ecosystem Processes: Applications in Global Change Research. Springer New York, New York, NY, pp. 87–117. https://doi.org/10.1007/978-1-4419-0026-5_4.
Richardson, A.D., Bailey, A.S., Denny, E.G., Martin, C.W., O'Keefe, J., 2006. Phenology of a northern hardwood forest canopy. Glob. Chang. Biol. 12, 1174–1188. https://doi.org/10.1111/j.1365-2486.2006.01164.x.
Rodriguez-Galiano, V.F., Dash, J., Atkinson, P.M., 2015a. Intercomparison of satellite sensor land surface phenology and ground phenology in Europe: inter-annual comparison and modelling. Geophys. Res. Lett. 42, 2253–2260. https://doi.org/10.1002/2015GL063586.
Rodriguez-Galiano, V.F., Dash, J., Atkinson, P.M., 2015b. Characterising the land surface phenology of Europe using decadal MERIS data. Remote Sens. 7, 9390–9409. https://doi.org/10.3390/rs70709390.
Schultz, P.A., Halpert, M.S., 1993. Global correlation of temperature, NDVI and precipitation. Adv. Space Res. 13, 277–280. https://doi.org/10.1016/0273-1177(93)90559-T.
Schuster, C., Estrella, N., Menzel, A., 2014a. Shifting and extension of phenological periods with increasing temperature along elevational transects in Southern Bavaria. Plant Biol. 16, 332–344. https://doi.org/10.1111/plb.12071.
Schuster, C., Kirchner, M., Jakobi, G., Menzel, A., 2014b. Frequency of inversions affects senescence phenology of *Acer pseudoplatanus* and *Fagus sylvatica*. Int. J. Biometeorol. 58, 485–498. https://doi.org/10.1007/s00484-013-0709-0.
Schwartz, M.D., Reed, B.C., White, M.A., 2002. Assessing satellite-derived start-of-season measures in the conterminous USA. Int. J. Climatol. 22, 1793–1805. https://doi.org/10.1002/joc.819.
Shang, R., Liu, R., Xu, M., Liu, Y., Zuo, L., Ge, Q., 2017. The relationship between threshold-based and inflexion-based approaches for extraction of land surface phenology. Remote Sens. Environ. https://doi.org/10.1016/j.rse.2017.07.020.
Simonetti, D., Simonetti, E., Szantoi, Z., Lupi, A., Eva, H.D., 2015. First results from the phenology-based synthesis classifier using Landsat 8 imagery. IEEE Geosci. Remote Sens. Lett. 12, 1496–1500. https://doi.org/10.1109/LGRS.2015.2409982.
Soudani, K., le Maire, G., Dufrêne, E., François, C., Delpierre, N., Ulrich, E., Cecchini, S., 2008. Evaluation of the onset of green-up in temperate deciduous broadleaf forests derived from moderate resolution imaging Spectroradiometer (MODIS) data. Remote Sens. Environ. 112, 2643–2655. https://doi.org/10.1016/j.rse.2007.12.004.
Spruce, J.P., Sader, S., Ryan, R.E., Smoot, J., Kuper, P., Ross, K., Prados, D., Russell, J., Gasser, G., McKellip, R., Hargrove, W., 2011. Assessment of MODIS NDVI time series data products for detecting forest defoliation by gypsy moth outbreaks. Remote Sens. Environ. 115, 427–437. https://doi.org/10.1016/j.rse.2010.09.013.
Stöckli, R., Rutishauser, T., Dragoni, D., O'Keefe, J., Thornton, P.E., Jolly, M., Lu, L., Denning, A.S., 2008. Remote sensing data assimilation for a prognostic phenology model. J. Geophys. Res. Biogeosci. 113. https://doi.org/10.1029/2008JG000781.
Stoner, D.C., Sexton, J.O., Nagol, J., Bernales, H.H., Edwards, T.C., 2016. Ungulate reproductive parameters track satellite observations of plant phenology across latitude and climatological regimes. PLoS One 11, e0148780. https://doi.org/10.1371/journal.pone.0148780.
Studer, S., Stöckli, R., Appenzeller, C., Vidale, P.L., 2007. A comparative study of satellite and ground-based phenology. Int. J. Biometeorol. 51, 405–414. https://doi.org/10.1007/s00484-006-0080-5.
Survey, U.S.G., 2015. MOD09A1|LP DAAC::NASA land data products and services [WWW document]. https://lpdaac.usgs.gov/dataset_discovery/modis/modis_products_table/mod09gq, Accessed date: 11 September 2017.
Tan, B., Woodcock, C.E., Hu, J., Zhang, P., Ozdogan, M., Huang, D., Yang, W., Knyazikhin, Y., Myneni, R.B., 2006. The impact of gridding artifacts on the local spatial properties of MODIS data: implications for validation, compositing, and band-to-band registration across resolutions. Remote Sens. Environ. 105, 98–114. https://doi.org/10.1016/j.rse.2006.06.008.
Tansey, C.J., Hadfield, J.D., Phillimore, A.B., 2017. Estimating the ability of plants to plastically track temperature-mediated shifts in the spring phenological optimum. Glob. Chang. Biol. 23, 3321–3334. https://doi.org/10.1111/gcb.13624.
Thackeray, S.J., Henrys, P.A., Hemming, D., Bell, J.R., Botham, M.S., Burthe, S., Helaouet, P., Johns, D.G., Jones, I.D., Leech, D.I., Mackay, E.B., Massimino, D., Atkinson, S., Bacon, P.J., Brereton, T.M., Carvalho, L., Clutton-Brock, T.H., Duck, C., Edwards, M., Elliott, J.M., Hall, S.J.G., Harrington, R., Pearce-Higgins, J.W., Høye, T.T., Kruuk, L.E.B., Pemberton, J.M., Sparks, T.H., Thompson, P.M., White, I., Winfield, I.J., Wanless, S., 2016. Phenological sensitivity to climate across taxa and trophic levels. Nature 535, 241–245. https://doi.org/10.1038/nature18608.
Venables, W.N., Ripley, B.D., Venables, W.N., William, N., 2002. Modern Applied Statistics with S, 4th ed. Springer.
Verger, A., Filella, I., Baret, F., Peñuelas, J., 2016. Vegetation baseline phenology from kilometric global LAI satellite products. Remote Sens. Environ. 178, 1–14. https://doi.org/10.1016/j.rse.2016.02.057.
Vermote, E.F., Wolfe, R., 2015. MOD09GA MODIS/Terra surface reflectance daily L2G global 1 km and 500 m SIN grid V006 [WWW document]. NASA EOSDIS L. Process. DAAChttps://doi.org/10.5067/MODIS/MOD09GA.006.
Walther, G.R., Post, E., Convey, P., Menzel, A., Parmesan, C., Beebee, T.J.C., Fromentin, J.M., Hoegh-Guldberg, O., Bairlein, F., 2002. Ecological responses to recent climate change. Nature 416, 389–395. https://doi.org/10.1038/416389a.
Wang, S., Yang, B., Yang, Q., Lu, L., Wang, X., Peng, Y., 2016. Temporal trends and spatial variability of vegetation phenology over the Northern Hemisphere during 1982–2012. PLoS One 11, e0157134. https://doi.org/10.1371/journal.pone.0157134.
Wang, Y., Xie, D., Hu, R., Yan, G., 2016. Spatial scale effect on vegetation phenological analysis using remote sensing data. In: 2016 IEEE International Geoscience and Remote Sensing Symposium (IGARSS). IEEE, pp. 1329–1332. https://doi.org/10.1109/IGARSS.2016.7729338.
Wang, X., Gao, Q., Wang, C., Yu, M., 2017. Spatiotemporal patterns of vegetation phenology change and relationships with climate in the two transects of East China. Glob. Ecol. Conserv. 10, 206–219. https://doi.org/10.1016/J.GECCO.2017.01.010.
White, M.A., Thornton, P.E., Running, S.W., 1997. A continental phenology model for monitoring vegetation responses to interannual climatic variability. Glob. Biogeochem. Cycles 11, 217–234. https://doi.org/10.1029/97gb00330.
White, M.A., de Beurs, K.M., Didan, K., Inouye, D.W., Richardson, A.D., Jensen, O.P., O'Keefe, J., Zhang, G., Nemani, R.R., van Leeuwen, W.J.D., Brown, J.F., de Wit, A., Schaepman, M., Lin, X., Dettinger, M., Bailey, A.S., Kimball, J., Schwartz, M.D., Baldocchi, D.D., Lee, J.T., Lauenroth, W.K., 2009. Intercomparison, interpretation, and assessment of spring phenology in North America estimated from remote sensing for 1982–2006. Glob. Chang. Biol. 15, 2335–2359. https://doi.org/10.1111/j.1365-2486.2009.01910.x.
Wylie, B.K., Zhang, L., Bliss, N., Ji, L., Tieszen, L.L., Jolly, W.M., 2008. Integrating modelling and remote sensing to identify ecosystem performance anomalies in the boreal forest, Yukon river basin, Alaska. Int. J. Digit. Earth 1, 196–220. https://doi.org/10.1080/17538940802038366.
Xie, Y., Wang, X., Silander, J.A., 2015b. Deciduous forest responses to temperature, precipitation, and drought imply complex climate change impacts. Proc. Natl. Acad. Sci. 112, 13585–13590. https://doi.org/10.1073/pnas.1509991112.
Xie, Y., Ahmed, K.F., Allen, J.M., Wilson, A.M., Silander, J.A., 2015a. Green-up of deciduous forest communities of northeastern North America in response to climate variation and climate change. Landsc. Ecol. 30, 109–123. https://doi.org/10.1007/s10980-014-0099-7.
Xin, Q., Olofsson, P., Zhu, Z., Tan, B., Woodcock, C.E., 2013. Toward near real-time monitoring of forest disturbance by fusion of MODIS and Landsat data. Remote Sens. Environ. 135, 234–247. https://doi.org/10.1016/j.rse.2013.04.002.
Yao, W., Krzystek, P., Heurich, M., 2012. Tree species classification and estimation of stem volume and DBH based on single tree extraction by exploiting airborne full-waveform LiDAR data. Remote Sens. Environ. 123, 368–380. https://doi.org/10.1016/j.rse.2012.03.027.
Yu, Q., Jia, D.-R., Tian, B., Yang, Y.-P., Duan, Y.-W., 2016. Changes of flowering phenology and flower size in rosaceous plants from a biodiversity hotspot in the past century. Sci. Rep. 6 (28302). https://doi.org/10.1038/srep28302.
Zeng, F.W., James Collatz, G., Pinzon, J.E., Ivanoff, A., 2013. Evaluating and quantifying the climate-driven interannual variability in global inventory modeling and mapping studies (GIMMS) normalized difference vegetation index (NDVI3g) at global scales. Remote Sens. 5, 3918–3950. https://doi.org/10.3390/rs5083918.
Zeppenfeld, T., Svoboda, M., Derose, R.J., Heurich, M., Muller, J., Cizkova, P., Stary, M., Bace, R., Donato, D.C., 2015. Response of mountain *Picea abies* forests to stand-replacing bark beetle outbreaks: neighbourhood effects lead to self-replacement. J. Appl. Ecol. 52, 1402–1411. https://doi.org/10.1111/1365-2664.12504.
Zhang, X., Wang, J., Gao, F., Liu, Y., Schaaf, C., Friedl, M., Yu, Y., Jayavelu, S., Gray, J., Liu, L., Yan, D., Henebry, G.M., 2017. Exploration of scaling effects on coarse resolution land surface phenology. Remote Sens. Environ. 190, 318–330. https://doi.org/10.1016/j.rse.2017.01.001.
Zhang, Y., Li, L., Wang, H., Zhang, Y., Wang, N., Chen, J., 2017. Land surface phenology of Northeast China during 2000–2015: temporal changes and relationships with climate changes. Environ. Monit. Assess. 189 (531). https://doi.org/10.1007/s10661-017-6247-1.
Zhao, H., Yang, Z., Di, L., Pei, Z., 2012. Evaluation of temporal resolution effect in remote sensing based crop phenology detection studies. In: IFIP Advances in Information and Communication Technology, pp. 135–150. https://doi.org/10.1007/978-3-642-27278-3_16.

Elevation linked-phenological lapse rates show differences in the pre-Alpine and Alpine regions of Bavaria: Overview from ground and satellite observations

Gourav Misra, Sarah Asam and Annette Menzel.

Abstract
The role of temperature in driving phenology of vegetation is well established. However, with the changing climate leading to differences in temperature regimes during the year and especially also during winter chilling, a pronounced variability in already established phenological rates is now being observed along the elevational gradient of mountains. In this study, we analysed the elevation linked lapse rates of phenological dates in the pre-alpine and alpine regions of the Bavarian Alps in Germany. The dates for the start of season (SOS) and the end of season (EOS) were extracted from a 4-day maximum value composite Moderate Resolution Imaging Spectrometer (MODIS) sensor's Normalised Difference Vegetation Index (NDVI) time series data for the years 2001-2016. Analyses of SOS data showed higher elevational lapse rates in the alpine areas than the pre-alpine areas, possibly due to longer duration of snow. Maximal differences in rates of SOS of alpine and pre-alpine areas were observed in years with preceding warm winters with lack of chilling. Minimum differences in the rates of SOS were found along the elevational gradient during cold spring and cold winter years. The MODIS based SOS showed the highest correspondence when validated against the gridded German Meteorological Service (DWD) leaf unfolding data. The EOS dates showed a comparatively lower correspondence to DWD data and their lapse rates in the pre-alpine and alpine regions were tricky to validate. Contrary to SOS, EOS dates revealed lower, but still positive lapse rate in the alpine areas than the pre-alpine areas.

Keywords: elevation, phenology, lapse rates, climate change, forest, Alps.

1. Introduction

Climate change induced shifts in phenology have been studied extensively in the past decades. Advances in spring phenology with warming are well established (Menzel and Fabian, 1999), however studies in recent years have also pointed to a decreased sensitivity to spring warming as consequence of lacking chilling in warmer winters (Laube et al., 2014). This timing of phenological events is crucial for key species interactions such as feeding habits, reproduction and migration, and are indicators of species abundance at any location (Burgess et al., 2018; Visser and Both, 2005). Moreover, climate change is known to not only affect occurrence of key phenophases (Menzel and Fabian, 1999), but it is also now changing the established phenological patterns regionally (Menzel et al., 2006; Vitasse et al., 2017). However, changing phenological timings of key species along with the now documented changes in phenological patterns could lead to mismatches or desynchrony in species interactions having far reaching consequences on ecosystem structure and functioning (Parmesan and Yohe, 2003; Vitasse et al., 2017). E.g. spatially more uniform phenological onset dates may influence the vulnerability of migratory species in terms of decreasing their choice of alternative sites in case of risk of mismatch (Diez et al., 2012).

Elevational gradients constitute powerful tools to study in a space-for-time approach triggers for phenological onset dates, providing a large set of meteorological conditions however with identical photoperiod. Few examples have also addressed the role of chilling and snow as additional phenological triggers across gradients. Vandvik et al. (2018) report a climate change induced decrease in the chilling period in lower elevations and an increase in the

effective chilling period in higher elevations of temperate regions. Additionally, the early melting of snow and the lengthening of the frost free period has led to early leaf out in trees across many regions of the world (Asam et al., 2018; Menzel et al., 2003). For e.g., such climate change impacts lead to earlier growth of trees and faster closure of overstory canopy which could pose challenges for growth of forest understory species. Thus, it is important to carefully study the challenges presented by the changing climate with respect to its varying effects on species at various gradients of environmental conditions and regions. Therefore knowledge of temporal and spatial variations in phenology and its drivers is necessary to develop mitigation and adaptation strategies. Although a few first studies have dealt with chilling influence on warming sensitivity at gradients based on ground phenological observations, not many studies based on remote sensing products exist.

Since, ground observation of phenology at higher elevation is severely limited due to a lack of permanent settlements and thus observers (Menzel et al., 2003), this study uses pioneer techniques such as remote sensing for repetitive mapping of forest seasonality at elevational gradients in the Alps. The main research questions of this study are: 1) are there differences in the annual elevational rates of phenology observed in the pre-alpine and alpine regions of the Bavarian Alps? and 2) how do the spring and (preceding) winter temperatures drive the elevational phenological response rates in forests?

2. Study Area and Data

This study was carried out in the Bavarian alpine region of Germany (corresponding to the administrative units of the alpine convention, Figure 1) for which we defined areas with elevations < 1000 m a.s.l. as pre-alpine and > 1000 m a.s.l. as alpine. The elevation of the forested area ranges from ~400 to 1800 m a.s.l. (see also Figure S1), and primarily consists of three classes (broad-leaved, coniferous and mixed forests). The species composition comprises mainly Norway spruce (*Picea abies* (L.) H.KARST) besides silver fir (*Abies alba* MILL.), European larch (*Larix decidua* MILL) as well as the deciduous tree species European beech (*Fagus sylvatica* L.) and sycamore (*Acer pseudoplatanus* L.), however with only spruce reaching elevation beyond 1500 m a.s.l.

Remote sensing information in the form of 4-day MODIS NDVI MVC data for the years 2001 to 2016 was used in this study. As described in detail in Asam et al. (2018), this NDVI product was generated from the daily MOD09GQ product collection 6 and used in conjunction with MOD09GA product for constraints on quality and viewing geometry of the pixels.

A CORINE land use cover map for year 2012 with 250 metre spatial resolution was used in this study which is freely available for download from the Copernicus Land Monitoring Service portal (EEA, 2012). A 30 meter resolution Shuttle Radar Topography Mission (SRTM) based digital elevation model was obtained from the earthexplorer portal of the United State Geological Survey website (USGS, 2018).
In the phenological network of the German Meteorological Service volunteers observe various phenological phases at up to 43 stations in the Bavarian study region. We selected the spring and autumn phenological phases of *Fagus sylvatica* L. (European beech), namely start of leaf unfolding, leaf colouring and leaf fall. This ground phenological information (GP, onset of phenophases in days of the year (DOY)) was retrieved in the form of gridded datasets at a 1 km resolution from the Climate Data Center portal of the German Meteorological Service (DWD, n.d.).. Further information on the methodology of the interpolation of point ground observations to the gridded phenology product is available at the DWD portal.

Furthermore, we used temperature data of three climate stations of the DWD in the study area (Garmisch 720 m, Mittenwald 981 m, Hohenpeißenberg 977 m a.s.l.) in order to generally characterise seasaonal temperatures for 2001 to 2016 (see Methods 3.3).

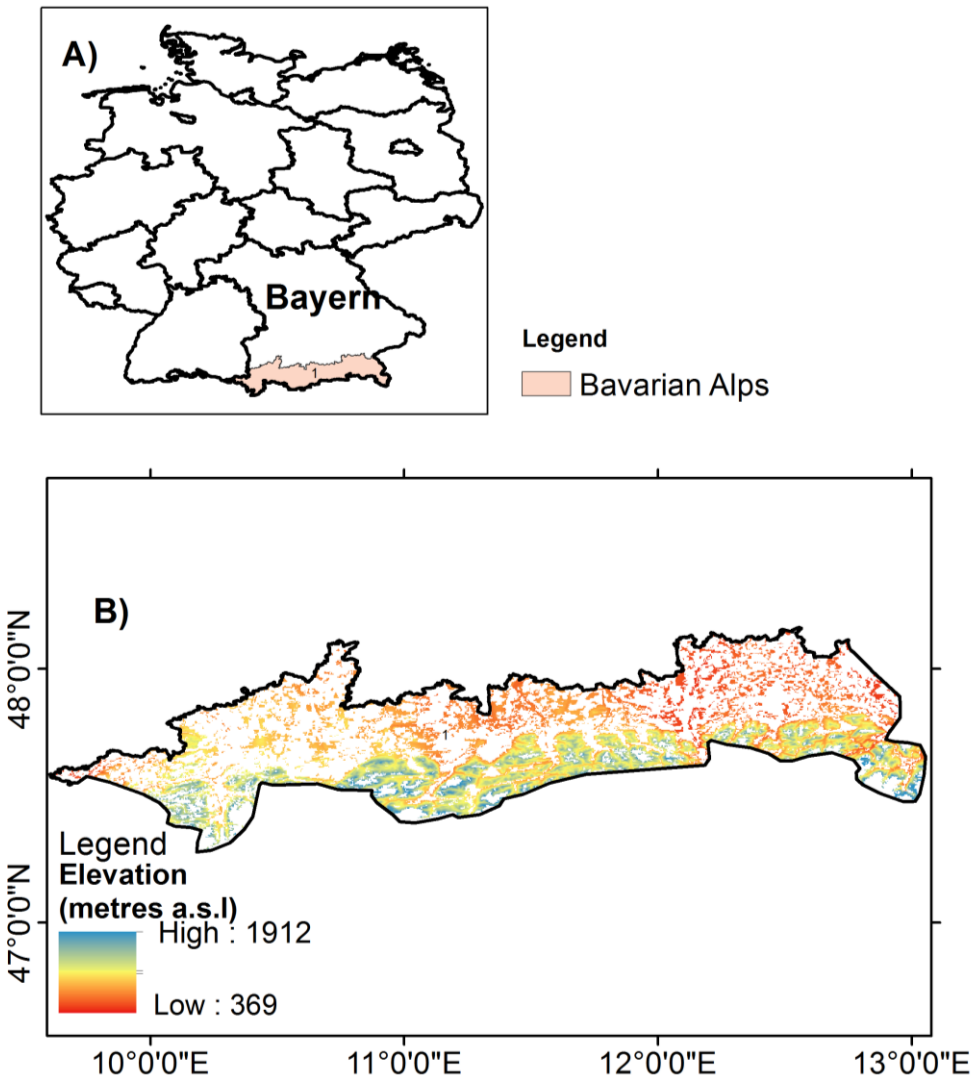

Figure1. A) Location of Bavarian Alps in Germany and, B) elevation (metre a.s.l.) of the forested region in the Bavarian Alps study area.

3. Methods

3.1 Estimation of Land Surface Phenology (LSP)

The 4-day MODIS NDVI data for the years 2001-2016 were first stacked in chronological order. The outliers in data were removed prior to calculation of NDVI using the pixel reliability and geometry (sun and solar zenith angle) information as described in Asam et al. (2018). Such gaps in the time series data were linearly interpolated and smoothed using a Gaussian function. The start (SOS) and end of season (EOS) dates were then calculated based on the 50% amplitude technique, i.e. the dates when the NDVI values cross the half-amplitude threshold in the respective ascending and descending part of the annual NDVI profile. The pre-processing of NDVI data and the calculation of LSP metrics are discussed in detail in Misra et al. (2018, 2016). Figure 2 displays the average LSP dates for start and end of the season in the study area.

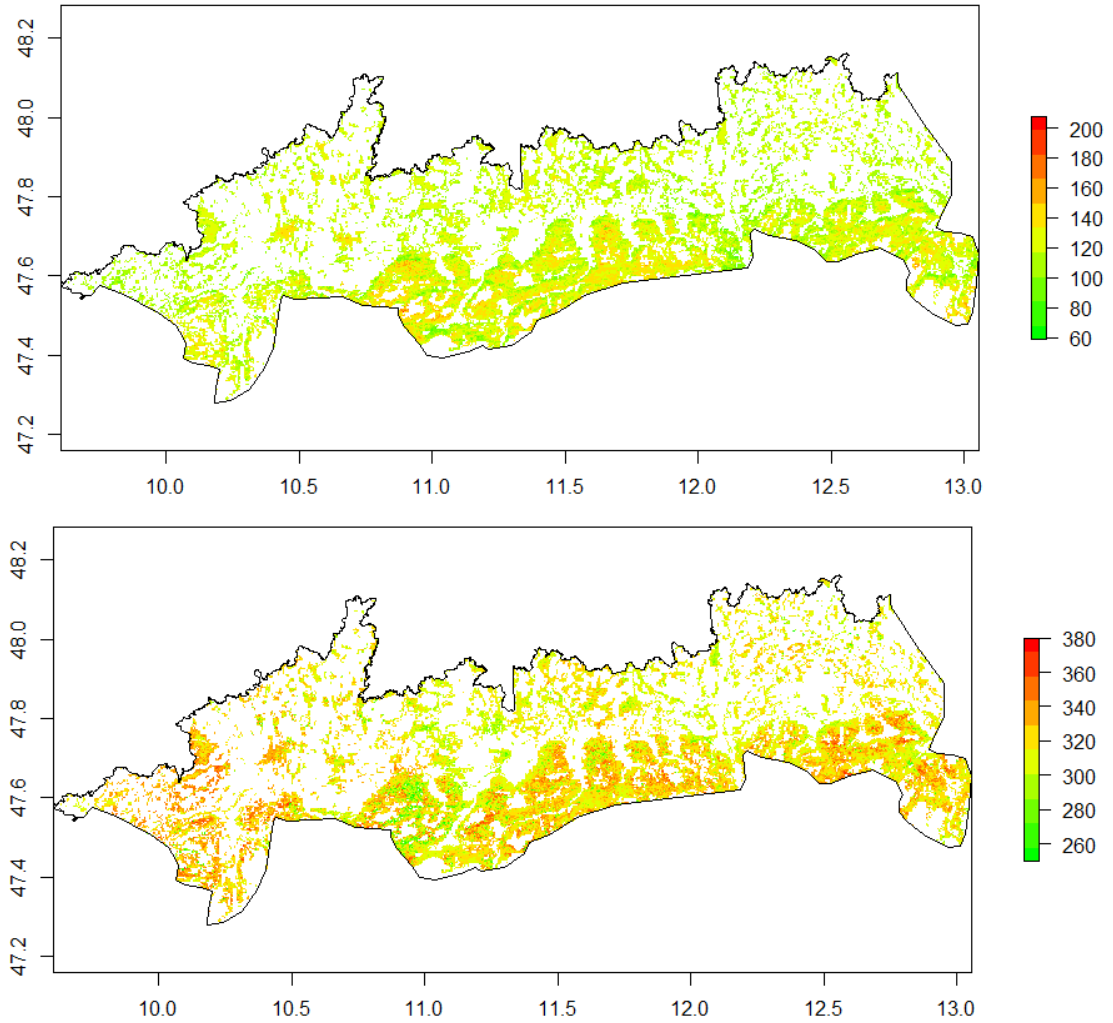

Figure 2. Mean LSP (DOY) of the forest pixels in the Bavarian alpine region during 2001-2016 derived from MODIS NDVI data. Upper panel: Start of season (SOS), lower panel: End of season (EOS).

3.2 Calculation of elevational rates of LSP and GP

The elevation data from SRTM was resampled from the native 30 m resolution to 250 m and 1 km to match the spatial resolution of MODIS-based LSP and ground phenology (GP) from DWD respectively. The pixels were then masked for the forest cover classes using a similarly resampled CORINE land cover map. Around 45,550 and 27,907 forest pixels lie in the pre-alpine and alpine region, respectively (Figure S1). The annual elevational rates of phenology were calculated using simple linear regression models over bootstrapped samples for pre-alpine and alpine regions of both MODIS-LSP and DWD-GP separately. For this, sampling of pixels containing information regarding phenological dates and their corresponding elevation was done and for each year (2001-2016) and region (pre-alpine, alpine), linear regression models between onset dates of phenology and elevation were run over 1000 iterations.

3.3 Testing of seasonal temperature driven differences in phenology and phenological lapse rates

The mean annual temperatures for the spring season (April and May) and winter season (January and February of current year, as well as November and December of previous year)

were calculated from the climate station data Based on these 16 annual seasonal temperatures, years were then grouped into the eight warmest and eight coldest years of spring and winter, respectively, yielding to four groups (CC cold spring-cold winter, CW cold spring-warm winter, WC warm spring-cold winter, WW warm spring-warm winter) which, by chance, were identical in size (4 years each) comprising the years 2002, 2006, 2010 and 2013 (CC), 2001, 2004, 2014 and 2016 (CW), 2005, 2009, 2011 and 2012 (WC) and 2003, 2007, 2008 and 2015 (WW).

The LSP and DWD-GP data were then grouped or classified based on the groups of spring and winter temperatures, and tested for significant differences using a Kruskal-Wallis test and a posthoc Dunn's test at $p<0.05$ significance level (using kruska.test and dunn.test functions in R). All data preparation, analysis and plotting of figures in this paper was carried out in the R statistical programming environment (Core Team, 2014).

4. Results

4.1 Annual Start of Season and End of Season

Annual LSP phenology for the pre-alpine and alpine region of the Bavarian Alps regions are shown in Figure 3 for spring (SOS dates) and in Figure 4 for autumn (EOS dates). Additionally, DWD-GP dates for leaf unfolding corresponding to SOS (Fig. 3) and leaf colouring and leaf fall representing EOS (Fig. 4) are also given for the pre-alpine region.
Based on remote sensing data, SOS on average starts between DOY 100 and 150 in the lowlands and between DOY 105 and 160 in the higher elevations. LSP-SOS and DWD-GP dates of the both regions show similar corresponding inter-annual variations with comparatively early SOS dates in 2007 and 2014 as well as to a lesser extent, in 2009, and late SOS dates in 2006, 2010 and 2012. LSP-SOS in 2011 exhibits a very high spatial variability in comparison with the other years. Mean annual leaf unfolding dates (DWD-SOS) occur between DOY 110 to 120, largely matching LSP-SOS, however with much smaller inter-annual variation.

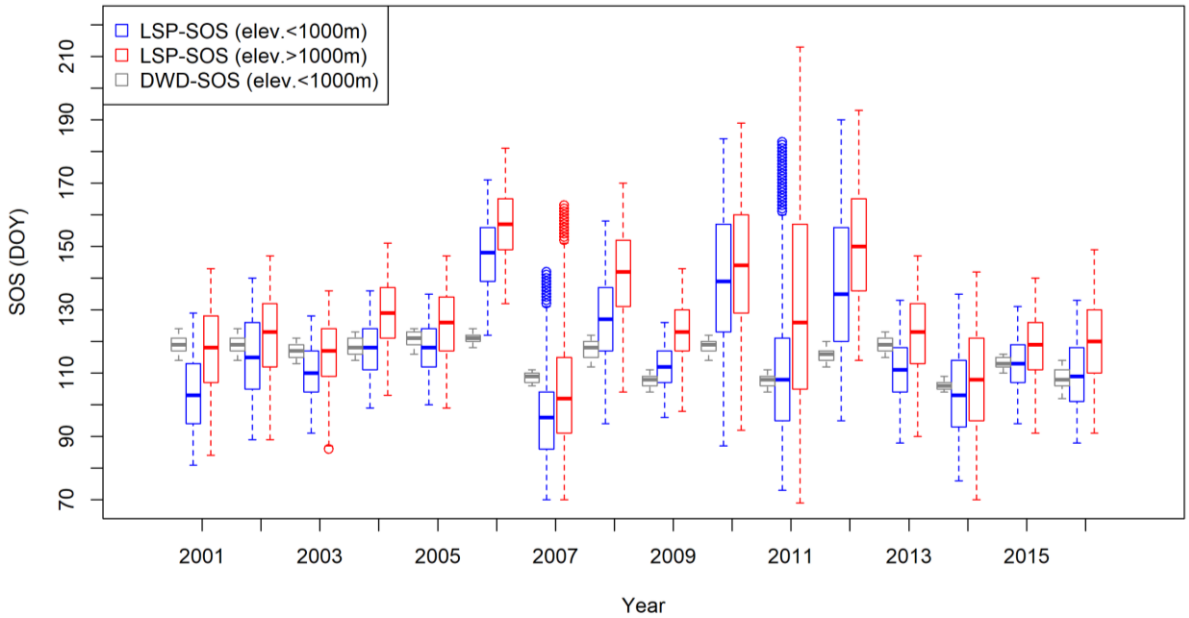

Figure 3. Annual LSP- and DWD-SOS for pre-alpine and alpine region of the Bavarian Alps from 2001 to 2016. LSP is derived from MODIS NDVI whereas DWD-SOS corresponds to leaf unfolding of European beech (see Data section).

Leaf colouring (around DOY 280) and leaf fall (around DOY 300) of European beech are observed considerably earlier than LSP-EOS from MODIS NDVI time series and exhibit smaller inter-annual variation (Fig. 4). Therefore, pre-alpine LSP-EOS corresponds (relatively) better to leaf fall than leaf colouring estimated from DWD-GP data.

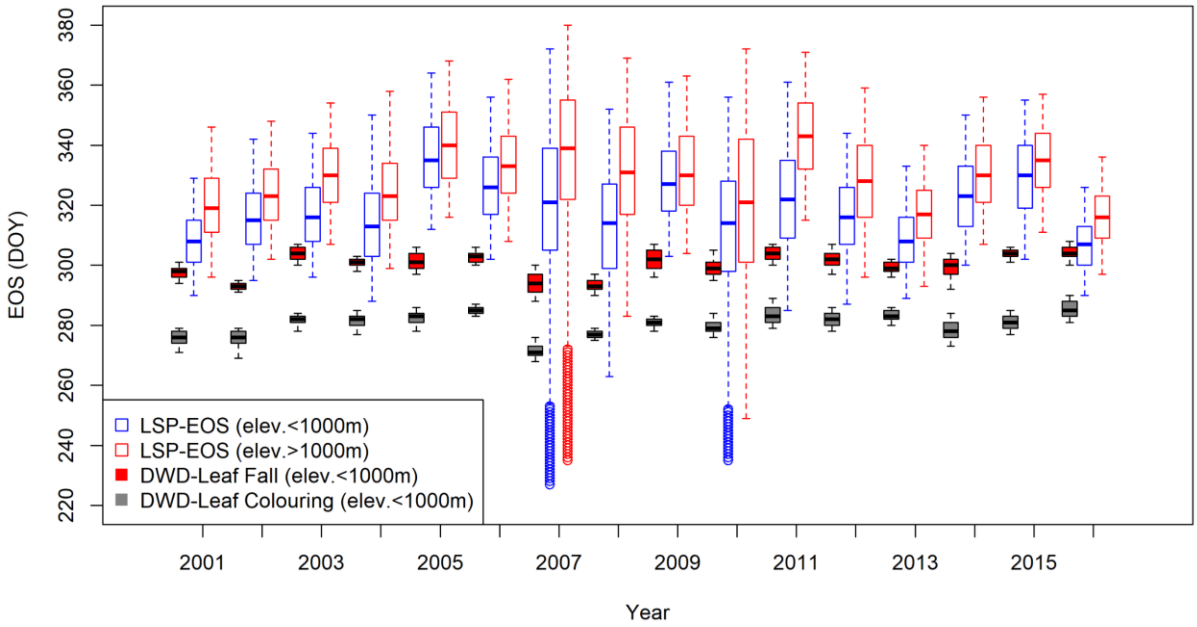

Figure 4. Annual LSP- and DWD-EOS for pre-alpine and alpine region of the Bavarian Alps from 2001 to 2016. LSP is derived from MODIS NDVI whereas DWD-EOS corresponds to leaf colouring and leaf fall of European beech (see Data section).

4.2 Annual elevational rates of Start of Season and End of Season

As expected, spring onset is delayed with elevation indicated by positive elevational rates. Overall, annual elevational rates of LSP-SOS in the alpine region are considerably higher than in the pre-alpine region with the exception of four years (2006, 2008, 2010, 2012) (see Figure 5). The annual elevational rates of DWD-GP (i.e. leaf unfolding) for the pre-alpine region strongly correlate to that of LSP-SOS rates in the pre-Alpine region. The inter-annual variability in the elevational rates of both the pre-alpine and alpine region largely matches with a few exceptions around the years 2006 / 2007 and 2011 / 2012.

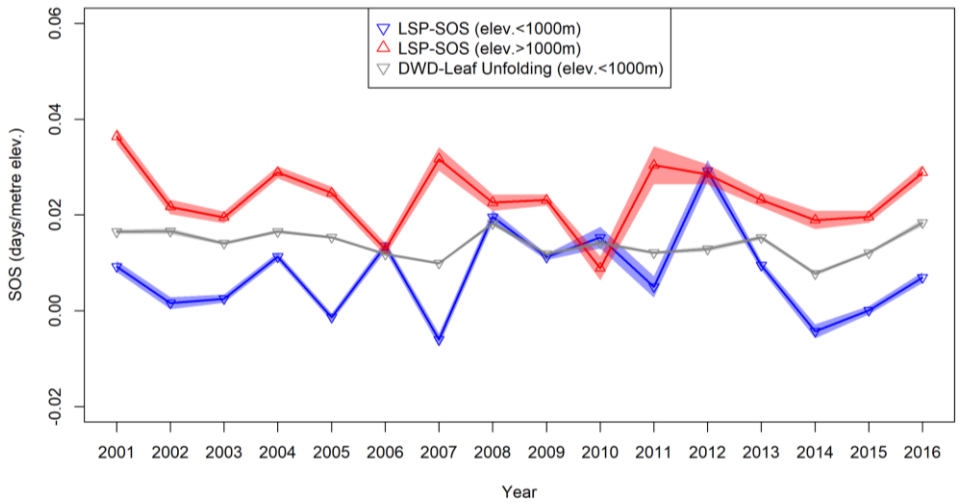

Figure 5. Annual elevational rates of SOS from MODIS-LSP and DWD-GP.

The annual EOS elevational rates based on MODIS NDVI data are still positive (sic !), however much smaller in absolute numbers than SOS elevational rates (Figure S2). They show contrasting behaviour in comparison to SOS rates, i.e. EOS rates in the pre-alpine region exhibit higher inter-annual variation than in the alpine region.

4.3 Differences in spring and warm temperature driven rates of annual phenology

When grouping the elevational rates in the pre-alpine and alpine region into the four spring-winter temperature groups, significant differences in their SOS rates become apparent (see Figure 6), apart from the groups CW and WC in the alpine region (Table S1). The smallest SOS elevational rates are revealed for pre-alpine WW, the largest for CW alpine. Differences between respective pre-alpine and alpine SOS rates are smallest in the group CC, followed by WC. In contrast, for the two groups with warm winters (WW, CW) the differences between elevational regions are considerably higher. In the case of warm springs (WW, WC), the variability of pre-alpine SOS rates is larger than for CC and CW.

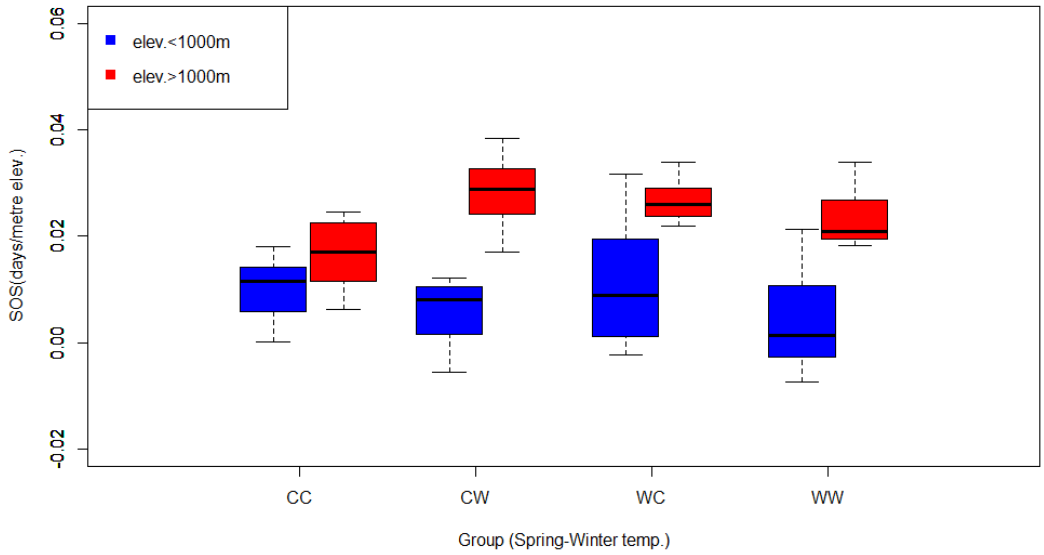

Figure 6. Annual LSP-SOS elevational rates grouped by spring and preceding winter temperatures as well as elevational regions. Note: The first letter of the group abbreviation is the assessed mean spring temperature (April, May) and the second corresponds mean winter temperature (November to February), e.g. CW is cold spring after a warm winter.

The EOS rates reveal opposing behaviour for the CC group in comparison to the EOS rates of other groups (Figure S3). The CC group shows a higher rate of EOS in the alpine region as compared to the pre-alpine region. The results of Kruskal-Wallis and posthoc Dunn's test reveal significant differences between the EOS rates of all groups (Table S2). Similarly to SOS, warm springs (WW, WC) are related to higher variability in pre-alpine EOS rates.

5. Discussion

In this study we found a close match in LSP-SOS estimates and GP observations of leaf unfolding dates. In agreement with previous research (Hamunyela et al., 2013; Luo et al., 2013), our analysis also indicates strong links between 50% amplitude based LSP-SOS and GP dates for leaf unfolding. The temperature dependent earliness in SOS is observed in the years 2007, 2009 and 2011 when the mean spring temperatures were higher than normal. The

high variability in the LSP-SOS during years 2010-2012 could not be supported by DWD-GP data which reveal a narrow range of SOS dates. Interestingly, the inter-annual patterns for both leaf colouring and leaf fall from DWD-GP strongly match with that of LSP-EOS. However, in comparison to leaf colouring, the LSP-EOS and leaf fall data show minimal differences in their absolute values. Therefore, only a correlation based measure in itself cannot sufficiently provide clues regarding a particular LSP method mirroring a specific phenophase on the ground i.e. GP. This observation corroborates suggestions from previous studies that recommend caution while comparing LSP based estimates with ground phenology (Misra et al., 2016).

The alpine elevational lapse rates of LSP-SOS were on average higher than the pre-alpine ones. This is most likely due to snow cover in the higher elevations which take disproportionately longer time to melt and warm the soil for creating favourable conditions for the starting of vegetation development. Previous research has indicated strong links between snow cover duration or snow melt and vegetation dynamics in high latitudes (Asam et al., 2018; C. Cornelius et al., 2013; Ide and Oguma, 2013). The significant differences in pre-alpine and alpine LSP-SOS of years with different spring and winter temperatures find agreement with Cook et al. (2012) who found flowering of plants to be strongly influenced by both spring and winter/ fall temperatures. Supporting Vitasse et al. (2017), we found maximum differences in the elevational rates of LSP-SOS in years of warm winters with lack of chilling. This study in this paper we have compared the pre-alpine and alpine rates of SOS and EOS in Bavaria, whereas, Vitasse et al. (2017) compares one elevational lapse rates across Switzlerland. Studies in the past have discussed the critical role of chilling in driving spring phenology, when warmer winters are known to delay the break of dormancy and the initiation of spring in plants (Laube et al., 2014; Yu et al., 2010). However, in case of years with cold spring following a cold winter, all the vegetation development is pretty late. In those years, the vegetation starts late and then has to speed up their development (leading to small elevational lapse rates). In such years the differences between pre-alpine and alpine rates of LSP-SOS are minimal possibly due to late melting of snow and the delayed start of season in higher elevations. The elevational rates of LSP-SOS were perfectly mirrored in the DWD-GP but only in the pre-alpine region. DWD-GP data are not shown in the analyses since gridded DWD-GP values in higher elevations seemed to be capped to a maximum value in the interpolation procedure.

In contrast, the LSP-EOS rates in the pre-alpine were generally higher than in the alpine region. No reasonable explanation was found for the significant differences observed between LSP-EOS rates of spring-winter temperature groups. This is possibly due to a complex interplay of factors other than temperature in driving EOS timings. Modelling of EOS phenology is known to be tricky and often reported to be triggered by combinations of temperature, photoperiod and precipitation (Hwang et al., 2011; Panchen et al., 2015; Stöckli et al., 2008). In light of the difficulties in modelling EOS and thus producing gridded products, the alpine DWD-GP rates of EOS were not included in analyses.

6. Conclusions

In this study we present analyses of spring and winter seasonal temperature-induced differences in regional phenological patterns. It is shown that not only spring temperatures but the preceding winter temperatures influence spring phenology in terms of elevational gradients. This study provides for the first time support to claims of previous studies (mostly based on ground observations) that suggest changing phenological patterns and the importance of seasonal temperature trends in high alpine regions. Both attempts hint to

reduced phenological variation at the landscape level with warming winters; however our study underlines that there are differences across altitudinal bands

References:

Asam, S., Callegari, M., Matiu, M., Fiore, G., Gregorio, L. De, Jacob, A., Menzel, A., Zebisch, M., Notarnicola, C., 2018. Relationship between Spatiotemporal Variations of Climate, Snow Cover and Plant Phenology over the Alps—An Earth Observation-Based Analysis. Remote Sens. 2018, Vol. 10, Page 1757 10, 1757. https://doi.org/10.3390/RS10111757

Burgess, M.D., Smith, K.W., Evans, K.L., Leech, D., Pearce-Higgins, J.W., Branston, C.J., Briggs, K., Clark, J.R., Du Feu, C.R., Lewthwaite, K., Nager, R.G., Sheldon, B.C., Smith, J.A., Whytock, R.C., Willis, S.G., Phillimore, A.B., 2018. Tritrophic phenological match-mismatch in space and time. Nat. Ecol. Evol. 2, 970–975. https://doi.org/10.1038/s41559-018-0543-1

Cook, B.I., Wolkovich, E.M., Parmesan, C., 2012. Divergent responses to spring and winter warming drive community level flowering trends. Proc. Natl. Acad. Sci. 109, 9000–9005. https://doi.org/10.1073/pnas.1118364109

Core Team, R., 2014. R: A language and environment for statistical computing. Vienna, Austria: R Foundation for Statistical Computing; 2014.

Cornelius, C., Estrella, N., Franz, H., Menzel, A., 2013. Linking altitudinal gradients and temperature responses of plant phenology in the Bavarian Alps. Plant Biol. 15, 57–69. https://doi.org/10.1111/j.1438-8677.2012.00577.x

Diez, J.M., Ibáñez, I., Miller-Rushing, A.J., Mazer, S.J., Crimmins, T.M., Crimmins, M.A., Bertelsen, C.D., Inouye, D.W., 2012. Forecasting phenology: From species variability to community patterns. Ecol. Lett. 15, 545–553. https://doi.org/10.1111/j.1461-0248.2012.01765.x

DWD, n.d. Climate Data Center- German Meteorological Service [WWW Document]. URL https://cdc.dwd.de/portal/201810240858/index.html (accessed 11.26.18).

EEA, 2012. CLC 2012 — Copernicus Land Monitoring Service [WWW Document]. URL http://land.copernicus.eu/pan-european/corine-land-cover/clc-2012/view (accessed 6.26.17).

Hamunyela, E., Verbesselt, J., Roerink, G., Herold, M., 2013. Trends in spring phenology of western European deciduous forests. Remote Sens. 5, 6159–6179. https://doi.org/10.3390/rs5126159

Hwang, T., Song, C., Vose, J.M., Band, L.E., 2011. Topography-mediated controls on local vegetation phenology estimated from MODIS vegetation index. Landsc. Ecol. 26, 541–556. https://doi.org/10.1007/s10980-011-9580-8

Ide, R., Oguma, H., 2013. A cost-effective monitoring method using digital time-lapse cameras for detecting temporal and spatial variations of snowmelt and vegetation phenology in alpine ecosystems. Ecol. Inform. 16, 25–34. https://doi.org/10.1016/j.ecoinf.2013.04.003

Laube, J., Sparks, T.H., Estrella, N., Höfler, J., Ankerst, D.P., Menzel, A., 2014. Chilling outweighs photoperiod in preventing precocious spring development. Glob. Chang. Biol. 20, 170–182. https://doi.org/10.1111/gcb.12360

Luo, X., Chen, X., Xu, L., Myneni, R., Zhu, Z., 2013. Assessing performance of NDVI and NDVI3g in monitoring leaf unfolding dates of the deciduous broadleaf forest in Northern China. Remote Sens. 5, 845–861. https://doi.org/10.3390/rs5020845

Menzel, A., Fabian, P., 1999. Growing season extended in Europe. Nature 397, 659. https://doi.org/10.1038/17709

Menzel, A., Jakobi, G., Ahas, R., Scheifinger, H., Estrella, N., 2003. Variations of the

climatological growing season (1951-2000) in Germany compared with other countries. Int. J. Climatol. 23, 793–812. https://doi.org/10.1002/joc.915
Menzel, A., Sparks, T.H., Estrella, N., Roy, D.B., 2006. Altered geographic and temporal variability in phenology in response to climate change. Glob. Ecol. Biogeogr. 15, 498–504. https://doi.org/10.1111/j.1466-822X.2006.00247.x
Misra, G., Buras, A., Heurich, M., Asam, S., Menzel, A., 2018. LiDAR derived topography and forest stand characteristics largely explain the spatial variability observed in MODIS land surface phenology. Remote Sens. Environ. 218, 231–244. https://doi.org/10.1016/j.rse.2018.09.027
Misra, G., Buras, A., Menzel, A., 2016. Effects of Different Methods on the Comparison between Land Surface and Ground Phenology—A Methodological Case Study from South-Western Germany. Remote Sens. 8, 753. https://doi.org/10.3390/rs8090753
Panchen, Z.A., Primack, R.B., Gallinat, A.S., Nordt, B., Stevens, A.D., Du, Y., Fahey, R., 2015. Substantial variation in leaf senescence times among 1360 temperate woody plant species: Implications for phenology and ecosystem processes. Ann. Bot. 116, 865–873. https://doi.org/10.1093/aob/mcv015
Parmesan, C., Yohe, G., 2003. A globally coherent fingerprint of climate change impacts across natural systems. Nature 421, 37–42. https://doi.org/10.1038/nature01286
Stöckli, R., Rutishauser, T., Dragoni, D., O'Keefe, J., Thornton, P.E., Jolly, M., Lu, L., Denning, A.S., 2008. Remote sensing data assimilation for a prognostic phenology model. J. Geophys. Res. Biogeosciences 113. https://doi.org/10.1029/2008JG000781
USGS, 2018. EarthExplorer - Home [WWW Document]. EarthExplorer. URL https://earthexplorer.usgs.gov/? (accessed 11.17.18).
Vandvik, V., Halbritter, A.H., Telford, R.J., 2018. Greening up the mountain. Proc. Natl. Acad. Sci. 115, 833–835. https://doi.org/10.1073/pnas.1721285115
Visser, M.E., Both, C., 2005. Shifts in phenology due to global climate change: The need for a yardstick. Proc. R. Soc. B Biol. Sci. https://doi.org/10.1098/rspb.2005.3356
Vitasse, Y., Signarbieux, C., Fu, Y.H., 2017. Global warming leads to more uniform spring phenology across elevations. Proc. Natl. Acad. Sci. 115, 201717342. https://doi.org/10.1073/pnas.1717342115
Yu, H., Luedeling, E., Xu, J., 2010. Winter and spring warming result in delayed spring phenology on the Tibetan Plateau. Proc. Natl. Acad. Sci. 107, 22151–22156. https://doi.org/10.1073/pnas.1012490107

Supplementary Information

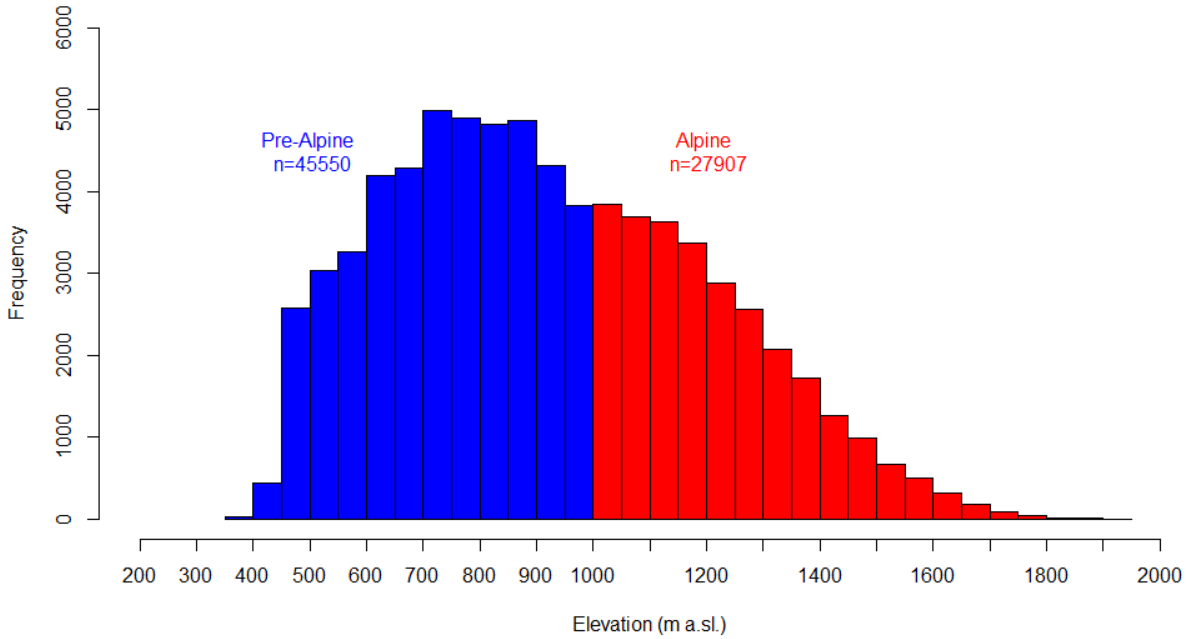

Figure S1. Frequency plot of forested pixels in the pre-alpine and alpine region of the study area.

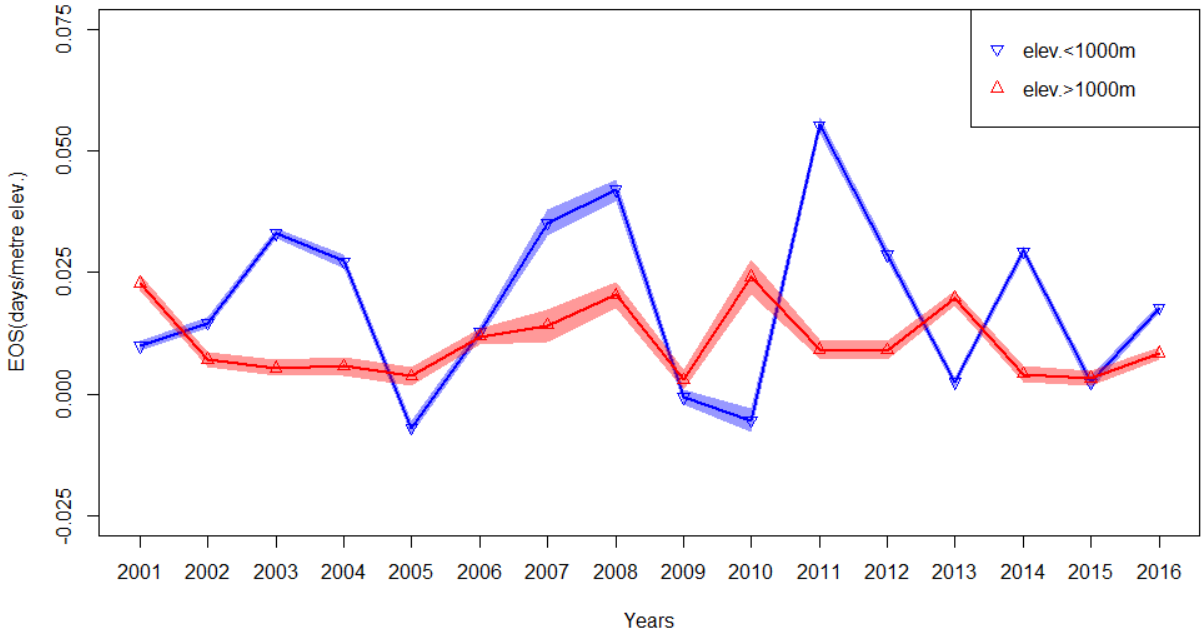

Figure S2. Annual elevational rates of LSP-EOS.

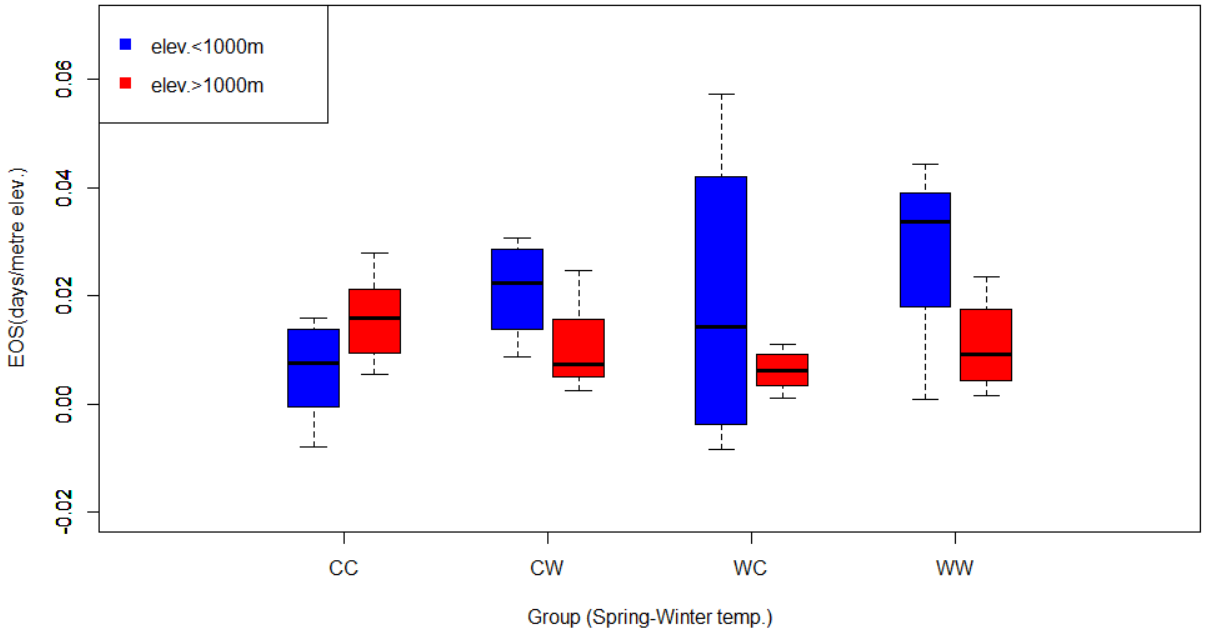

Figure S3. Annual LSP-EOS elevational rates grouped by spring and preceding winter temperatures as well as elevational regions. Note: The first letter of the group abbreviation is the assessed mean spring temperature (April, May) and the second corresponds mean winter temperature (November to February), e.g. CW is cold spring after a warm winter.

Table S1. Kruskal-Wallis test (stats package in R) followed by Dunn's test (dunn.test package in R) for testing differences in SOS rates for different groups in alpine and pre-alpine areas, i.e. from Fig 6 (aCC is alpine- cold spring- cold winter, and prCC is prealpine- cold spring following a cold winter)

```
Kruskal-Wallis rank sum test
Kruskal-Wallis chi-squared = 19591.3008, df = 7, p-value = 0

                           Comparison of x by group
                             (Benjamini-Hochberg)
Col Mean-|
Row Mean |         aCC         aCW         aWC         aWW        prCC      prCW
---------+-----------------------------------------------------------------------
-
      aCW |   -44.52444
          |     0.0000*
          |
      aWC |   -44.31971    0.204728
          |     0.0000*      0.4189
          |
      aWW |   -27.19651    17.32793    17.12320
          |     0.0000*     0.0000*     0.0000*
          |
     prCC |    26.41004    70.93449    70.72976    53.60655
          |     0.0000*     0.0000*     0.0000*     0.0000*
          |
     prCW |    43.17128    87.69572    87.49099    70.36779    16.76123
          |     0.0000*     0.0000*     0.0000*     0.0000*     0.0000*
          |
     prWC |    21.10517    65.62962    65.42489    48.30168 -5.304870 -22.06610
          |     0.0000*     0.0000*     0.0000*     0.0000*    0.0000*  0.0000*
          |
     prWW |    46.45781    90.98225    90.77752    73.65432 20.04776    3.286530
          |     0.0000*     0.0000*     0.0000*     0.0000*    0.0000*  0.0005*
Col Mean-|
Row Mean |        prWC
---------+-----------
     prWW |    25.35263
          |     0.0000*

alpha = 0.05
Reject Ho if p <= alpha/2
```

Table S2. Kruskal-Wallis test (stats package in R) and Dunn's test (dunn.test package in R) for Testing differences in eos rates of broadleaf forests for different groups in alpine and pre-alpine areas, i.e. from Figure S7.

```
Kruskal-Wallis rank sum test

data: x and group
Kruskal-Wallis chi-squared = 7855.7159, df = 7, p-value = 0

                           Comparison of x by group

                             (Benjamini-Hochberg)


Col Mean-|
Row Mean |         aCC         aCW         aWC         aWW        prCC      prCW
---------+-----------------------------------------------------------------------
-
     aCW |    23.69851
         |     0.0000*
         |
     aWC |    40.66801    16.96950
         |     0.0000*     0.0000*
         |
     aWW |    20.90552   -2.792990   -19.76249
         |     0.0000*     0.0027*     0.0000*
         |
    prCC |    38.22196    14.52344   -2.446058    17.31643
         |     0.0000*     0.0000*     0.0072*     0.0000*
         |
    prCW |   -17.28513   -40.98364   -57.95315   -38.19065   -55.50709
         |     0.0000*     0.0000*     0.0000*     0.0000*     0.0000*
         |
    prWC |    15.86532   -7.833183   -24.80268   -5.040192   -22.35663
33.15046
         |     0.0000*     0.0000*     0.0000*     0.0000*     0.0000*  0.0000*
         |
    prWW |   -22.45755   -46.15606   -63.12557   -43.36307  -60.67951 -5.172424
         |     0.0000*     0.0000*     0.0000*     0.0000*     0.0000*  0.0000*
Col Mean-|
Row Mean |        prWC
---------+------------
    prWW |   -38.32288
         |     0.0000*

alpha = 0.05
Reject Ho if p <= alpha/2
```